Functional Studies on Par14/Par17 with Emphasis on Chromatin, the Cell Cycle, and Protein-Protein Interactions

Inaugural-Dissertation

zur

Erlangung des Doktorgrades

Dr. *rer. nat.*

der Fakultät

Biologie und Geografie

an der

Universität Duisburg-Essen

vorgelegt von

Akuma Divine Saningong

aus Mankon, Bamenda, Kamerun

April 2010

The experiments for this doctoral thesis were conducted at the Centre of Medical Biotechnology (ZMB), Department of Structural and Medicinal Biochemistry, University of Duisburg-Essen.

First Examiner: Prof. Dr. Peter Bayer

Second Examiner: Prof. Dr. George Iliakis

Chairwoman of the Board of Examiners: Prof. Dr. Ann Ehrenhofer-Murray

Date of the *viva voce*: 21st June 2010

Die der vorliegenden Arbeit zugrunde liegenden Experimente wurden am Zentrum für Medizinische Biotechnologie (ZMB), Arbeitsgruppe Strukturelle und Medizinische Biochemie an der Universität Duisburg-Essen durchgeführt.

1. Gutachter: Prof. Dr. Peter Bayer

2. Gutachter: Prof. Dr. George Iliakis

Vorsitzende des Prüfungsausschusses: Prof. Dr. Ann Ehrenhofer-Murray

Tag der mündlichen Prüfung: 21. Juni 2010

Dedication

I dedicate this work to my parents, **Helen Nanga Saningong born Ndefru** and **Anye Henry Saningong**, who toiled and went endless miles to ensure that their children got the best education possible. They instilled in us that education shall be our shield, our sword and our olive branch.

It would be unfair not to mention the contribution of my “white parents” **Elfriede** and **Helmut Lotz** whose unshakable support, encouragement and care have been relentless since the early years of my education in their beloved country, Germany. *Liebe, Elfriede, Lieber Bundesbruder Helmut, ich danke euch für alles. Ich bin gerührt.*

$$Equation\ of\ Life$$

$$Phenotype\ = \int_{<birth}^{now} genome\ \times environment$$

„There is no easy walk to freedom anywhere, and many of us will have to pass through the valley of the shadow death again and again before we reach the mountaintop of our desires."
Nelson Mandela

„My humanity is bound up in yours, for we can only be human together." ***Desmond Tutu***

TABLE OF CONTENTS

Abbreviations

AP-MS	Affinity Purification-Mass Spectrometry
Av	Average
bp	base pairs
BSA	Bovine Serum Albumin
ChAP	Chromatin Affinity Purification
ChIP	Chromatin Immunoprecipitation
CHUD	Chromatin Unfolding Domain
C_t	Crossing Point Value in qRT-PCR
CTD	Carboxyl Terminal Domain
DAPI	4',6-Diamidino-2-Phenylindole
DMEM	Dulbecco's Modified Eagle Medium
DNA	Deoxyribonucleic Acid
DNase	Deoxyribonuclease
dpi	dots per inch
DTT	Dithiothreitol
E. coli	*Escherichia coli*
ECL	Enhanced Chemoluminescence
EDTA	Ethylene Diamine Tetraacetic Acid
EGFP	Ehanced Green Fluoresence Protein
EGTA	Ethylene Glycol Tetraacetic Acid
EMSA	Electromobilty Shift Assay
EP	European Patent
ESI-QTOF	Electrospray Quadrupole - Time of Flight Mass Spectrometry
et al.	et alii (and others)
FACS	Fluorescence Activated Cell Sorting
FBS	Foetal Bovine Serum
FCS	Foetal Calf Serum
FPLC	Fast Performance Liquid Chromatography
g	gram
GFP	Green Fluorescent Protein
GST	Glutathion-S-Transferasen
CNBr	Cyanogen bromide
HEPES	4-(2-hydroxyethyl)-1-Piperazineethanesulfonic Acid

HFF	Human Foreskin Fibroblast
HKG	Housekeeping Gene
HMG	High Mobility Group
HPLC	High Pressure/Performance Liquid Chromatography
IPI	International Protein Index
KD	Knock-down
kDa	Kilodalton
LacZ	α-galactosidase gene
LC-MS/MS	Liquid Chromatography Tandem Mass Spectrometry
mAU	milli Absorbance per Units
MEFs	Mouse Enthodelial Fibroblasts
MEK	MAPK and ERK Kinase
MEM	Minimum Essential Medium
min	minute
MNase	Micrococal Nuclease
mRNA	messenger Ribonucleic Acid
MS	Mass Spectrometry
mtDNA	mitochondrial DNA
MW	Molecular Weight
MWCO	Molecular Weight Cut Off
NLS	Nuclear Localisation Signal
NMR	Nuclear Magnetic Resonance
PAGE	Polyacrylamide Gel Electrophoresis
PI	Propidium Iodide
PBS	Phosphate Buffered Saline
Pen/Strep	Penicillin/Streptomycin
PMSF	Phenylmethylsulfonylfluoride
Pol II	RNA Polymerase II
PPIase	Peptidyl-Prolyl *Cis-Trans* Isomerase
qRT-PCR	quantitative Real-Time Polymerase Chain Reaction
rDNA	ribosomal DNA
rhPar14	recombinant Par14
RIPA	Radio Immuno Precipitation Assay
RNA	Ribonucleic Acid
RNase	Ribonuclease
rpm	revolutions per minute

RT	Room Temparature
SDS	Sodium Dodecyl Sulfate
sec	seconds
SHD	Schuffled Decoy Protein
shRNA	short hairpin RNA
siRNA/RNAi	small interfering RNA/RNA interference
SNP	Single Nucleotide Polymorphism
TBST	Tris-Buffered Saline Tween-20
TCE	Total Cell Extract
TEMED	Tetramethylethylenediamine
TIFF	Target Image File Format
Tris	Tris-(hydroxymetheyl)-aminomethane
U	Unit (enzyme activity)
UV	Ultraviolet Light
x g	Gravitational Acceleration

List of Figures

List of Tables

Abstract

Par14 and Par17 are members of the parvulin family of peptidyl-prolyl *cis-trans* isomerases. Par14 has been shown to be enriched in the nucleus and Par17 was demonstrated to be located in the mitochondrial matrix. It has been suggested that Par14 plays a role in chromatin remodeling on basis of sequence and structural identities to HMGB and HMGN proteins. Both Par14 and Par17 have been shown to bind to double-stranded DNA *in vitro*. However, the cellular functions of both proteins have not been characterised, and we aimed in this study to give insights to their function.

By means of biochemical fractionations, we have shown that Par14 is enriched in chromatin 3-fold higher than in the nuclear matrix. In the same experiments, we also observed that Par14 was released from the chromatin fraction after treatment with DNase I indicating its binding to DNA. In the light of this, we performed another biochemical fractionation scheme enriching nucleic acid-binding proteins. Using a phospho-cellulose column, we eluted Par14 at 0.35 and 1 M NaCl from the nucleic acid-binding fraction. This gave credit to the fact that Par14 was associated with DNA *in vivo*. Following Par14's association with chromatin, pilot experiments were initiated using Chromatin Affinity Purification (ChAP) to search for DNA-binding motifs for Par14.

Pin1 is the other member of the parvulin family and it has been characterised as a mitotic regulator. As a result, we were interested to investigate the role of Par14/Par17 in the cell cycle. Using our established cell cycle synchronisation system by serum deprivation, we showed with the aid of qRT-PCR that Par14 and Par17 were 2- and 3-fold up-regulated respectively during the S-phase at the mRNA level. A 3- and 5-fold up-regulation was seen for Par14 and Par17 in the G2/M phase respectively. The transcriptional increase of Par14 in the S and G2/M phases was correlated with a 4-fold translational increase as analysed by western blotting. As concerns Par17, we observed that Par17 was 4- and 3-fold up-regulated when cellular lysates from the individual cell cycle phases were used. Moreover, there was the oc-

currence of a 28 kDa variant of Par17 in all the phases of the cell cycle before and after the fractionation of the cellular lysates.

As a strategy to elucidate the function of Par14/Par17, we used affinity purification coupled with mass spectrometry to find their interaction partners. A Par17 construct fused to *Strep*-tag was transfected in HCT116 cells and the cellular lysates were passed over a modified streptavidin (*Strep*-Tactin) column. Elution was done with desthiobiotin and the eluted proteins were sent for tandem mass spectrometry. After filtering spurious and non-specific binders, EZR was among the 17 potential interaction partners of both parvulin proteins. EZR plays a role in the cytoskeletal network; but it remains to be validated by other techniques whether it is a *bona fide* Par14/Par17 interactor.

We were interested to know if some of the potential interaction partners found were up- or down-regulated in the advent of a successful Par14/Par17 knock-down. Our protein-protein interaction data paved the way to perform gene knock-down experiments for Par14/Par17 using siRNA technology. HeLa and HCT116 cells were transfected and knock-down was investigated by performing qRT-PCR and western blot experiments. No appreciable knock-down of Par14/Par17 mRNAs and their gene products was registered. Fluorescence microscopic studies were also done on transfected cells to check for any morphological abnormalities as a result of Par14/Par17 loss. Still, no visible phenotypic changes were observed.

Taken together, Par14 can be described as a chromatin and DNA-binding protein. The transcriptional up-regulation of Par14 and Par17 was directly proportional to their translational up-regulation. If EZR is validated as an interaction partner of Par14/Par17, this may suggest a role of Par14/Par17 as anchor proteins that link the cytoskeletal apparatus to a DNA-related process in the nucleus or in the mitochondria.

Zusammenfassung

Bei Par14 und Par17 handeln es sich um Peptidyl-Prolyl *cis-trans* Isomerasen, die zur Familie der Parvuline gehören. Es wurde gezeigt, dass Par14 im Zellkern und Par17 in der Mitochondrien-Matrix lokalisiert ist. Es wurde angenommen, dass Par14 eine Rolle im *Chromatin Remodeling* spielt, da es sequentielle und strukturelle Ähnlichkeiten mit HMGB and HMGN Proteinen aufweist. Sowohl für Par14 als auch für Par17 konnte *in vitro* die Bindung an doppelsträngige DNA nachgewiesen werden. Jedoch wurden die Funktionen beider Proteine in der Zelle bis jetzt nicht näher charakterisiert. Unsere Untersuchungen sollen zu einem besseren Verständnis der Funktionen dieser Proteine beitragen.

Mit biochemischen Fraktionierungen konnten in dieser Arbeit gezeigt werden, dass Par14 in Chromatin dreimal stärker angereichert ist, als in der nuklearen Matrix. In diesen Experimenten konnten wir außerdem beobachten, dass Par14 sich nach Zugabe von DNase I von der Chromatinfraktion löste, was auf seine Bindung an DNA hindeutet. Aufgrund dieser Beobachtungen, haben wir ein biochemisches Fraktionierungsschema genutzt, in welchem nukleinsäurebindende Proteine angereichert wurden. Unter der Annahme, dass Par14 *in vivo* DNA-gebunden vorliegt, wurde Par14 mit 0,35 M und 1 M NaCl unter Verwendung einer Phospho-Cellulose-Säule aus der nukleinsäurebindenden Fraktion eluiert. Da Par14 Chromatin-bindende Eigenschaften aufweist, wurden mit Hilfe einer Chromatin-Affinitäts-Reinigung (ChAP) Pilotexperimente durchgeführt, um mögliche DNA-Bindungsmotive für Par14 zu finden.

Pin1 ist ein weiteres Mitglied der Parvulin-Familie. Dieses Protein spielt nachweislich bei der Regulation der Mitose eine Rolle. Da Par14 und Par17 ebenfalls der Parvulin-Familie angehören, wurde die Funktion dieser Proteine im Zellzyklus näher untersucht. Mit Hilfe unseres etablierten Zellzyklus-Synchronisations-Systems und qRT-PCR konnte gezeigt werden, dass die relative Menge an mRNA von Par14 und Par17 in der S-Phase zwei- bis dreimal so hoch war. Des Weiteren konnte eine drei- bzw. fünffach höhere Expression der Par14- und Par17-Gene in der G2/M-Phase beobachtet werden. Wie mit Hilfe von Western-Blots gezeigt werden konnte, war die

erhöhte Transkription von Par14 in der S- und G2/M-Phase mit einer vierfach erhöhten Translation von Par14 mRNA korreliert. Eine entsprechende Korrelation konnte bei Par17 ebenfalls nachgewiesen werden. Eine erhöhte Transkription von Par17 in der S- und G2/M-Phasen wurde in Zelllysaten der einzelnen Phasen eine drei- und vierfache höhere Konzentration an Par17 nachgewiesen. Darüber hinaus wurde eine 28 kDa-Variante von Par17 in allen Phasen des Zellzyklus vor und nach der Fraktionierung beobachtet.

Um die Funktion von Par14/Par17 näher zu untersuchen und jeweilige Interaktionspartner zu finden, wurde eine Massenspektrometrie-gekoppelte Affinitätschromatographie angewendet. Hierzu wurde zuerst das *Strep*-tag-gekoppelte Par17-Konstrukt in HCT116-Zellen transfiziert und die Zelllysate wurden über eine modifizierte Streptavidin (*Strep*-Tactin)-Säule gereinigt. Die Elution wurde mit Desthiobiotin durchgeführt und die eluierten Proteine wurden massenspektroskopisch analysiert. Nach der Entfernung von Verunreinigungen und unspezifisch gebundenen Proteinen, konnte EZR unter den 17 potentiellen Bindungsproteinen beider Parvulinproteine, als Interaktionspartner nachgewiesen werden. EZR spielt eine Rolle im Netzwerk des Cytoskeletts. Es bleibt jedoch in weiteren Experimenten zu klären, ob Par14/Par17 tatsächlich Interaktionspartner sind.

Mit Hilfe von siRNA-Techniken wurde überprüft, ob einige der gefundenen potentiellen Interaktionspartner bei einem erfolgreichen Knock-Down von Par14/Par17 hoch- oder Herunterreguliert werden. Hierzu wurden HeLa und HCT116-Zellen mit entsprechender siRNA transfiziert und der Knock-Down wurde mit qRT-PCR und Western-Blots analysiert. Es konnte kein signifikanter Knock-Down von Par14/Par17-mRNA und der entsprechenden Genprodukte nachgewiesen werden. Es wurden ebenfalls fluoreszenzmikroskopische Untersuchungen mit transfizierten Zellen durchgeführt, um diese auf morphologische Veränderungen zu untersuchen, die auf das Fehlen von Par14/Par17 zurückzuführen sein könnten. Es konnten keine phänotypischen Veränderungen beobachtet werden.

Zusammenfassend konnten in dieser Arbeit erstmals Hinweise gefunden werden, die darauf hindeuten, dass es sich bei Par14 um ein Chromatin- und DNA-bindendes Protein handelt. Jedoch bleibt ungeklärt, warum bei Hochregulierung von Par17-Transkripten in der S- und G2/M-Phase eine entsprechende Zunahme des Genprodukts ausbleibt und warum dieses eher abzunehmen scheint. Wenn EZR als Interaktionspartner von Par14/Par17 bestätigt wird, könnte das auf eine Ankerfunktion von Par14/Par17 hindeuten, die den Cytoskelettapparat in einem DNA-abhängigen Prozess an den Zellkern oder die Mitochondrien bindet.

1. Introduction

Proteins are homologous when they share sequence similarities or identities. Homology will imply a conserved structure. A conserved structure is an indication of a conserved function. However, function is a fussy concept. It can range from same biochemical activity, same identical expression or tissue-specific expression pattern, to same cellular localisation et cetera. The catalytic core sequence of peptidyl-prolyl *cis-trans* isomerases occurs in all three domains of life, Archaea, Prokarya and Eukarya. Implicitly, it has been conserved through the course of evolution and purports a conserved function.

1.1 Peptidyl-Prolyl *cis-trans* Isomerases (PPIases)

The primary catalytic function of PPIases (EC 5.2.1.8) is to accelerate *cis-trans* isomerisation of Xaa-Pro peptide bonds within polypeptide chains (Fanghanel and Fischer, 2004). Hence, a role for PPIases in the folding of newly synthesised proteins was inferred and chaperone-like activity has been associated with several PPIases (Kruse et al., 1995; Schmid, 1995).

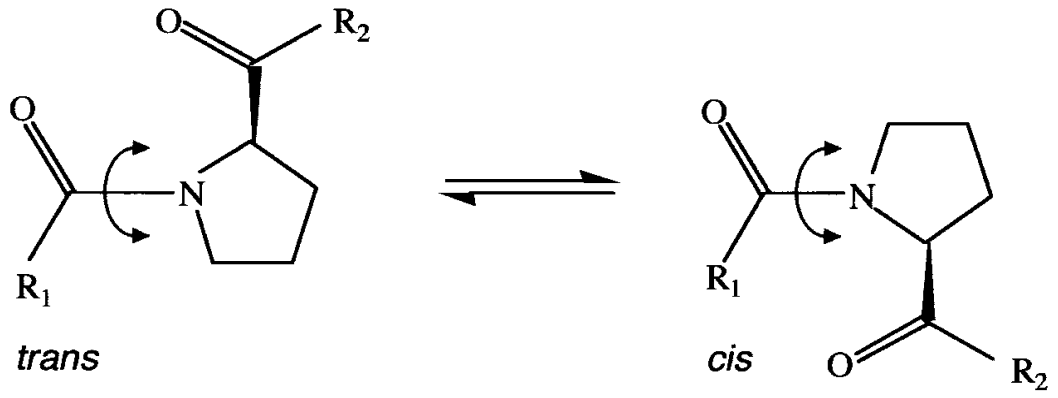

Fig 1.1 *Cis-trans* isomerisation of a peptidyl-prolyl bond (Gothel and Marahiel, 1999)

PPIases are ubiquitous proteins expressed in Eukarya, Prokarya and Archaea. Hitherto, they have been classified into three main distinct families according to their amino acid sequence homology and structural similarity. These are the cyclophilins (Cyps), FK506-binding proteins (FKBPs), and the parvulins. In Prokarya, the periplasmic space of *Escherichia coli* contains all three classes of PPIases, namely PpiA,

a cyclophilin-type PPIase, FkPA, a FK506-binding PPIase, and 2 members of the parvulin-family, SurA and PpiD (Hennecke et al., 2005; Stymest and Klappa, 2008; Weininger et al., 2009; Weininger et al., 2010). Members of cyclophilins and FKBPs have also been identified in Achaea (Maruyama et al., 2004). PinA from the cryophilic Cenarchaeum symbiosum (SwissProt: O74049) and NmPin from the mesophilic *Nitrosopumilus maritimus* (Schouten et al., 2008) are parvulin-type PPIases that have been identified in Achaea.

The prototypical member of the cyclophilin family, cytosolic cyclophilin 18 (Cyp18) also known as cyclophilin A in mammalian cells specifically catalyses *cis-trans* isomerisation of amide peptide bonds (Fischer et al., 1984). FKBP12 is the prototypic human enzyme of the FKBPs and was identified as a FK506 binding module; the term FKBP includes all proteins that share amino acid sequence homology with FKBP12, although high-affinity FK506 binding is not a common property of all FKBPs (Harding et al., 1989).

The cyclophilins and the FKBPs are sometimes termed the immunophilins. Cyps and FKBPs have been implicated in the cellular action of the immunosuppressive drugs cyclosporine A (CsA) (Fischer et al., 1989; Takahashi et al., 1989) and FK506 (tacrolimus) (Harding et al., 1989; Siekierka et al., 1989) respectively. The immunosuppressive actions exerted by CsA and FK506 on T cells and B cells have been discussed in numerous reviews (Schreiber and Crabtree, 1992; Clardy, 1995; Ho et al,. 1996). The FKBP-FK506, as well as the cyclophilin-CsA complexes, bind to calcineurin and inhibit its phosphatase activity. Calcineurin, a calcium/calmodulin-dependent serine-threonine phosphatase, dephosphorylates the nuclear factor of activating T cells (NF-AT). In its dephosphorylated form, NF-AT is able to cross the nuclear membrane to function as a transcription activator of IL-2/4 (interleukin 2 and 4), granulocyte-macrophage colony stimulating factor (GM-CSF), and gamma-interferon expression. As a result, cyclophilins and FKBPs, together with their specific immunosuppressive-acting ligands CsA and FK506, respectively, are able to interfere with this signal transduction pathway. Thus, it is not their isomerisation property but

their peptide binding ability that brings about immunosuppression (Schreiber and Crabtree, 1992).

The third family of PPIases, the parvulins (Pin1, Par14 and Par17) does not belong to immunophilins because family members do not show affinity to immunosuppressive drugs. Protein phosphatase 2A (PP2A) phosphatase activator (PTPA) has been described recently as the new family of PPIases (Jordens et al., 2006; Leulliot et al., 2006). It is an essential and specific activator of PP2A and the PP2A-like enzymes. PTPA was shown to induce conformational changes by means of isomerase activity similar to cyclophilin A and FKBP12 but similar to the isomerase activity of Pin1. The detailed treatment of this new family of PPIases is beyond the scope of this work. Two members of the parvulin family (Par14 and Par17) were the focus of this thesis.

1.2 Parvulins

In 1994, the PPIase family of parvulins was discovered by characterising the prototypical enzyme Par10 from *E. coli* (Rahfeld et al., 1994b; Rahfeld et al., 1994a). The name parvulin originates from the Latin word *parvulus*, which means tiny or very small because of its molecular weight of 10 kDa. This PPIase does not exhibit sequence similarity to either cyclophilins or FKBPs. The mature enzyme with its sole domain of 92 amino acids is enzymatically active in its monomeric state.

Many multidomain parvulins have since then been characterised in prokaryotes. In Gram-positive bacteria such as *Staphylococcus aureus* and *Bacillus subtilis*, a parvulin-type PPIase PrsA has been identified and the solution structure characterised (Heikkinen et al., 2009; Tossavainen et al., 2006). Par27 in *Bordella pertussis* was identified as a prototype of a new group of parvulins in Gram-negative bacteria (Hodak et al., 2008). The existence of only two genes, PIN1 and PIN4, encoding human parvulin proteins have been described, which is a low frequency when compared with both Cyp and FKBP sequences (Mueller et al., 2006; Rahfeld et al., 1994a).

Pin1, a parvulin family member, is irreversibly inhibited by juglone (5-hydroxy-1, 4-naphtoquinon (Hennig et al., 1998). Juglone is a benzoquinone that covalently modi-

fies thiol groups of cysteine residues in parvulins followed by a subsequent slower protein inactivation process, which is thought to be a partial unfolding of the PPIase domain (Fila et al., 2008). Juglone can also inhibit other proteins as it was reported to interact with RNA polymerase Pol II, which then led to a block in transcription (Chao et al., 2001). Derivatives of juglone such as PiB (diethyl-1,3,6,8-tetrahydro-1,3,6,8-tetraoxobenzo[lmn][3,8] phenanthroline- 2,7-diacetate) where shown to bind to the PPIase domain of Pin1 (Uchida et al., 2003). The authors also purported that Pin1 inhibitors could be used as a novel type anticancer drug that acts by blocking cell cycle progression. This line of thinking was verified by Bayer and colleagues where they identified Pin1 inhibitors that induced apoptosis in a mammalian Ras transformed cell line. Pepticinnamin E was one such inhibitor that destabilised Pin1 in solution in a juglone-like manner but did not covalently modify the protein (Bayer et al., 2005). Recently, indole 2-carboxylic acid was demonstrated in a PPIase assay to be a potent inhibitor of Pin1's PPIase activity (Potter et al., 2010). But the authors failed to confirm the ligand binding potency by biophysical techniques such as surface plasmon resonance and nuclear magnetic resonance.

1.2.1 Pin1

Pin1 was discovered in a yeast two-hybrid screen aimed to identify proteins that interact with Never in Mitosis gene A (NIMA), an essential mitotic kinase in *Aspergillus nidulans* (Lu et al., 1996). Pin1 is a 18 kDa protein composed of two functional domains, an amino terminal WW domain (amino acids 1-39) involved in protein-protein interaction, and a C-terminal PPIase domain (amino acid 45-163) that functions in catalysis (Lu et al., 1996). These two domains are separated by a short flexible linker region (Bayer et al., 2003). Pin1 is unique from other parvulin family members because it recognises phosphorylated Ser/Thr-Pro motifs, and increases the rate of *cis* and *trans* amide isomer inter-conversion by as much as 1300-fold compared to unphosphorylated peptides (Yaffe et al., 1997). The isomerisation of proteins by Pin1 results in an alteration of protein structure and/or function, which is often coupled to a change in protein stabilisation. Ess1/Ptf1 is the Pin1 orthologue in *Saccharomyces cerevisiae.* Gemmill and co-workers provided evidence that fewer than 400 molecules per cell of Ess1 were sufficient for growth although wild type cells contain about

200,000 molecules (Gemmill et al., 2005). They demonstrated *in vitro* and *in vivo* that the isomerase activity of Ess1 on the heptad-repeat (YSPTSPS) on the carboxyl-terminal domain (CTD), the largest subunit of RNA polymerase II (Pol II) was required for growth only at diminishing low levels (Gemmill et al., 2005). It will be worthwhile to decipher if human Pin1 also shows such tendencies.

The over-expression of Pin1 in yeast prevented the premature chromosome condensation followed by cell death whereas the over-expression of NIMA induced this effect. Thus, it was suggested that Pin1 might function as a negative regulator of mitosis (Lu et al., 1996). Besides, the deletion of Ess1 induced a terminal mitotic arrest (Hanes et al., 1989). The addition of Pin1 to *Xenopus* egg extracts led to the inhibition of mitotic entry and this gave more weight to the role of Pin1 in mitosis (Crenshaw et al., 1998; Shen et al., 1998; Stukenberg and Kirschner, 2001; Winkler et al., 2000c).

Dodo is the Pin1 orthologue in *Drosophila melanogaster* (Maleszka et al., 1996). Flies deficient of Dodo had no lethal phenotype. Dodo-deficient flies displayed abnormalities in the dorsal-ventral patterning of the egg chamber (Hsu et al., 2001) owing to an alteration in the fly signalling pathway that is homologous to the mammalian epidermal growth factor (EGF)-mediated pathway. A similar scenario was observed in Pin1-null mice, which had no lethal phenotype but revealed several defects (Liou et al., 2002). Pin1-null mice developed retinal atrophy, decreased body weight, testicular atrophy, and lack of breast epithelial expansion during pregnancy. These defects resembled those that occurred in cyclin D1-null mice (Liou et al., 2002). Fujimori and colleagues found that Pin1-null mouse embryonic fibroblasts (MEFs) developed normally but showed slower asynchronous growth than wild-type MEFs and were markedly delayed in cell cycle re-entry in response to re-stimulation with serum after G0 arrest (Fujimori et al., 1999). Additional studies confirmed these growth defects by showing that serum-arrested $Pin1^{-/-}$ MEFs were resistant to cell cycle re-entry in response to insulin-like growth factor 1 (IGF1) (You et al., 2002). In addition, in Pin1-null mice primordial germ cells (PGC) demonstrated a prolonged G1-S phase transition (Atchison and Means, 2003).

Pin1 is over-expressed in some human cancers (colorectal cancer, oral squamous cell carcinoma, thyroid tumours) in correlation with cyclin D1 and α-catenin over-expression (Kim et al., 2005; Li et al., 2006; Miyashita et al., 2003; Nakashima et al., 2004). Such correlations have led to the idea that Pin1 might be tumour promoting. On the contrary, the loss of Pin1 also promotes the stabilisation of two important proto-oncogenes, MYC and cyclin E. The germ line deletion of Pin1 promotes rapid genomic instability in MEFs in a p53-dependent manner that encourages more aggressive Ras-induced transformation of these Pin1-null cells (Yeh et al., 2004; Yeh et al., 2006; Zheng et al., 2002). Therefore, it has been suggested that Pin1 might act as a tumour suppressor and as an anti cancer drug target (Xu and Etzkorn, 2009). The contradictory experimental observations regarding the function of Pin1 in cancer remains enigmatic but raises the possibility that Pin1 can function as either a tumour promoter or conditional tumour suppressor. This gives rise to the question, if Pin1 can be used as a diagnostic marker of cancer or to stage the disease. Perhaps, the diagnostic values of quantifying the level of Pin1 will probably only pertain to specific cancers. Moreover, to be of use clinically, a sensitive and specific high-throughput assay for Pin1 must be developed. Hence, irrespective of how attractive it might be to present Pin1 as a therapeutic and prognostic target for cancer, much more work is required to understand the functions of Pin1 in the pathogenesis of cancer, and a large body of precaution is mandatory to ensure the specificity, selectivity, and safety of antagonists awaiting discovery (Yeh and Means, 2007).

Pin1 has also been involved in ubiquitylation and protein degradation. Pin1 was shown to control the NF-αB-related Spt23 transcription factor involved in the synthesis of unsaturated fatty acids (Siepe and Jentsch, 2009). Low ubiquitylation of Spt23 is associated with high Pin1 activity, which then triggers Spt23 precursor processing and subsequent transcription activation and *vice versa* with decreased Pin1 activity that leads to the poly-ubiquitylation of Spt23 and proteosomal degradation. Evidence has also been provided that the inhibition of Pin1 changes the ubiquitylation status of the tumour suppressor gene p53 from oligo-ubiquitylation to poly-ubiquitylation that leads to its degradation (Siepe and Jentsch, 2009; Wulf et al., 2002). The oligo-ubiquitylation of p53 is responsible for nuclear export.

Pin1 also regulates the post-transcriptional level of some cytokines, associated with asthma that possess 3' untranslated region AU-rich elements (AREs) via interaction with AUF1, the nucleoprotein in the ARE-binding complex (Esnault et al., 2006; Shen et al., 2005). Pin1 has also been identified as the molecular partner of tau and amyloid precursor protein (APP), the key factors of Alzheimer's disease (AD) (Neve and McPhie, 2006). It interacts with the phosphorylated Thr-231 of tau and regulates its activity to bind microtubules. It further interacts with the phosphorylated Thr-668 of APP and affects its metabolism (Lu, 2004; Lu et al., 1999; Zhou et al., 2000). Hence, Pin1 is probably involved in the pathogenesis of asthma and AD.

1.2.2 Par14/Par17 (PIN4)

The second and third members of the parvulin family are Par14 and Par17. For unexplained reasons, the name PIN4 was assigned to both proteins in public databases meaning protein interacting with NIMA kinase 4, although such an interaction has never been shown. PIN4 is located on the human genome on chromosome Xq13.1 that encodes two protein species, Par14 and Par17 (Mueller et al., 2006). There are two intron-less parvulin pseudogenes on chromosome 1 and 15 found on the human genome but they are truncated at the 5' end and they posses several point mutations and, hence they are not expressed (Mueller et al., 2006). The human parvulin promoter is TATA-less and situated in a CpG island typical of housekeeping genes.

Par14 consists of a 1.0 kilo-base cDNA encoding 131 amino acids and it was first cloned as a homologue of human Pin1 and *E. coli* Par10 (Uchida et al., 1999a) and has a molecular weight of 14 kDa. It is also known as Eukaryotic Homologue of Parvulins (EHPV) (Thorpe et al., 1999). Par14 has an N-terminal basic domain consisting of amino acids 1 - 35 and a PPIase domain of amino acids 36 – 131 (Sekerina et al., 2000; Terada et al., 2001).

Par17 is an elongated isoform of Par14 that resulted by alternative transcription initiation (Mueller et al., 2006). This isoform, Par17, contains a 5' extension including a 75 bp extended open reading frame with two coupled SNPs leading to amino acid substitutions Q16R (rs6525589) and R18S (rs7058353) (Riva and Kohane, 2002).

The gene product of Par17 mRNA contains an extra N-terminal consisting of 25 amino acids in addition to the N-terminal basic domain and PPIase domain of Par14. Thus, Par17 has a molecular weight of approximately 16.6 kDa and is made of 156 amino acids. The names Par14 and Par17 are derived from the nomenclature of Par10 (Rahfeld et al., 1994b). The digits 10, 14, and 17 are a reflection of their molecular weights.

1.2.3 Structure of Par14/Par17

The N-terminal region of Par14 contains 35 amino acids and it is unstructured. It is rich in lysine, serine, and glycine residues (Sekerina et al., 2000; Terada et al., 2001). Par17 differs from Par14 within the N-terminus by 25 amino acids. The N-terminal sequence between Met3 and Ala23 of Par17 is suggested to form an amphipatic α-helix as shown by the secondary structure prediction package NPS (Kessler et al., 2007). The coupled SNPs resulting in Q16R and R18S substitutions within the predicted α-helix does not compromise its amphipatic character. It has been reported that positively charged amphipatic N-terminal α-helices are typical mitochondrial targeting signals (Model et al., 2002).

Using nuclear magnetic resonance spectroscopy (NMR), two groups independently solved the solution structure of the PPIase domain of Par14 and Par17 (Sekerina et al., 2000; Terada et al., 2001). The fold of residues 36-131 of the C-terminal PPIase domain consists of a twisted four-stranded α-sheet wrapping around the C-terminal helix and the other three α-helices stacking on the other side of the central α-sheet (**Fig. 1.2**). The three dimensional structure of the PPIase domain of Par14/Par17 shows a high degree of similarity with the crystal structure of the PPIase domain of Pin1 (Sekerina et al., 2000). Par14/Par17 PPIase domain have a 34 % and 39 % sequence identity with the PPIase domains of *E. coli* Par10 and human Pin1, respectively (Mueller and Bayer, 2008).

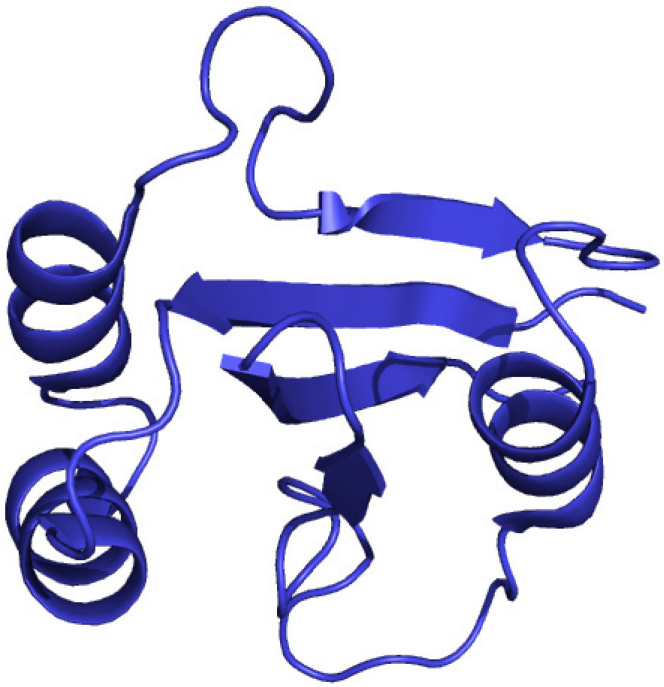

Fig 1.2 NMR solution structure of the PPIase domain of Par14/Par17 (Sekerina et al., 2000), (PDB ID: 1EQ3)

In comparison to Par10, Par14 contains an N-terminal extension of 35 amino acid residues. This extension does not possess a polyproline II helix-binding motif typical of eukaryotic Pin1-like parvulins (Mueller and Bayer, 2008). Par14 does not accelerate the *cis* to *trans* inter-conversion of oligopeptides with side chain-phosphorylated Ser/Thr-Pro moieties as in Pin1. Contrastingly, Par14 and Par10 show preference of arginine residues adjacent to N-terminal prolines. With the aid of conventional chymotrypsin-coupled assay, the enzymatic activity and substrate specificity for Par14 (Arg-Pro-Phe-NH-Np) was 3.95/mM/s that was 3-fold lower than that of Par10, 1.35/mM/s (Uchida et al., 1999a).

1.2.4 Occurrence of Par14/17

The core sequence (PPIase domain) of Par14 and Par17 is present in metazoans. The expression of Par14 was up-regulated in heart and skeletal muscles but very week in brain and lung tissues. This expression patterns were seen after analysing Par14 mRNA via northern blot (Thorpe et al., 1999; Uchida et al., 1999a; Uchida et

al., 1999b). Besides, the expression of Par14 in placenta, liver, kidney, and pancreas was present at moderate levels.

About 1 % of PIN4 mRNA transcribes Par17 as quantified by RT-PCR. Par17 is encoded in the human genome but is absent from rodent, bovine and non-mammalian genomes (Mueller et al., 2006). Our group reported that Par17 is present only in the genomes of great apes (man, chimpanzee, gorilla and orang-utan), but not in those of other primates, as shown by parvulin sequences from different primate genomic DNA samples (Kessler et al., 2007). Quantitative RT-PCR experiments also revealed that Par17 mRNA was transcribed in human tissues such as brain, blood vessels, kidney, liver, mammary gland, parotis gland, skeletal muscle, small intestine and submandibularis.

When an antibody against the N-terminal extension of Par17 was used in HeLa and HepG2 cellular lysates, a 17 kDa band was seen together with a band of 28 kDa, a putative Par17 variant (Mueller et al., 2006). The 28 kDa band suggests a potential posttranslational modification, which warranted further experimental investigation. The difference of approximately 10 - 11 kDa provoked the thinking that it was a possible SUMOylation or ubiquitylation. But western blot analyses using antibodies for ubiquitin, SUMO1 and SUMO2/3 failed to justify this assumption (Mueller et al., 2006).

1.2.5 Cellular Localisation of Par14/Par17

1.2.5.1 Par14 Localises to the Nucleus and binds to dsDNA

From cellular fractionation studies, Par14 showed an uneven distribution pattern between the cytosol and the nucleus (Surmacz et al., 2002). Par14 was 2-fold higher in the nucleus than in the cytoplasm. In confirming this enriched localisation of Par14 to the nucleus, Par14 and its deletion mutants were fused to green fluorescent protein and expressed in HeLa cells. It was observed that the deletion mutant with sequence Ser7-Gly-Ser-Gly-Lys-Ala-Gly-Lys14 found in the N-terminus of Par14 was necessary

for the nuclear targeting (Surmacz et al., 2002). DNA-cellulose affinity experiments also demonstrated that Par14 could also bind to double-stranded native DNA *in vitro*. Based on homologies and similarities of Par14 to members of the high mobility group of proteins, double-stranded DNA constructs were developed and tested for their Par14 binding affinity in fluorescence titration assays (Surmacz et al., 2002). Par14 bound preferentially in a 10 - 50 mM range to bent AT-rich DNA octamers. Experiments with truncated Par14 (amino acids 25-131) showed that the unstructured basic N-terminal part with sequence similarity to the chromatin-unfolding domain of HMGN proteins was indispensable for high affinity DNA binding. Such bent AT-rich segments of DNA are supposed to dictate nucleosome positioning (Segal et al., 2006) and play a role in transcription initiation. Electromobility shift assays were also employed to confirm the binding of Par14 to double-stranded DNA (Surmacz et al., 2002). Par14 induced a band-shift that corresponded to the DNA-protein complex.

Subsequent experiments demonstrated that the phosphorylation of Par14 on Ser19 regulated its sub-cellular localisation to the nucleus and its ability to bind DNA (Reimer et al., 2003). In HeLa cells, Par14 is most likely modified by casein kinase 2 (CK2) as phosphorylation of Par14 is inhibited *in vitro* and *in vivo* by 5, 6-dichloro-1-α-D-ribofuranosyl benzimidazole (DRB), a specific inhibitor of CK2 activity. Mutation of Ser19 to Ala abolishes phosphorylation and alters the sub-cellular localisation of Par14 from predominantly nuclear to significantly cytoplasmic. Immunostaining showed that a Glu19 mutant of Par14, which mimics the phosphorylated state of Ser19, is localised around the nuclear envelope, but does not penetrate into the nucleoplasm. As opposed to wild-type Par14, the *in vitro* DNA binding affinity of the Glu19 mutant was strongly reduced, indicating that only the de-phosphorylated protein is active in DNA-binding in the cellular nucleus.

In a GST pull-down coupled with mass spectrometry experiment, Par14 associated with pre-ribosomal ribonucleoprotein particles (Fujiyama et al., 2002). Intriguingly, in the same study, it was shown that the basic domain alone was sufficient for most of these interactions. Fujiyama-Nakamura and co-authors reported that Par14 exists in both phosphorylated and unphosphorylated forms in the cell and argued that only the

unphosphorylated form is associated with pre-40S and pre-60S ribosomal complexes (Fujiyama-Nakamura et al., 2009). They used sucrose density gradient ultracentrifugation to fractionate cytoplasmic and nuclear extracts. It was seen that phosphorylated Par14 was detected in non-ribosomal fractions while unphosphorylated Par14 was present in both non-ribosomal fractions as in pre-40S and pre-60S ribosomal fractions. In sum, Par14 enrichment in the nucleus suggests a function of a highly conserved protein involved in a DNA/RNA-dependent process like chromatin remodelling, replication, transcription, translation, or ribosome biogenesis.

1.2.5.2 Par17 Localises to the Mitochondrial Matrix and binds to dsDNA

Kessler and co-workers performed cellular fractionation studies in which HeLa cells were subdivided to obtain the constituents of the cytosol, nucleus, and mitochondria (Kessler et al., 2007). This fractionation procedure was followed by western blot analysis using an antibody targeted against the N-terminus of Par17. A 17 kDa band was detected for Par17 in the mitochondria. The mitochondrial localisation of Par17 was confirmed by transfection and fluorescence microscopic studies. Fusion constructs of Par17 to EGFP were transfected and MitoTracker, a dye that stains the mitochondria, was used for mitochondrial detection.

To check if the N-terminal pre-sequence is solely responsible for targeting the protein to the mitochondria, fusion constructs from the pre-sequence coupled to EGFP and the entire protein coupled to EGFP were transfected and stained as aforementioned. Their EGFP fluorescence overlapped with the MitoTracker signal to a lesser extent than the full length Par17 constructs. From this observation, it was deduced that the mitochondrial association of Par17 is dependent on the pre-sequence. In addition, Kessler and colleagues in the same study demonstrated with the aid of *in vitro* mitochondrial import experiments that Par17 associated with mitochondrial surfaces and it was imported to the mitochondrial matrix in a time and membrane potential-dependent manner (Kessler et al., 2007).

In DNA cellulose binding experiments, Par17 was shown to bind to dsDNA. Par17 was eluted at physiological salt concentrations as Par14 does (Kessler et al., 2007).

Hence, Par17 could be associated with the mitochondrial nucleoid. Par17 is thus a Hominid-specific DNA-binding constituent of the mitochondrial matrix and the pre-peptide (N-terminus) represents the most recently evolved functional mitochondrial targeting peptide (Kessler et al., 2007).

1.2.6 Comparing Par14/Par17 with Pin1

Par14 partially compensated for Pin1 loss in mammalian cells as its mRNA and protein levels were up-regulated in Pin1-null mouse endothelial fibroblasts (MEFs) (Uchida et al., 2003). In the same study, it was inferred that siRNA knock-down of Par14 inhibited growth of Pin1-null MEFs stronger than Pin1-null MEFs re-expressing Pin1. In an independent and different experiment, knock-down of Par14 transcript using siRNA technology lead to suppressed growth and the appropriate expression of Par14 was necessary for normal cell growth in HEK293 cells (Fujiyama-Nakamura et al., 2009). Moreover, Par14 has been suggested to complement Pin1 function in the context of cell cycle regulation and chromatin remodeling (Reimer et al., 2003). Nevertheless, the compensation of the absence of Pin1 was not complete as Par14 was unable to rescue the deletion of the yeast Ess1 (Metzner et al., 2001). Furthermore, its comparably low activity was not for phosphorylated peptide motifs (Mueller and Bayer, 2008). This might suggest divergent, but partially overlapping cellular functions for the Par14 and Pin1.

1.3 Peptidyl-Prolyl cis-trans Isomerases and their Role in DNA-Dependent Processes

Pin1 has been suggested to have overlapping functions with Phosphorylated CTD Interacting Factor (PCIF1) in vertebrate cells (Yunokuchi et al., 2009). PCIF1 is a human WW domain-containing protein that interacts with the phosphorylated carboxyl-terminal domain (CTD) of RNA polymerase II (Pol II). CTD is constituted of up to 52 tandem repeats of the heptapeptide consensus sequence YSPTSPS. When phosphorylated at Ser 2 and Ser 5, it serves as a scaffold to recruit proteins, which are pivotal in transcription and RNA processing. Yunokuchi group's reported that Pin1 was significantly up-regulated in PCIF1-deficient chicken DT40 cell lines. However, the reconstitution of PCIF1 in the mutant cell lines did not abrogate the expression of Pin1. They reasoned that Pin1 over-expression might suppress defects

caused by PCIF1 deficiency in DT40 cells. They compared the functional properties of Pin1 and PCIF1 and it was revealed that both proteins had similar substrate specificity as compared to other CTD-binding WW proteins. PCIF1 and Pin1 had overlapping sub-cellular localisation and showed comparative inhibitory effects on transcriptional activation by Pol II in human cultured cells (Yunokuchi et al., 2009).

Xu *et al* reported that Pin1 was able to modulate CTD phosphorylation both *in vitro* and *in vivo* (Shaw, 2007; Xu et al., 2003). They argued that inducible over-expression of Pin1 resulted in enhanced Pol II phosphorylation on both Ser 2 and Ser 5, which gave rise to the hyper-phosphorylated Pol IIOO isoform. In 2007, they demonstrated with the aid of transcription *in vitro* assays that Pin1 inhibited transcription in nuclear extracts as opposed to an inactive mutant that stimulated transcription (Xu and Manley, 2007). An inducible Pin1 cell line showed that Pin1 over-expression was sufficient to release Pol II from chromatin, which accumulated in a hyper-phosphorylated form in nuclear speckle-associated structures. Their data is congruent with those of Yunokuchi and co-workers mentioned above. From several assays, they inferred that inhibition reflected Pin1's activity during transcription initiation and not elongation. Hence, suggesting that Pin1 modulates CTD phosphorylation and Pol II activity during an early stage of the transcriptional cycle.

The *Xenopus laevis* Pin1 orthologue has been found to be required for the DNA replication check point (Winkler et al., 2000b). Pin1 depleted egg extracts were unable to transit the G2 to M phase of the cell cycle in the presence of aphidicolin, an inhibitor of DNA replication. The inability to transit the G2 to M boundary was exacerbated when an isomerase inactive mutant of Pin1 was added. But upon addition of wild-type recombinant Pin1, entry from the G2 to the M phase was possible (Winkler et al., 2000a). These observations speculate that Pin1 in *Xenopus laevis* maybe required for the checkpoint delaying the onset of mitosis in the advent of incomplete replication.

Ess1 has been proposed to positively regulate the function of Pol II and to be linked to chromatin remodeling complexes (Wu et al., 2000). Work from the laboratory of

Wu and co-workers have demonstrated that Ess1 interacts both physically and genetically with CTD of RNA Pol II. They suggested that Ess1 binds to the phosphorylated form of CTD of Pol II and thereby catalysing its isomerisation. Ess1 coordinates sequential steps of transcription by changing the three-dimensional structure of CTD, thus, altering the affinity of protein-CTD interactions. In the light of this, Ess1 might act as a regulatory switch for loading proteins required for transcription initiation, elongation, termination and mRNA processing (Wu et al., 2000).

Intriguingly, it was demonstrated in both genetic and biochemical approaches that cyclophilin A and Ess1 interacted with the Sin3-Rpd3 histone deacetylase complex (HDAC) by a mechanism that required prolyl isomerisation (revalo-Rodriguez et al., 2000) and thus, modulating its silencing activity. HDAC regulates transcriptional repression and gene silencing in yeast and mammalian cells (Struhl, 1998). Sin3 and Rpd3 contain multiple Ser-pro or Thr-Pro sites. It was suggested that Ess1 is a direct target of Sin3 and acted as a negative regulator to Sin3-Rpd3 HDAC. Cyclophilin A on its part targeted Rpd3 and served as positive regulator to Sin3-Rpd3 HDAC. The authors proposed a model with their findings that Ess1 and cyclophilin A modulate the activity if the Sin3-Rpd3 complex, and that excess histone deacetylation provoked mitotic arrest in Ess1 mutants (revalo-Rodriguez et al., 2000).

As aforementioned, the FKBPs constitute a subfamily of peptidyl-prolyl isomerases. Kuzuhara gave evidence to the fact that a nuclear FKBP (SpFkbp39p) from *Schizosaccharomyces pombe* could influence chromatin structure (Kuzuhara and Horikoshi, 2004). They showed that the endogenous FKBP gene was required for the *in vivo* silencing of gene expression at the rDNA locus and that SpFkbp39p had a histone chaperone activity *in vitro*. Both of these activities depended on the N-terminal non-PPIase domain of the protein. They further alluded that the C-terminal PPIase domain was not essential for the histone chaperone activity *in vitro*, but was required for the regulation of rDNA silencing *in vivo* (Horikoshi et al., 2004; Kuzuhara and Horikoshi, 2004).

Fpr4, a member of the FKBPs in *Saccharomyces cerevisiae* was reported by Nelson and colleagues how its prolyl isomerisation activity as a non-histone modification could regulate transcription and they provided evidence for cross-talk between histone lysine methylation and proline isomerisation (Nelson et al., 2006). Fpr4 binds to the amino-terminal tail of both histone H3 and H4 and in doing this it catalyses the isomerisation of H3 on proline P30 and P38 *in vitro*. Nelson and co-authors further described that P38 was mandatory for the methylation of K36 and that the isomerisation of Fpr4 inhibited the ability of Set2 to methylate H3 K36 *in vitro*. Thus, the conformational state of P38 that is controlled by Fpr4 is important for methylation of H3K36 by Set2. *In vivo*, the abrogation of Fpr4 activity resulted in increased levels of H3K36 methylation and delayed transcriptional kinetics of specific genes in yeast (Nelson et al., 2006).

In a yeast two-hybrid screen, FKB52 was identified as a potential interaction partner of IRF-4 (Mamane et al., 2000). The interferon regulatory factors (IRFs) are a family of transcriptional factors involved in the early host response to pathogens (Mamane et al., 1999). IRF-4 plays a crucial role in immunoregulatory gene expression in B and T lymphocytes. The work from Mamane's laboratory lended circumstantial support that FKBP52 inhibited IRF-4 DNA binding and and that transactivation functions by a posttranslational modification of IRF-4 that was dependent on the PPIase activity of FKBP52 (Mamane et al., 2000). The proline-rich region of IRF-4 (amino acids 150-237) and the C-terminal tetratricopeptide repeats were characterised as the domains required for the interaction. While IRF-4 and PU.1 function as a transactivator complex, their activity was suppressed due to the association of IRF-4 and FKBP52 and this effect was dependent on the PPIase activity of FKBP52 (Mamane et al., 2000). PU.1 is a member of the E-twenty six (Ets) family of transcription factors. Taken together, the authors inferred that FKBP52 induces a conformational change in IRF-4 by *cis-trans* prolyl isomerisation that interfered with the binding of IRF-4 to DNA and PU.1 and thus, demonstrating a posttranslational mechanism inducing transcription repression.

1.4 HMG Proteins in DNA-Dependent Processes

The high mobility group (HMG) proteins are a superfamily of abundant and ubiquitous nuclear proteins that bind to DNA and nucleosome and induce structural changes in the chromatin fiber. They are non-histone architectural proteins, which influence multiple DNA-related activities such as chromatin remodeling, transcription, replication, recombination, DNA repair and genomic stability (Bustin, 2001; Hock et al., 2007; Ueda and Yoshida, 2010). The HMG proteins were originally isolated from mammalian cells and named according to their electrophoretic mobility in polyacrylamide gels due to a high content of positively and negatively charged amino acid residues (Goodwin et al., 1973). The HMGs are divided into 3 families (HMGB, HMGA, and HMGN), and each family member has a characteristic functional sequence motif but they all share a carboxyl terminus rich in acidic amino acids. The names of the genes are named in sequential order for example HMGB1, HMGB2. Spice variants are indicated by small letters such as HMGA1a, HMGA1b and HMGA1c.

The functional motif of the HMGB (formerly HMG-1/-2) family is called the HMG-box. The HMGB proteins can contain up to six HMG boxes in tandem. The boxes are formed by three α-helices folded together to an L-shaped structure which can penetrate the minor groove of DNA. Binding of HMG-boxes to the DNA minor groove causes unwinding and widening of the minor groove accompanied by bending (Stros, 2010). Mammalian HMG-box containing proteins are usually classified into two major groups. The first group consists of HMGB-type non-sequence-specific DNA binding proteins with two HMG-box domains and a long highly acidic C-tail. The second group is highly diverse and consists of proteins having mostly a single HMG-box and no acidic C-tails and they bind DNA specifically. Transcription factors of SRY/Sox and TCF/LEF family of proteins belong to this second group of HMG-box proteins. The consensus DNA binding motif for SRY proteins is A/TAACAA/ (Stros et al., 2007). Both types of HMG-box domains bind non-B-type DNA structures (bent, kinked and unwound) with high affinity.

The HMGA (formerly HMG-I/Y/C) family contains three AT-hooks that serve as the functional motif. Through these hooks, HMGAs bind preferably to the minor groove of AT-rich stretches in B-form DNA and induce conformational changes that promote subsequent recruitment of additional components to the binding sites (Hock et al., 2007). The HMGN family (formerly HMG-14/-17) is characterised by a positively charged region of 30-amino acids residues, the nucleosome binding domain (NBD), the chromatin unfolding domain (CHUD), and a bipartite nuclear localisation signal (NLS). HMGNs bind in a non-specific manner to the 147-base pair nucleosome core particle and alter both the local and the higher order structure of the chromatin fiber (Hock et al., 2007).

Proteins containing any of these functional motifs embedded in their sequences are known as “HMG motif proteins.” Par14 and Par17 are HMG motif proteins. The N-terminus of Par14 reveals a 45 % sequence identity with the CHUD and the flanking sequences of HMGN2, whose residues are involved in contacts to nucleosome DNA (Surmacz et al., 2002). Furthermore, Par14/Par17 shows sequence and structural homology to SRY and LEF-1 sequence-specific transcription factors, which both contain a single HMG-box (Mueller and Bayer, 2008; Surmacz et al., 2002). On grounds of the sequence and structural homology to HMG proteins it is worthwhile to speculate that Par14/Par17 could be involved in a DNA-related event such as transcription, chromatin architecture and/or chromatin remodeling.

1.5 Purpose of the Thesis

There is considerable data supporting the fact that Par14 is a nuclear protein and binds to double stranded DNA *in vitro*. Besides, Par14 shares sequence and structural homology to HMG proteins. Par17 an isoform of Par14 has been presented as a mitochondrial protein which also binds to double-stranded DNA and was eluted at physiological salt concentrations in the same manner as Par14. Above all, Pin1, a paralogue to Par14 and Par17, is a nuclear PPIase and it has been reported to be involved in the regulation of the cell cycle. In the light of these evidences, it was of paramount importance to investigate the function of nuclear Par14 and its mitochondrial counterpart Par17. For this reason, we employed the following approaches:

- To determine the sub-nuclear localisation of Par14 by means of biochemical fractionations;
- To verify the binding of Par14 to nuclear DNA *in vivo* and to search for the DNA-binding motifs for Par14/Par17;
- To investigate the regulation of Par14/Par17 within the cell cycle making use of cell cycle synchronisation, qRT-PCR and western blotting;
- To search for novel potential interaction partners of Par14/Par17 by means of affinity purification followed by tandem mass spectrometry, and;
- To perform Par14/Par17 gene knock-down studies with the aid of siRNA-technology.

2. Materials and Methods

2.1 Materials

2.1.1 Laboratory Apparatus

AGFA Curix 60 Developer	AGFA, Düsseldorf, Germany
ÄKTApurifier 10/100 UPC-900	GE Healthcare, Munich, Germany
Beckman Tabletop GS-6R centrifuge	Beckman, CA, USA
Biophotometer	Eppendorf, Hamburg, Germany
CCD-Camera, Fuji LAS-4000x	Fujifilm, Düsseldorf, Germany
Cell Culture Bench, (HeraSafe)	Heraeus, Hanau, Germany
Cell Scraper	Eppendorf, Hamburg, Germany
Centrifuge 5415 R	Eppendorf, Hamburg, Germany
Centrifuge 5810 R	Eppendorf, Hamburg, Germany
Chromatography Column (20 ml)	Bio-Rad, Munich, Germany
Concentrator 5301	Eppendorf, Hamburg, Germany
Cover Glas	Menzel-Gläser, Braunschweig, Germany
Coulter Counter	CASY^{R}, Schärfe System, Reutlingen, Germany
CO_2 –Incubator (C200)	Labotect, Göttingen, Germany
Dry Block Heat Bath	VLM, Bielefeld, Germany
ESI-QTOF Mass Spectrometer	Bruker Daltonics, Bremen, Germany
FACSCalibur	Becton Dickson Science, CA, USA
Fastblot	Biometra, Göttigen, Germany
Inverted Phase Contrast Microscope	Olympus CK2, Hamburg, Germany
Laminar Flow Hood	Heraeus, Hanau, Germany
Master Cycler Gradient (PCR)	Eppendorf, Hamburg, Germany
Microtiter Pipettes	Gilson, Villiers-Le-Bel, France
Thermomixer Comfort	Eppendorf, Hamburg, Germany
NanoDrop ND-1000 Spectrometer	PeQLab Biotechnologies, Erlangen, Germany
Nanoflow HPLC (Ultimate 3000)	Dionex, Idstein, Germany
Novex MiniCell Chamber	Invitrogen, Karlsruhe, Germany
Olympus BX61 Fluorescence	

Microscope	Olympus, Hamburg, Germany
Overnight Culture Shaker	INFORS, Bottmingen, Germany
pH-Meter	Knick, Feldchen, Germany
Pipettes	Eppendorf, Hamburg, Germany
Roller Mixer SRT6	Stuart, Asbach, Germany
Sonicator	Bandelin Sonopuls HD 2200, Berlin, Germany
Vortexer (Vortex-Genie 2)	Scientific Industries, INC, N.Y, USA
Water Bath	Memmert, Büchenback, Germany
Weighing Machines	Kern, Balingen, Germany

2.1.2 Disposable Elements

Ultra 15 Centrifugal Device (3000 MWCO)	Amicon, MA, USA
Cassettes for SDS-PAGE	Invitrogen, CA, USA
Cell Culture Dishes, Pipettes & Flasks	Greiner, Frickenhausen, Germany
1.5 & 2 ml Tubes	Eppendorf, Hamburg, Germany
0.2 & 0.5 PCR Tubes	Brand, Wertheim, Germany
15 & 50 ml Centrifuge Tubes	Greiner, Neu-Ulm, Germany
ECL on CL-XPosure Film	Thermo Scientific, Rockford, USA
Gel Blotting Paper	Schleicher & Schuell, Dassel, Germany
Glas Round-Bottom Tubes	Greiner, Neu-Ulm, Germany
Gloves	VWR, Leuven, Thailand
Nitrocellulose Membrane	Whatman, Dassel, Germany
Polystyrene Round-Bottom Tubes	BD Falcon, MA, USA
UV Cuvettes	Roth, Karlsruhe, Germany

2.1.3 Chemical Reagents

The chemicals used were of analytical grade.

Albumin, Bovine (BSA)	Sigma, Steinheim, Germany
CNBr-activated Sepharose 4	GE Healthcare, Munich, Germany

Desthiobiotin	IBA BioTAGnology, Göttingen, Germany
Bromophenol Blue	Sigma-Aldrich, Steinheim, Germany
DAPI	Roth, Karlsruhe, Germany
DMEM + GlutaMAX	Gibco™, Invitrogen, Karlsruhe, Germany
DTT	Roth, Karlsruhe, Germany
Freezing Medium	Gibco™, Invitrogen, Karlsruhe, Germany
Ethanol	Roth, Karlsruhe, Germany
EDTA	Roth, Karlsruhe, Germany
FCS/FBS	Gibco™, Invitrogen, Karlsruhe, Germany
Glycine	Roth, Karlsruhe, Germany
Glycerol	Roth, Karlsruhe, Germany
Isopropanol	Roth, Karlsruhe, Germany
MagicMark (Protein Ladder)	Invitrogen, Karlsruhe, Germany
MEM	Gibco™, Invitrogen, Karlsruhe, Germany
$NaHCO_3$	Roth, Karlsruhe, Germany
NaCl	Roth, Karlsruhe, Germany
Nonidet P40	Roche, Mannheim, Germany
Opti-MEM® I	Gibco™, Invitrogen, Karlsruhe, Germany
PBS	Sigma-Aldrich, Steinheim, Germany
Penicillin/Streptomycin	Gibco™, Invitrogen, Karlsruhe, Germany
PreScissionPlus (Dual Colour)	Biorad, CA, USA
Propidium Iodide	Roth, Karlsruhe, Germany
Rotiphorese Gel 30	Roth, Karlsruhe, Germany
TransPass D2	New England BioLabs, Frankfurt, Germany
TEMED	Roth, Karlsruhe, Germany
Tris-HCl	Roth, Karlsruhe, Germany
Tryple Express	Gibco™, Invitrogen, Karlsruhe, Germany
Tween-20	Roth, Karlsruhe, Germany
Triton X-100	Roth, Karlsruhe, Germany

2.1.4 Commercial Kits, Columns, and Recombinant Enzymes

ABsolute QPCR SYBR Green Mix	Thermo Scientific, Bonn, Germany
DNase I	New England BioLabs, Frankfurt, Germany
ECL Western Blotting Reagents	Thermo Scientific, Bonn, Germany

Qproteome Mitochondria Isolation Kit	Qiagen, Hilden, Germany
Qproteome Nuclear Subfractionation Kit	Qiagen, Hilden, Germany
Micrococal Nuclease	Sigma-Aldrich, Munich, Germany
NAP 10	Column GE Healthcares, Munich, Germany
NucleoBondR Xtra Midi kit	Macherey-Nagel, Düren, Germany
peqGOLD Total RNA Kit	PeqLab, Erlangen, Germany
Reverse-iT MAX 1st Strand Synthesis Kit	Thermo Scientific, Bonn, Germany
SYBR-RT-Mastermix/RT-Mix	Qiagen, Hilden, Germany
RNase	Sigma-Aldrich, Munich, Germany
StrepTrap HP Column	GE Healthcare, Munich, Germany

2.1.5 Human Cell Lines

Table 2.1 Human cell lines used in cell culture experiments

Name	Description	Culture Medium	Reference
HCT 116 Cells	Colorectal Carcinoma	D-MEM, 10 % foetal calf serum, 1 % Pen/Strep	ATCC, USA
HeLa Cells	Adenocarcinoma, Cervix	D-MEM, 10 % foetal calf serum, 1 % MEM & Pen/Strep	DSMZ, Germany
HFF Cells	Human Foreskin Fibroblasts	D-MEM, 10 % foetal calf serum, 1 % Pen/Strep	ATCC, USA

2.1.6 Primers and siRNAs/shRNAs Sequences

Table 2.2 Sequences of primers of used in qRT-PCR experiments

Name of Primers		Sequence 5´-3´	Reference
Cyclin B2	forward	AAA GTT GGC TCC AAA GGG TCC TT	Wasner et al., 2003
	reverse	GAA ACT GGC TGA ACC TGT AAA AAT	
GAPDH	forward	GCTTGTCATCAATGGAAATCCC	EP2108705, 2009
	reverse	AGCCTTCTCCATGGTGG	
Par14	forward	253-TGG GAG TGA CAG TGC TGA CAA	Mueller et al., 2006
	reverse	254- CAT GTT TTT CAC ATA GAA TGT GTC TGA C	
Par17	forward	251- CGG CTT TCA GGC ATT TGT TTA G	Mueller et al., 2006
	reverse	252- GCGGCATCTTGGAAGCTTGTT	
Ribosomal Protein L13A	forward	GGTGGTCGTACGCTGTG	EP2108705, 2009
	reverse	GGTCCGCCAGAAGATGC	
snRNA U6	forward	CTC GCT TCG GCA GCA CA	-
	reverse	AAC GCT TCA CGA ATT TGC GT	

Table 2.3 siRNA and shRNA sequences used for Par14/Par17 knock-down studies

siRNA/shRNA		Sequence 5´-3´	Manufacturer	Comments
siRNA-1	sense strand	CCCAAAGGTG GTGGCAATGC AG	Dharmacon, Bonn, Germany	all four siRNAs in a pool
	antisense strand	GGGTTTCCAC CACCGTTACG TC		
siRNA-2	sense strand	GTTAAAGTCT GGGATGAGAT		
	antisense strand	CAATTTCAGA CCCTACTCTA		
siRNA-3	sense strand	GGCCGCACAGTATAGTGAAG ATA		
	antisense strand	CCGGCGTGTC ATATCACTTC TAT		
siRNA-4	sense strand	AGCATTTGCC TTGCCTGTAA		
	antisense strand	TCGTAAACGG AACGGACATT		
shRNA-1	sense strand	GAGTGACAGTGCTGACAAGA	Genscript, New Jersey, USA	loop sequence TTGATATCCG
	antisense strand	CTCACTGTCACGACTGTTCT		
shRNA-2	sense strand	CGCACAGTATAGTGAAGATAA		
	antisense strand	GCGTGTCATATCACTTCTATT		
shRNA-3	sense strand	TTATTATGGTCGAAGGAAGA		
	antisense strand	AATAATACCAGCTTCCTTCT		
shRNA-Luc	sense strand	CTTACGCTGAGTACTTCG		
	antisense strand	GAATGCGACTCATGAAGC		

2.1.7 Antibodies

Table 2.4 Antibodies used in western blotting analyses

Antibody	MW (kDa)	Type	Manufacturer	Dilution
Primary Antibodies				
αPar17-Ext	17	Rabbit Polyclonal	Eurogentec, Cologne, Germany	1 to 1000
αPPIase	14/17	Rabbit Polyclonal	Eurogentec, Cologne, Germany	1 to 1000
ß-Actin	42	Rabbit Polyclonal	Abgent, San Diego, USA	1 to 5000
Cyclophilin B	21	Rabbit Polyclonal	Abcam, Cambridge, UK	1 to 3000
Cytochrome C	15	Mouse Monoclonal	Abcam, Cambridge, UK	1 to 2000
GFP	27	Rabbit Polyclonal	Abcam, Cambridge, UK	1 to 4000
Histone H3	15	Rabbit Polyclonal	Abcam, Cambridge, UK	1 to 4000
Lamin B1	68	Rabbit Polyclonal	Abcam, Cambridge, UK	1 to 1000
MEK2	46	Rabbit Polyclonal	Abcam, Cambridge, UK	1 to 1000
Nuclear Matrix Protein p84	84	Mouse Monoclonal	Abcam, Cambridge, UK	1 to 1000
Secondary Antibodies				
Anti-Mouse HRP-linked (from Sheep)			Amersham, Freiburg, Germany	1 to 2000
Anti-Rabbit HRP-linked (from Donkey)			Amersham, Freiburg, Germany	1 to 2000

2.1.8 Plasmids and Bacterial Cells

Escherichia coli strain BL21 (DE3), home-made

Par17QR-GFP, home-made

Par17QR*Strep*-GFP, home-made

pCR®2.1-TOPO® vector, Invitrogen, Karlsruhe, Germany

pRNATin-H1.3/Hygro/siFluc vector, GenScript, New Jersey, USA

pRNATin-H1.2/Hygro vector, GenScript, New Jersey, USA

2.1.9 Buffers and Solutions

Binding Buffer

100 mM Tris-HCl, 1 mM EDTA, pH 8.0

Coomassie Brilliant Blue R 250

0.5 mg/l in 40 % methanol and 10 % acetic acid

Coupling Buffer

0.1 M $NaHC0_3$ pH 8.3, 0.5 M NaCl

Developing Solution

6 % sodium carbonate, 0.0185 %, (v/v) 37 % formaldehyde and 0.0005 % sodium thiosulfate pentahydrate

Elution Buffer

100 mM Tris-HCl, 150 mM NaCl, 2.5 mM desthiobiotin, 1 mM EDTA, pH 8.0

Extraction Buffer

1 % Triton X-100, 50 mM HEPES, pH 7.4; 150 mM NaCl, 30 mM $Na_4P2O_7.10H_2O$, 10 mM NaF, 1 mM EDTA) containing a cocktail of protease inhibitors (Roche Diagnostics) and 100 mM phenylmethylsulfonyl fluoride

Fixing Solution

50 % ethanol, 12 % acetic acid and 0.0185 %, (v/v) 37 % formaldehyde

Low Salt Lysis Buffer

10 mM HEPES, pH 7.4, 10 mM KCl, 0.1 % Triton X-100 supplemented with a cocktail of protease inhibitors (Roche Diagnostics) and 100 mM phenylmethylsulfonyl fluoride

Resolving Gel Buffer

1.8 M Tris-HCl, pH 8.8

Running Buffer for SDS-PAGE

50 mM Tris-HCl, 380 mM glycine, 0.1 % (w/v) SDS, pH 8.3

Sample Buffer

10 mM Tris-HCl, pH 7.6, 0.5 % (w/v) SDS, 25 mM DTT, 10 % (w/v) glycerol, 0.018 mg/ml bromophenol blue

Sensitisation Solution

0.02 %, sodium thiosulfate pentahydrate

Silver Nitrate Solution

0.02775 %, (v/v) 37 % formaldehyde, 0.2 % silver nitrate

Sonication Buffer

10 mM HEPES, pH 7.8; 10 mM KCl, 1 % sodium deoxycholate, 0.1 % IGEPAL CA-630 (NP-40), 1 mM DTT, 50 mM NaF, 40 mM glycerol phosphate, 10 mM Na_3VO_4, 5 µg/ml PMSF, protease inhibitor cocktail from Roche Diagnostics, Germany

Stacking Gel Buffer

1.25 M Tris-HCl, pH 6.8

Stopping Solution

50% methanol and 12 % acetic acid

Stripping Buffer

0.05 M Glycine, pH 2.5, 1 % SDS, 1 mM EDTA

TBST-500 Buffer

50 mM Tris-HCl, pH8.0, 500 mM NaCl; 0.3 % (v/v) Tween

TBST-150 Buffer

50 mM Tris-HCl, pH8.0, 150 mM NaCl; 0.3% (v/v) Tween; 3 % (w/v)

Transfer Buffer

25 mM Tris-HCl, pH 8.0 – 8.3, 192 mM Glycine, 20 % Methanol

Urea Buffer

8 M urea, 100 mM NaH_2PO_4, and 10 mM Tris-HCl, pH 8.0

2.2 . Methods

2.2.1 Molecular Biology Methods

2.2.1.1 RNA Extraction and RT-PCR Analysis

The RNA extractions and qRT-PCR analyses were done from two different perspectives to answer different questions. The first-fold of the protocol was carried out by Dr Levin Böhlig at the Department of Molecular Oncology affiliated to the *Universitäts-frauenklinik* in Leipzig, Germany. At that time, they had the expertise in doing cell cycle synchronisation per serum deprivation and were in possession of human foreskin fibroblasts (HFF), which are suitable for the mentioned kind of synchronisation. The transcriptional regulation of Par14 and Par17 in the course of the cell cycle was the matter of interest. Their protocol was as follows:

Extraction of total RNA from HFF cells was performed with TRIzol Reagent (Invitrogen, Germany) according to the supplier's instructions. Real-time RT-PCR mRNA-quantification was done with the LightCycler system (Roche, Germany). Each reaction consisted of: 10 µl 2 × SYBR-RT-Mastermix, 0.2 µl Quanti Tect RT-Mix (Qiagen, Germany), and 7.2 µl RNase free aqua dest. This mastermix was added to 1.5 µl total-RNA (50 ng/µl) respectively. For each RT-PCR reaction 18.4 µl of this solution was pipetted into a capillary. Finally, specific primers were added to a final concentration of 2 µM. The following primers were used (5' to 3'): Par14: 253-TGG GAG TGA CAG TGC TGA CAA and 254- CAT GTT TTT CAC ATA GAA TGT GTC TGA C Par17: 251- CGG CTT TCA GGC ATT TGT TTA G and 252- GCGGCATCTTGGAAGCTTGTT (Mueller et al., 2006). The reverse transcriptase reaction was performed at 50°C for 20 min. Each cycle of the following PCR included 15 sec denaturation at 95°C, 20 sec of primer annealing at 60°C, and 15 sec of extension/synthesis (72°C). Expression of U6 snRNA (GenBank accession number NR_004394) was used as an internal control that was believed to remain relatively constant during the cell cycle and it was analysed as described above with the following primers: forward: CTC GCT TCG GCA GCA CA and reverse: AAC GCT TCA CGA ATT TGC GT. As a positive control, expression of the cell cycle regulating protein Cyclin B2-gene was measured (Wasner et al., 2003). Cyclin B2-mRNA was detected with the following primers: forward: AAA GTT GGC TCC AAA GGG TCC TT, reverse: GAA ACT GGC TGA ACC TGT AAA AAT. Relative expression changes

were calculated using the $2^{-\alpha\alpha CT}$ method (Livak and Schmittgen, 2001; Schmittgen and Livak, 2008). All PCR-products used in LightCycler mRNA quantifications were confirmed by sequencing to check their identity.

The second-fold of our RNA extractions and qRT-PCRs experiments was conducted to investigate the level of Par14/Par17 knock-down after treatment with shRNAs specific to them. After the cultivation and transfection of HCT116 cells with the respective shRNA constructs, Tina Stratmann at the Department of Medicinal and Structural Biochemistry, Center of Medical Biotechnology, University of Duisburg-Essen, Germany conducted the experimental part of the qRT-PCR analyses. The author of this thesis performed the data analysis.

In brief, HCT116 cells were transfected with shRNA-1, shRNA-2, shRNA-3 and shRNA-Luc in 12-well plates using the transfection reagent nanofectamin (PAA, Germany) according the manufacturer's manual. shRNA-1, 2, and -3 are short hairpins specific to Par14/Par17 while shRNA-Luc is a short hairpin specific to luciferase and was used as a negative control. Transfection was done for 72 hrs, and total RNA was extracted using peqGOLD Total RNA Kit, (PeqLab, Germany) following the manufacturer's protocol. The RNAs from three independent wells for each construct was isolated. The concentrations of the RNAs were measured using NanoDrop photometer (PeqLab, Germany). The synthesis of cDNAs was conducted with the Reverse-iT MAX 1st Strand Synthesis Kit (Thermo Scientific, Bonn, Germany). qRT-PCR was performed on Rotor-Gene3000 (Corbett Life Science now Qiagen, Germany) using ABsolute QPCR SYBR Green Mix (Thermo Scientific, Germany) according to the manufacturer's instructions. Each reaction consisted of: 12, 5 µl Absolute QPCR SYBR Green Mix, 2 µl of respective forward primer, 2 µl of respective reverse primer RT-Mix, 8 µl RNase free aqua dest. This was done in a "master mix" manner. The Par14/Par17 primers mentioned above in the first-fold of qRT-PCR experiments were used and primers for GAPDH and ribosomal protein L13A were employed as housekeeping genes **(Table 2.2)**. The reverse transcriptase reaction was activated at 95 °C for 15 min. PCR amplification was done for 35 cycles at 95 °C for 15 sec, 56 °C for 30 sec, 72 °C for 30 sec. Relative expression changes were calculated with the $2^{-\alpha\alpha CT}$ method (Livak and Schmittgen, 2001; Schmittgen and Livak, 2008).

2.2.2 Cell Biology Methods

2.2.2.1 Eukaryotic Cell Culture

HCT 116 cells (ATCC, USA) and HeLa cells (DSMZ, Germany) were cultured in growth medium (D-MEM, 1 % MEM, 10 % heat-inactivated foetal calf serum and 1 % penicillin/streptomycin; Gibco, Germany) in T-75 cm^2 culture flasks (Greiner, Frickenhausen) and incubated at 37°C in a 5 % CO_2 incubator. Note that the growth medium for HCT116 cells was not supplemented with 1 % MEM. HFF cells were also grown in the same culture medium like HCT116 cells devoid of 1 % MEM. Besides, HFF cells were cultured in T-300 cm^2 flasks (TPP, Germany). HFFs are very large fibroblastic cells and need much space for proliferation.

Cells were allowed to grow to 80 - 90% confluence and were sub-cultured as follows: culture medium was discarded and cells were washed briefly two times with pre-warmed PBS, pH 7.4. Thereafter, cells were trypsinised with 1 ml Tryple Express per flask (Gibco, Germany) and incubated for 3 min at 37°C and 5 % CO_2. Cell detachment from the culture flasks with Tryple Express was halted by adding 10 ml of culture medium and the cell suspension was transferred to a 15 ml centrifuge tube. Centrifugation was done for 5 min at 200 x g and the cell pellet was re-suspended in 3 - 5 ml culture medium. Cell number from a 50 µl aliquot was determined by using a Coulter counter (CASY^R, Schärfe System, Germany) and the settings for the respective cell line was maintained as recommended by the manufacturer. The required density of cells was re-cultured or cryoconserved.

Routinely, 1 x 10^5 cells were plated in 10 ml growth medium and 2 x 10^6 cells were cryoconserved in 1 ml of Recovery ^{TM} cell culture freezing medium (Gibco, Germany). For the latter, the vials were first stored at -80°C overnight before they were transferred to -196°C until use. For use after cryopreservation, a vial was removed and was just allowed to thaw by exposing it to a water bath at 37°C. The cells in the vial were immediately transferred to a T-25 cm^2 culture flask containing pre-warmed culture medium. Incubation and sub-cultivation were performed as described as above.

2.2.2.2 Transient Transfection

Plasmid DNAs (Par17QR-GFP and Par17QR*Strep*-GFP) and shRNAs specific for Par14/Par17 in pRNTin-H1.2/Hygro and pRNATin-H1.3/Hygro/siFluc vectors were isolated, precipitated sequentially with isopropanol, 100 % and 70 % ethanol, and dissolved in 10 mM Tris-HCl (pH 8) using the NucleoBond^R Xtra Midi kit (Macherey-Nagel, Germany). One day before transfection, 1.5 x10^6 HCT116 or HeLa cells were seeded on 15 cm^2 petri dishes (Greiner Bio-One, Germany) and incubated over night at 37 °C and 5 % CO_2. Transfection experiments were carried out using 34 µl TransPass D2 (New England BioLabs, Germany) transfection reagent per 12 µg plasmid DNA (Par17QR-GFP and Par17QR*Strep*-GFP). For the transfection of shRNAs and siRNAs, nanofectamin (PAA, Germany) and Dharmafect I (Dharmacon, Germany) were used respectively. The transfection procedures were performed according to the instructions of the suppliers. Transfection from 48 and up to 96 hrs was conducted. Transfection efficiency was validated by the use of a fluorescence microscope since our plasmid DNAs and shRNAs constructs carried the coding sequence of the GFP reporter gene. The siRNAs were co-transfected with siGLO green, which also served as a transfection indicator **(Section 2.4)**. The transfected cells were washed twice with pre-warmed PBS, pH 7.4 and either scrapped or trypsinised and centrifuged (300 x g, 5 min, RT) for down-flow experiments.

2.2.2.3 Preparation of Cell Lysates

Transfected HCT116 cellular lysates of Par17QR-GFP and Par17QR*Strep*-GFP were lysed each in 4 ml sonication buffer (10 mM HEPES, pH 7.8; 10 mM KCl, 1 % sodium deoxycholate, 0.1 % IGEPAL CA-630 (NP-40), 1 mM DTT, 50 mM NaF, 40 mM glycerol phosphate, 10 mM Na_3VO_4, 5 µg/ml PMSF, protease inhibitor cocktail from Roche Diagnostics, Germany). The lysates were sonicated with five pulses of 20 sec each, with a 30 sec rest on ice between each pulse (Bandelin Sonopuls HD 2200, Germany). Centrifugation of the sonicated transfected lysates was done at 12,000 x g, 4°C for 10 min to get rid of cellular debris. The supernatants were collected and stored at -20°C until use for *Strep*-tag II pull-down experiments.

The transfected cellular lysates obtained after transfection with shRNAs or siRNAs were lysed, sonicated and processed in the same manner as described above. They

were later used for SDS-PAGE and western blot analyses to check for knock-down efficiency.

2.2.2.4 Cell Cycle Syncrhonisation

In the present protocol, we describe a simple, reliable, and reversible procedure to synchronise human foreskin fibroblasts (HFF) culture by serum deprivation in which the cells were arrested in the G0 phase before re-entry into the cell cycle (Davis et al., 2001; Merrill, 1998). 1.5 x 10^6 HFFs were seeded and allowed to grow to about 65 % confluence in culture medium (D-MEM 10 % foetal calf serum and 1 % Pen/Strep; Gibco, Germany) in a T-300 cm^2 culture flask (TPP, Germany) at 37°C and 5 % CO_2. The medium was aspirated and the cells were thoroughly washed 3 times with pre-warmed PBS, pH 7.4 to remove any trace of serum. Cells were allowed to starve for 30 - 36 hrs by incubating them in culture medium without foetal calf serum. After 30 - 36 hrs of serum deprivation, 4 culture flasks that were labelled G0 were taken out of the incubator (**Section 2.3.2.1** for sub-cellular fractionation). Cells were spun down in an Eppendorf tabletop 5810 R centrifuge at 800 x g and 4°C for 5 min. The supernatants were aspirated and the cells were first trypsinised and re-suspended in 5 ml PBS to facilitate cell counting. Cell counting was done using a Coulter Counter as described above. An aliquot of 1 x 10^5 cells was kept aside for analysis by flow cytometry. The remaining aliquot of cells was spun down as mentioned above and the pellet was kept at -20°C until use.

HFF cells in the other culture flasks were re-stimulated to enter the cell cycle by aspirating the old culture medium and giving them new culture medium supplemented with 20 % foetal calf serum. Cells in G1, S, and G2/M phases were harvested after 14, 20, and 24 hrs after re-stimulation respectively. 10 % foetal calf serum is normally needed for cells that have not been deprived of growth factors. They were prepared and stored as cells gained from the G0 phase and the respective aliquots for flow cytometry were kept till further analyses. In general, 1.3 x 10^7 cells per cell cycle phase were harvested for subsequent downstream cellular fractionations.

2.2.2.5 Fixation

Cells gained from the different phases of the cell cycle were permeabilised by fixation rendering them fit for intracellular staining. 1 x 10^5 HFF cells from each phase of the cell cycle were re-suspended in 200 µl PBS, pH 7.4. 200 µl of ice-cold 70 % ethanol was added dropwise to the cells under gentle agitation (750 rpm) in a thermormixer and incubated for 15 – 60 min at 4°C. The cells were pelleted at 750 x g for 4 min at RT. Respective pellets were washed with PBS; pH 7.4 supplemented with 1 % foetal bovine serum (FBS) and allowed to equilibrate for 20 min at RT while rocking on a shaker. Cells were centrifuged in a swing bucket centrifuge at 1800 x g for 5 min. From a practical point of view, a fixed-radius centrifuge did not pellet the cells at this step even at high centrifugal forces. The pelleted cells were ready for use or were stored at -20°C until use. The fixation of HeLa cells for microscopic investigations has been described in **Section 2.4**.

2.2.2.6 Propidium Iodide Staining and Flow Cytometry Analysis

In this study, propidium iodide (PI) was used as a DNA-staining dye. PI binds to DNA by intercalating between the bases with little or no sequence preference and with a stoichiometry of one dye molecule per 4 – 5 base pairs of DNA. PI also binds to RNA, necessitating treatment with nucleases to distinguish between RNA and DNA staining. Once the dye is bound to nucleic acids, its fluorescence is enhanced from 20- to 30-fold, the fluorescence excitation maximum is shifted ~30 – 40 nm to the red and the fluorescence emission maximum is shifted ~15 nm to the blue. Since the fluorescence of cells stained with PI is directly proportional to its DNA content and thus reflecting which phase of the cell cycle, this property is exploited to analyse cells in the different phases of the cell cycle by a flow cytometer.

Before staining with propidium iodide, the cells (**Section 2.2.2.5**) were washed once with PBS, pH 7.4 and re-suspended in 750 µl PBS in the same buffer. After treatment of the cells with 10 µl of 50 µg/ml RNase (Sigma-Aldrich, Germany) for 30 min under gentle agitation with a thermomixer at 37°C. 15 µl of 50 µg/ml propidium iodide (Roth, Germany) were added to the cells and incubated for 5 min making them ready for fluorescence activated cell sorting (FACS) analysis. FACSCalibur flow cytometer (Becton Dickson Science, Germany) was used. The PI-stained cells were carried to

the laser intercept in a fluid stream. When the cells passed through the laser intercept, they scattered laser light and the PI molecules incorporated in them showed fluorescence. The counting of doublets (that is two cells, which might have clogged and passed throught the laser together) was circumvented by adjusting the instrument settings for a FL-2A histogram. FL-2A is the peak area that is directly proportional to the DNA content of the cells. G1 doublets have the same DNA content, as G2/M cells but need a longer time to go through the laser and will not be considered on the histogram. In this way, doublets were excluded and they did not falsify the populations of the respective cell cycle phases. The cells were excited with an Argon laser (488 nm) and the fluorescence emission was recorded on a FL-2 detector (585/42 band pass filter). Data processing was done with the software CellQuest^{TM} Pro (Becton Dickson Science, Germany). For each sample, 1 x 10^4 cells were analysed.

2.3 Protein Biochemistry Methods

2.3.1 Antibody Production and Purification

2.3.1.1 Production and Affinity Purification of anti serum against the PPIase Domain of Par14/Par17 (αPPIase)

To generate αPPIase polyclonal antibodies, amino acids 36 - 131/61 - 156 corresponding to the PPIase domain of full length Par14/Par17 was cloned into the expression vector pET-41 according to standard procedures, which has been modified with PreScission protease restriction sites (Grum et al., 2010). Alma Rüppel from the Department of Structural and Medicinal Biochemistry, University Duisburg-Essen, Germany kindly provided the cloned plasmid. For protein production, the plasmid was over-expressed in *Escherichia coli* strain BL21 (DE3) and purified as a glutathione S-transferase (GST) fusion protein. After cleavage of the GST moiety with PreScission protease (GE Healthcare, Germany), the PPIase domain was further purified on a superdex 75 column by gel filtration and used as the antigen. A total of 2 mg of the recombinant PPIase was sent for immunisation of a rabbit (Eurogenetec, Belgium) and analysis of the test bleeds were conducted. The final antiserum αPPIase was purified by affinity chromatography as described below.

CNBr-activated Sepharose 4 fast Flow (GE Healthcare, Germany) was equilibrated according to the manufacturer's protocol in a 20 ml chromatography column (Bio-Rad, Germany). Before coupling of 10.5 mg (21 mg/ml in 0.5 ml) recombinant PPIase on the equilibrated sepharose, it was first re-buffered with coupling buffer (0.1 M $NaHC0_3$, pH 8.3, 0.5 M NaCl) using a NAP 10 column (GE Healthcare, Germany). Coupling was done for 5 hrs at RT under gentle agitation. Excess PPIase was washed off with at least 5 medium volumes of coupling buffer. One medium volume corresponded to 1 ml. The PPIase concentration in the washed-off medium volumes was determined by Bradford assay to 5 mg/ml (2.5 mg in 0.5 ml). This implied that 8 mg of PPIase was immobilised to the column. The non-reacted groups on the medium were blocked after coupling by transferring to 0.1 M Tris-HCl buffer, pH 8.0 and allowed to stand for 2 hrs. 3 medium volumes of buffers 0.1 M acetate, pH 3 - 4 and 0.1 M Tris-HCl, pH 8-9 both containing 0.5 M NaCl were used alternately 5 times to wash the coupled medium after this incubation procedure. 5 ml of antiserum PPIase-Par14/Par17 was diluted with 14.5 ml PBS, pH 7.4 and 0.5 ml 5 mM NaN_3 and the

solution was poured onto the coupled medium and incubated overnight under gentle agitation on an end-over-end shaker at 4°C. The bottom cap of the column was opened and the unbound serum flew through. The column was washed 3 times with 20 ml of PBS, pH 7.4.

For elution, 2 ml microcentrifuge tubes were prepared each containing 1 ml 1 M Tris HCl, pH 8.8. The column was placed on the first tube and 1 ml of elution buffer (25 mM glycine, pH 2.2) was given onto it and allowed to flow through into the tube underneath. This procedure was repeated for all tubes until no antibody flew through. To find this out, the viscosity of the flow-through was visually examined. A non-viscous flow-through justified that no antibody was present. The components of all the microcentrifuge tubes used to capture the eluates were pooled and concentrated to a final volume of 0.2 ml with an Amicon Ultra 15 centrifugal device 3000 MWCO. The antibody concentration was determined using UV/Vis absorption and the formula of Warburg and Christian (Warburg and Christian, 1940). The formular corrects the contamination and the absorbption of nucleic acids at 260 nm. C is the protein concentration and A_{280} is the absorbance of proteins at 280 nm.

$$C_{Protein}\ (mg/ml) = 1.55A_{280} - 0.76A_{260}$$

0.77 mg/ml in 0.2 ml of αPPIase was purified and diluted with 0.2 ml sterile 87 % glycerol, making the end concentration of the antibody to be 0.38 mg/ml in 0.4 ml.

2.3.1.2 Production and Affinity Purification of anti serum against the N-Terminal Extension of Par17 (αPar17-Ext)

The antiserum for the N-Terminal extension for Par17 was done at Eurogenetec, Belgium and as previously described by Mueller and co-workers (Mueller et al., 2006). The final antiserum was subjected to affinity purification as elucidated below to reduce background and to increase specificity and sensitivity for the detection of Par17.

Affinity purification was done in the same manner as described in **Section 2.3.1.1** for the purification of antiserum PPIase Par14/Par17. A main difference in the procedure was the use of the solid phase synthesised 25-amino acid peptide for coupling to the

equilibrated CNBr-activated Sepharose 4 fast Flow (GE Healthcare, Germany). Sascha Gentz from the Department of Physical Biochemistry at the Max Planck Institute for Molecular Physiology, Dortmund, Germany kindly provided this synthetic peptide. The final concentration of αPar17-Ext antibody diluted to a 1:1 ratio in 87 % glycerol stood at 1 mg/ml in 0.5 ml.

2.3.2 Biochemical Fractionations

2.3.2.1 Sub-cellular Fractionation

Qproteome mitochondria isolation kit (Qiagen, Germany) was used to separate HFF G0, G1, S and G2/M cell populations into cytosolic, nuclear, and mitochondrial fractions. 1.3 x 10^7 cells were centrifuged at 500 x g 4°C for 10 min and the supernatant was aspirated. The pellets were washed in 1 ml 0.9 % NaCl solution and centrifuged again at 500 x g, 4°C for 10 min. The pellets were re-suspended in 0.5 ml ice-cold lysis buffer (composition of the lysis buffer was not disclosed by the manufacturer) supplemented with protease inhibitor solution and an incubation step followed for 10 min at 4°C on an end-over-end shaker. The cell pellets were centrifuged at 1000 x g for 10 min at 4°C and the supernatants were termed S1, which primarily contained cytoplasmic proteins **(Fig. 2.1)**. The pellets (P1) were washed 2 times with lysis buffer to remove cytosolic contaminants and re-suspended in 1 ml ice-cold disruption buffer (composition of the disruption buffer not disclosed by the manufacturer) supplemented with protease inhibitor solution. The supernatants (S2) collected after a centrifugation step at 1000 x g, 4°C for 10 min were transferred to 2 ml centrifuge tubes. The pellets (P2) which contained nuclei, cell debris, and unbroken cells were further extracted with 0.5 ml disruption buffer and the first and second S2s were pooled. The resulting P2s (containing nuclei, unbroken cells and cell debris) were dissolved in 300 µl disruption buffer and sonication was performed at 3 pulses for 30 sec with a 30 sec rest on ice between each pulse at 17 - 20 % amplitude (Bandelin Sonopuls HD 2200, Germany). Thereafter, the sonicated P2 pellets were clarified by centrifugation at 16,000 x g (Eppendorf Centirfuge 5415R), 4°C for 5 min and the resulting supernatants (S3) were kept at -20°C until further analysis. The supernatants S2 from above were centrifuged for 30 min at 12,000 x g (Eppendorf Centirfuge 5415R) at 4°C. The resulting supernatants S4 were aspirated and the pellets (P4) were believed to contain mitochondria. The mitochondrial pellets were washed

with 1 ml mitochondria storage buffer (composition not disclosed by the manufacturer) by pipetting up and down and centrifuged at 12,000 x g (Eppendorf Centirfuge 5415R) for 20 min at 4°C. These pellets were re-suspended in 50 µl of mitochondria storage buffer for further analysis. Storage of all the samples was done at -20°C.

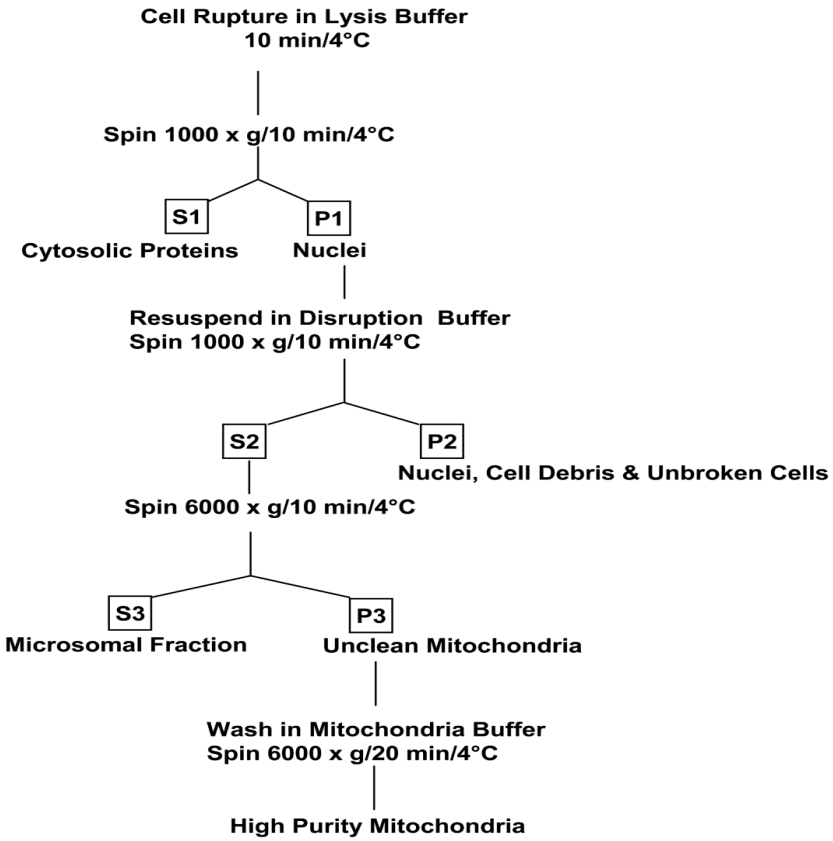

Fig 2.1 Small scale biochemical cellular fractionation scheme

Final fractions used for SDS-PAGE and western blot analysis were S1 (cytosolic fraction), P2 (fraction containing nuclei, cell debris and unbroken cells) and P3 (high purity mitochondria).

Protein determination for S1, P2 and P3 each resulting from the synchronised G0, G1, S and G2/M HFF cell populations respectively was achieved by Bradford assay. Equal amounts of protein from the respective fractions of the cell cycle were used for SDS-PAGE and subsequent immunoblotting procedures.

2.3.2.2 Sub-nuclear Fractionation 1

A small-scale biochemical sub-nuclear fractionation scheme was adapted from the protocols of (Mendez and Stillman, 2000; Wysocka et al., 2001) in which the nucleus was separated from its soluble components leaving behind an insoluble pellet believed to be enriched in chromatin-nuclear matrix bound material. 4 x 10^7 HeLa cells

were harvested with a cell scraper or by trypsination and centrifuged at 200 x g for 2 min. The supernatant was discarded and the cell pellet was washed 2 times with 2 ml PBS and centrifuged like above. The pellet was re-suspended in 1 ml of buffer A (10 mM HEPES, pH 7.9; 10 mM KCl, 1.5 mM $MgCl_2$, 0.34 M sucrose, 10 % glycerol, 1 mM DTT, 1 mM PMSF and protease inhibitor cocktail from Roche Diagnostic, Germany). Triton X-100 was added to a 0.1 % final concentration. Incubation followed for 10 min on ice and centrifugation was performed at 1300 x g, 4°C for 5 min. The supernatant S1 was separated from the nuclei pellet P1. S1 was clarified by high-speed centrifugation at 20,000 x g for 20 min at 4°C and the supernatant S2 was kept that contained cytosolic proteins (**Fig. 2.2**). The nuclei pellet P1 was washed twice with 2 ml of buffer A and centrifuged at 1300 x g, 4°C for 5 min. At this stage, P1 was divided in two equal amounts of 0.5 ml (P1+/P1-) in buffer B (3 mM EDTA, 0.2 mM EGTA, 1 mM DTT, protease inhibitors as described above). P1- was lysed for 1 hr at 4°C and spinning was done at 1700 x g for 5 min at 4°C. Soluble nucleoplasmic proteins (supernatant, S3-) were separated from the pellet P3- that consisted of insoluble chromatin-nuclear matrix bound proteins.

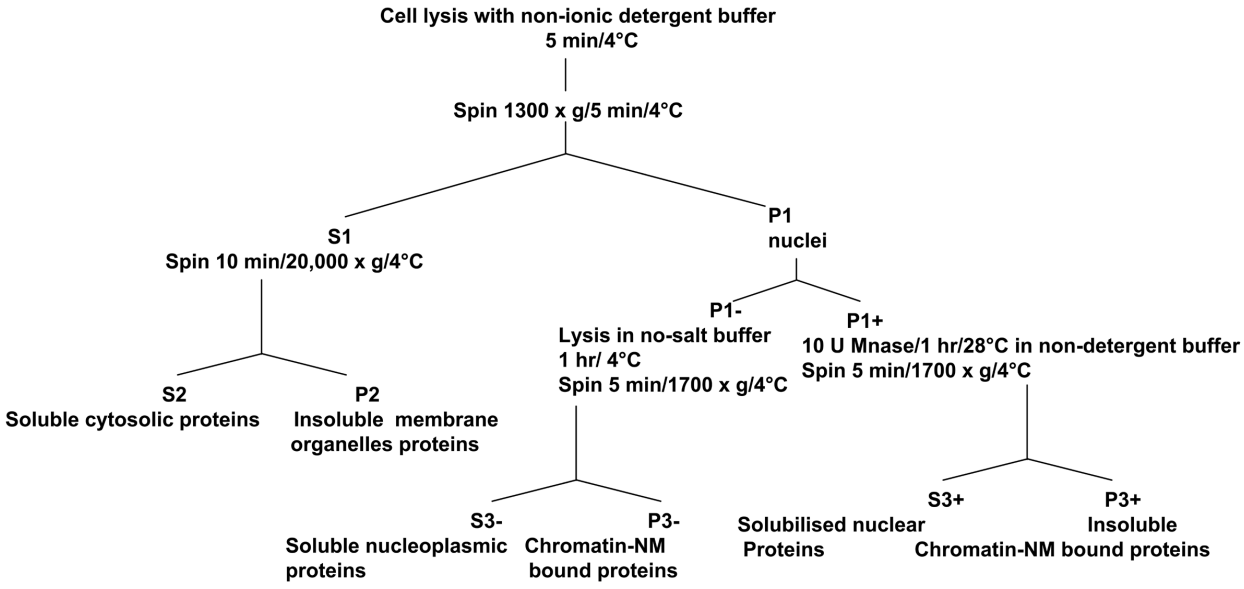

Fig 2.2 Scheme of biochemical sub-nuclear fractionation 1

Final fractions used for SDS-PAGE and western blot analysis were S1 (soluble cytosolic proteins), S3- (soluble nucleoplasmic proteins), S3+ (solubilised nuclear proteins with micrococal nuclease), P3- (chromatin-nuclear matrix bound proteins) and P3+ (solubilised chromatin-nuclear matrix bound proteins with micrococal nuclease). NM stands for nuclear matrix.

To release chromatin and nuclear matrix bound proteins, P1+ as separated above was first centrifuged at 1300 x g for 5 min at 4°C. The supernatant was discarded and the pellet was treated in 0.5 ml buffer A supplemented with 10 U of micrococal nuclease (MNase) and 0.05 M $CaCl_2$ solution for 1 hr at 28°C. MNase treatment was stopped by adding 1mM EGTA. P1+ was spun at 1700 x g, 4°C for 5 min and the supernatant S3+ believed to consist of solubilised nuclear proteins was separated from the pellet P3+ containing solubilised chromatin-nuclear matrix bound proteins. Protein determination of the isolated fractions S2, S3+, S3-, P2, P3+, and P3- was done by the Bradford method. SDS-PAGE and western blot analysis were carried out with equal amounts of the isolated fractions.

2.3.2.3 Sub-nuclear Fractionation 2

Procedures for permeabilsation and sequential small-scale biochemical sub-nuclear fractionation were adapted from the method of (Qiao et al., 2001). These procedures differed from the sub-nuclear fractionation I described above by separately enriching chromatin and the nuclear matrix. This distinction was not that clear-cut in the sub-nuclear fractionation 1 protocol.

In summary, 4 x 10^7 HeLa cells were harvested by using a cell scraper and spun at 200 x g for 2 min and the supernatant was discarded. The pellet was washed two times with PBS, pH 7.4 and spun down at 200 x g for 2 min. The re-suspension and permeabilsation of the pellet was done in 5 ml low salt lysis buffer (10 mM HEPES, pH 7.4, 10 mM KCl, 0.1 % Triton X-100) supplemented with a cocktail of protease inhibitors (Roche Diagnostics, Germany) and 1 mM PMSF for 15 min at 4°C. The permeabilised nuclei pellet (P1) was recovered at 200 x g, 5 min at 4°C and the supernatant collected was termed the cytosolic fraction, S1 (**Fig. 2.3**). P1 was washed again three times with low salt lysis buffer to remove any cytoplasmic contaminants and centrifugation was done like above. The nuclei pellet was re-suspended in 800 µl lysis buffer and separated in two equal volumes of 400 µl and termed P1- and P1+ respectively. Incubation of P1- on ice was done for 1 hr. At the same time, P1+ was treated with 30 U DNase I (RNase free, New England BioLabs, Germany) and incubated for 15 min at RT and later for an extra 15 min at 37°C. DNase I in P1+ was inactivated for 10 min at 75°C. Chromatin proteins were extracted from P1- and P1+ by adding 500 µl of extraction buffer (1 % Triton X-100, 50 mM HEPES, pH 7.4;

150 mM NaCl, 30 mM $Na_4P_2O_7 \cdot 10H_2O$, 10 mM NaF, 1 mM EDTA) containing a cocktail of protease inhibitors (Roche Diagnostics, Germany) and 1 mM PMSF, for 15 min at 4°C respectively.

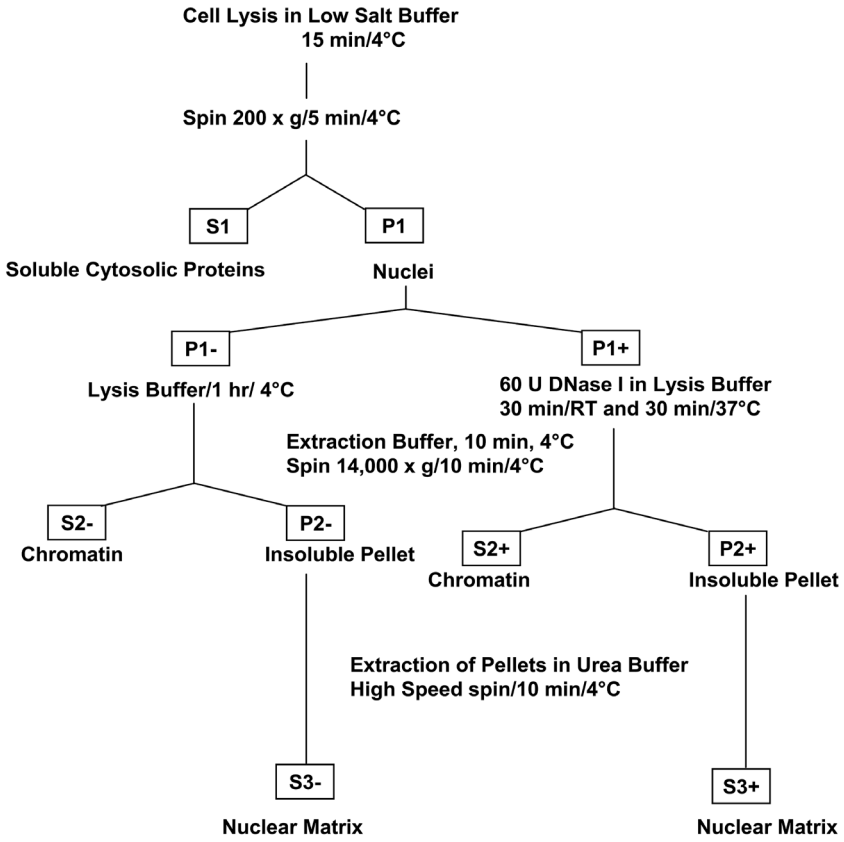

Fig 2.3 Scheme of biochemical sub-nuclear fractionation 2

Final fractions used for SDS-PAGE and western blot analysis were S1 (soluble cytosolic proteins), S2+/- (chromatin fraction treated with and without DNase I), S3+/- (nuclear matrix fraction treated with and without DNase I).

Both P1-/P1+ were centrifuged at 14,000 x g for 10 min at 4°C and the respective supernatants S2-/S2+ were collected and named chromatin fractions. The resulting pellets P2-/P2+ were solubilised in 250 µl urea buffer (8 M urea, 100 mM NaH_2PO_4, and 10 mM Tris-HCl, pH 8.0) and clarified by centrifugation at high-speed in a microcentrifuge for 10 min at 4°C. The supernatants S3- and S3+ collected respectively were called nuclear matrix fractions. Protein determination was performed by Bradford assay and equal amounts of S1, S2-/+ and S3-/S3+ were loaded on an SDS-PAGE gel for subsequent immunoblot analysis.

2.3.2.4 Fractionation of Nuclear and Nucleic Acid Binding Proteins

Qproteome nuclear subfractionation kit (Qiagen, Germany) was used for the fractionation procedure and the extraction of nucleic acid binding proteins. 4 x 10^7 HeLa cells were harvested using a cell scraper. They were washed two times with 5 ml of ice-cold PBS and centrifuged at 450 x g, 4°C for 5 min. The lysis of the pelleted cells was achieved by re-suspending them in 1 ml lysis buffer (components not disclosed by the manufacturer) supplemented with 10 µl protease inhibitor solution and 5 µl of 0.1 M DTT followed by a 15 min incubation on ice. Thereafter, 50 µl of detergent solution were added to the cell suspension and vortexed at maximum speed. The cell suspension was centrifuged for 5 min at 10,000 x g in a microcentrifuge (Eppendorf Centirfuge 5415R) pre-cooled to 4°C. The supernatant collected was termed cytosolic fraction (S1). The pellet (P1) that contained cell nuclei was re-suspended in 0.5 ml lysis buffer supplemented with 5 µl protease inhibitor solution and 2.5 µl of 0.1 M DTT by vortexing at maximum speed. Centrifugation of the nuclear pellet was done for 5 min at 10,000 x g in a pre-cooled microcentrifuge at 4°C. This step was repeated twice to remove cytosolic contaminants. The supernatants (S2) were discarded and the nuclear pellet (P2) was re-suspended in 100 µl extraction buffer supplemented with 1 µl protease inhibitor solution and incubated for 30 min with gentle agitation (750 rpm in a thermomixer) at 4°C. The nuclei suspension was centrifuged for 10 min at 12,000 x g in a microcentrifuge pre-cooled (Eppendorf Centirfuge 5415R) to 4°C. The supernatant (S3) that was believed to contain nucleic acid-binding proteins was transferred into a microcentrifuge tube. 0.3 ml of dilution buffer supplemented with 3 µl protease inhibitor solution and 6 µl of 0.1 M DTT was added to 0.1 ml of the nucleic-acid binding protein supernatant S3 (**Fig. 2.4**).

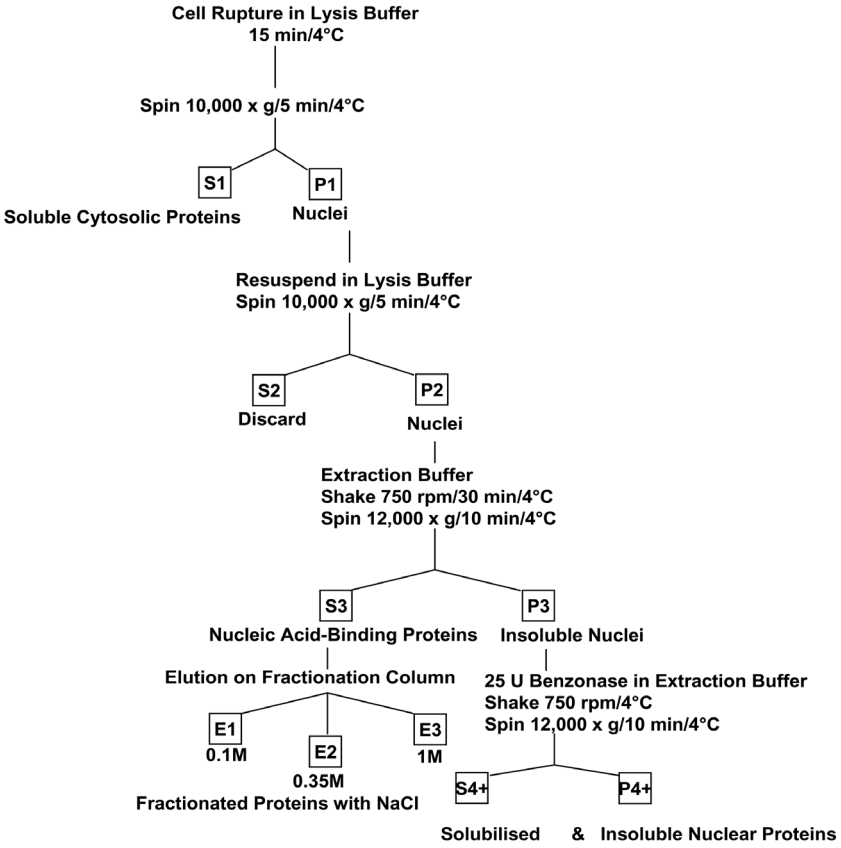

Fig 2.4 Scheme of biochemical fractionation of nuclear and nucleic acid binding proteins

Final fractions used for SDS-PAGE and western blot analysis were S1 (soluble cytosolic proteins), E1-E3 (eluted nucleic acid-binding proteins with 0.1, 0.35 and 1 M NaCl), and S4+ (solubilised nuclear proteins).

The remaining pellet (P3) was re-suspended in 0.1 ml extraction buffer that has been supplemented with benzonase, 1 µl protease inhibitor solution and the suspension was incubated by gentle agitation for 1 h (750 rpm in a Thermomixer) at 4°C. The pellet suspension (P3) was centrifuged for 10 min at 12,000 x g in a pre-cooled microcentrifuge (Eppendorf Centirfuge 5415R) at 4°C. The supernatant S4+ (solubilised nuclear proteins) obtained was stored. In order to obtain nucleic acid-binding proteins, a phospho-cellulose fractionation column was prepared by adding the re-suspended nuclear protein fractionation resin (0.4 ml) to the column and allowing it to settle. The resin was a component of the kit and it was ready for use. 0.4 ml elution buffer NE1 containing 5 µl protease inhibitor solution and 1.5 µ of 1 M DTT was added to the nuclear protein fractionation column and allowed to flow through the column by gravity. The now diluted 0.4 ml nucleic acid binding protein solution (S3) from above was poured onto the equilibrated phosphor-cellulose fractionation col-

umn. The first 0.4 ml that flew through was discarded. After this procedure, another 0.5 ml of elution buffer NE1 was given onto the equilibrated phosphor-cellulose column and the flow-through E1 was captured and stored. 0.4 ml of elution buffer NE2 also supplemented with 5 µl protease inhibitor solution and 5 µl of 1 M DTT was poured onto the column and the flow-through E2 was captured and stored as well. The last elution step was done by adding elution buffer NE3 to the column and the eluate E3 was also collected and stored. The eluates E1, E2 and E3 were concentrated and desalted by chloroform/methanol precipitation (Wessel and Flugge, 1984). Bradford assay was used to determine the concentrations of S1, E1, E2, E3 and S4+ and equal amount of protein from each of them was loaded for electrophoresis and subsequent western blotting analysis.

2.3.3 Preparation of Polytene Chromosome Squashes

Polytene chromosomes were also used as a measure to test the association of Par14 with chromatin. Polytene chromosome squashes from *Drosophila melanogaster* were prepared and kindly provided to us by Dr Corinna Schirling from the Department of Genetics at the Center of Medical Biotechnology affiliated to the University of Duisburg-Essen, Germany. For further reading on how polytene chromosomes are prepared, please refer to (Schirling et al., 2010) and *Drosophila Protocols*, eds. W. Sullivan, M. Ashburner, R. Scott Hawley, Cold Spring Harbour Press, New York, 2000.

2.3.4 Chromatin Affinity Purification (ChAP)

In order to search for the DNA-binding motifs of Par17/Par14, we employed a modified form of Chromatin Immunoprecipitation (ChIP) experiment that we termed Chromatin Affinity purification (ChAP). Here, a Par17 construct fused to *Strep*-tag II and GFP (Par17QR*Strep*-GFP) was transfected into HCT116 cells. A Par17 construct without the *Strep*-tag II but fused to GFP (Par17QR-GFP) was used as negative control. A quick overview on *Strep*-tag II has been elucidated in **Section 2.3.5.1**. This modified version of conventional ChIP experiments was a measure to circumvent large amounts of highly purified, specific and sensitive antibodies normally needed.

HCT116 cells were grown to 70 – 80 % confluency in 10 cm^2 culture dishes and transiently transfected as described in **Section 2.2.2.2**. After 2 – 3 days of transfection, the medium was aspirated and the cells were washed 2 times with pre-warmed 1x PBS. 10 ml of 1 % formaldehyde was added to the culture dishes. Incubation in 1 % formaldehyde was done at RT on a shaker for 10 and 30 min respectively. Formaldehyde was used as a cross-linking reagent. The formaldehyde solution was aspirated and cells were washed 2 times with pre-warmed 1x PBS. 1 ml of 0.125 M glycine was added to each plate and gently swirled to mix for 5 min at RT. This step served to stop the cross-linking reaction. The glycine solution was decanted and cells were washed again 2 times with pre-warmed 1x PBS. Thereafter, the cells were scrapped from the dishes using RIPA buffer (50 mM Tris-HCl, pH 8; 150 mM NaCl, 2 mM EDTA, pH 8; 1 % NP-40, 0.5 % sodium deoxycholate, 0.1 % SDS, protease inhibitor cocktail from Roche Diagnostics, Germany) and pooled in two 15 ml canonical tubes i.e. for cells transfected with Par17QR*Strep*-GFP and Par17QR-GFP constructs respectively. The cells were pelleted for 5 min at 200 x g, 4°C. The supernatants were discarded leaving behind the pellet, which could be stored at -80°C until further use. A total of 8 culture dishes were used, 4 being for the negative control.

The pellets (total cell extract) were re-suspended in RIPA buffer and incubated for 10 – 30 mins on ice. Before chromatin shearing was done, we first performed pilot experiments with untransfected cellular lysates to optimise the appropriate sonication conditions **(Fig. 3.6)**. The final sonication was done at 8 pulses for 15 sec with a 30 sec rest on ice between each pulse at 17 - 20 % amplitude (Bandelin Sonopuls HD 2200, Germany). The sheared chromatin samples were centrifuged at 12000 x g at 4°C for 10 min. The supernatants were transferred to 2 ml tubes while avoiding any pelleted material and stored either at -80°C or directly used. The reversal of the cross-linking was done by adding 4 µl 5 M NaCl and 2 µl RNase A (0.5 mg/ml) to 100 µl of each the sheared chromatin samples. They were vortexed and incubated for 4 hrs or overnight at 65°C. After this incubation procedure, the samples were briefly centrifuged for 15 sec to collect the liquid from the sides of the tube and allowed to return to RT. 5 µl of the Proteinase K (20 mg/ml) solution and 0.5 % SDS were added to each tube and incubated at 52°C for 2.5 hours. Proteinase K works at an optimum temperature of 50 – 60°C; 0.5 -1 % SDS. Proteinase K cleaves peptide bonds adjacent to the carboxylic group of aliphatic and aromatic amino acids. The

chromatin samples were ran on a 1 % agarose gel to determine the sizes of the sheared DNA. We loaded varying amounts of each sample (10 and 20 µl) to avoid overloading. The sheared chromatin samples were pre-cleared on a 1 ml engineered streptavidin (*Strep*-Tactin) hand column (IBA, Germany). The elution was done with 2.5 mM desthiobiotin. The eluates for the samples that were treated with Par17QR*Strep*-GFP and Par17Q-GFP constructs were further purified with Nucleo-Spin® Extract II (Macherey-Nagel, Germany) to obtain DNA free from proteins or any other contaminants. DNA concentrations were measured using NanoDrop ND-1000 Spectrometer (PeqLab, Germany). The respective DNA samples were cloned in to a pCR®2.1-TOPO® vector according to the manufacturer's instructions (Invitrogen, Germany).

2.3.5 Protein-Protein Interaction Studies

2.3.5.1 Background to *in vivo* Protein-Protein Interaction Analysis

In living cells, protein-protein interactions are indispensible for virtually every process. The study of protein-protein interactions has become a formidable challenge in modern day biological sciences to understand the principles underpinning the concerted action of proteins in time and space that elicit cellular functions. The interactions of proteins could be transient or stable in which they form a complex. A protein may be a carrier of other proteins as it is the case of importins, which translocate between the nucleus und the cytoplasm. Another form of interaction is the case in which kinases or phosphotases add or remove phosphate groups from proteins thus modifying them. These modifications usually lead to change in their interaction patterns with other proteins and thus elicit different signal transduction pathways. For these reasons, the interactome can be a very dynamic network of protein complexes with changing compositions strictly depending on the given physiological state (One-*STrEP*-tag and *Strep*-tag® comprehensive manual, Version PR27-0001; IBA Bio-Tagnology, Germany).

In our quest for interaction partners of Par14/Par17, we made use of the *Strep*-tag II/*Strep*-Tactin system. The *Strep*-tag II is a short peptide of 8 amino acid residues (Trp-Ser-His-Pro-Gln-Phe-Glu-Lys) with a molecular weight of approximately 1 kDa that binds to an engineered streptavidin called *Strep*-Tactin. We used *Strep*Trap HP

that is a ready to use 1 ml column pre-packed with *Strep*-Tactin sepharose (GE-Healthcare, Germany). The binding between *Strep*-Tactin and *Strep*-tag II is reversible and elution of our *strep*-tagged II protein was enabled by competitive binding with desthiobiotin, a derivative of biotin, which is the natural occurring binder to streptavidin (Schmidt and Skerra, 2007). One of the strengths of *strep*-tag II lies in its small size making it not to hamper protein folding and thus not interfering with the function of the protein in question. *Strep*-tag II is also biochemical inert, hence rendering the use of buffers at physiological condition possible. *Strep*-tag II has been successfully applied in the identification of protein interaction partners, (Junttila et al., 2005; Witte et al., 2004) and this gave us the credibility to use it for the search of binding partners of Par14/Par17.

2.3.5.2 Search of Interaction Partners of Par14/17 using the *Strep*-Tag II/*Strep*-Tactin System

This protocol describes the approach used to search for potential binding partners of Par14/Par17 in the cell. *Strep*-tag II and *His*-tag were fused to Par17QR in a vector carrying the coding sequence of the GFP reporter gene. The construct was defined as Par17QR*Strep*-GFP. As a negative control, Par17QR in the GFP vector was used devoid of tags (Par17QR-GFP). Both constructs were transfected in HCT116 cells, and the gene products were expressed at least for 48 hrs and up to 72 hrs. The cellular lysates were prepared as described in **Section 2.2.2.3**. Before loading the transfected HCT116 lysates on the 1 ml *Strep*Trap HP column, the lysates were concentrated to a volume of 1 ml each using a 15 ml Amicon® 3,000 MWCO Ultra-15 centrifugal device (Millipore, Germany). The 1 ml from each lysate was diluted to an end volume of 2 ml with 1 ml of binding buffer (100 mM Tris-HCl, 1 mM EDTA, pH 8.0).

For the remaining part of the affinity purification procedure and regeneration of the 1 ml column, ÄKTApurifier 10/100 UPC-900 (GE Healthcare, Germany) was used. The column was mounted as recommended in the manufacturer's handbook. The column was equilibrated with 10 column volume (1 column volume = I ml) of binding buffer (100 mM Tris-HCl, 1 mM EDTA, pH 8.0) at 1 ml/min. The lysate of Par17QR*Strep*GFP was applied on the column using a syringe fitted to luer adapter. The column was washed with 20 column volumes until no material appeared in the effluent. A step gradient elution with 50, 150, and 500 mM NaCl was done. This was

a measure applied to investigate if the protein-protein interactions were electrostatic in nature. When the salt elution was done, the column was washed again with 10 column volumes of binding buffer which was salt free. Elution with 2.5 mM desthiobiotin in elution buffer (100 mM Tris-HCl, 150 mM NaCl, 1 mM EDTA, pH 8.0) was performed with 20 column volumes. The column was regenerated with 10 column volumes of double distilled water followed by 10 column volumes of 0.5 M NaOH and again with 10 column volumes of double distilled water. Salt and desthiobiotin elutions and the regeneration step were done at 1ml/min at 4°C. Before use, the column was first flushed again with binding buffer and the lysate of Par17QR-GFP was loaded upon, and the purification cycle was repeated as described above. 2 ml of flow-through, wash-through, salt and desthiobiotin-eluted fractions for both lysate types were collected and stored at -20°C until the analyses with SDS-PAGE and silver staining were conducted.

2.3.6 SDS-PAGE and Immunoblotting

SDS-PAGE and immunoblotting were carried out according to standard protocols with the following notations. After determining the protein concentrations by the Bradford method using a BioPhotometer (Eppendorf, Germany), 30 µg protein per lane except otherwise stated and 3 µl of Prescision Plus Protein Standards Dual Colour protein ladder (Bio-Rad, USA) were separated by SDS-PAGE (Laemmli, 1970). The protein samples were re-suppended in sample buffer consisting of 10 mM Tris-HCl, pH 7.6; 0.5 % (w/v) sodium dodecylsulphate (SDS), 25 mM dithiothreitol (DTT), 10 % (w/v) glycerol, 0.018 mg/ml bromophenol blue and boiled at 95°C for 5 min. Electrophoretic separation was carried out for about 2 hrs at 125 V in a Novex MiniCell Chamber (Invitrogen, Germany). Thereafter, the protein samples were resolved on 12.5 or 15 % SDS-PAGE gels. Blotting was done on a nitrocellulose membrane (Invitrogen, Germany) in transfer buffer (25 mM Tris-HCl, pH 8.0 – 8.3, 192 mM glycine, 20 % methanol) at 30 V for 1 hr using the semi-dry Fastblot apparatus (Biometra, Germany). The gel left after transfer was subsequently stained with Coomassie Brilliant Blue R 250 (0.5 mg/l in 40 % methanol and 10 % acetic acid) for 30 min under gentle agitation. The gels were de-stained overnight under agitation with 40 % methanol and 10 % acetic acid and scanned. Images were stored in TIFF format at a resolution of 300 dpi.

Blocking of the membrane to minimise non-specific binding of the antibody was done for 1 hr in TBST-150 buffer [(50 mM Tris-HCl pH8.0, 150 mM NaCl; 0.3 % (v/v) Tween; 3 % (w/v) milk powder (Instant-Magermilchpulver, Granovita, Germany)] at 4°C and incubated with the respective antibody overnight at 4°C on a end-over-end roller. Washing of the membranes after incubation with the primary antibody was first done in 5 ml TBST-500 buffer (50 mM Tris-HCl pH8.0, 500 mM NaCl; 0.3 % (v/v) Tween) for 5 min and later in 5 ml TBST-150 buffer like above with the exception of milk powder. The latter washing step was repeated for a second time. The washings took place at 4°C on a shaker and they served as a measure to wash off excess unbounded primary antibody. Anti-rabbit horseradish conjugated secondary antibody from donkey or anti-goat horseradish conjugated secondary antibody from sheep (Amersham Biosciences, UK) were used at a 1:2000 dilution in TBST-150 buffer in 3 % powdered milk and incubated for 2 hrs at 4°C. The membrane was washed again 3 times for 5 min in 5 ml TBST-150 buffer in the absence of 3 % powdered milk. Immunoreactions were visualised with use of an enhanced chemiluminescence (ECL western blot reagents) kit followed by exposure on CL-XPosure Film (Thermo Scientific, Germany). Protein bands on the film were developed using the AGFA Curix 60 developer (AGFA, Germany). The films were scanned and stored. The images were saved in TIFF format at a resolution of 300 dpi.

Used membranes were stripped-off of antibodies when necessary with stripping buffer (0.05 M glycine, pH 2.5, 1 % SDS, 1 mM EDTA) for 30 mins at RT under gentle agitation on a shaker. They were washed 2 times with 2 ml TBST-150 buffer for 2 mins and were ready for use.

2.3.7 Silver Staining

Silver staining is about 10 – 100 times more sensitive than various staining techniques like coomassie blue stain. It is a staining technique with a detection level down to 0.3 – 10 ng (Switzer, III et al., 1979). The basic mechanism behind this method is that silver ions will react with the carboxyl and sulfhydryl groups of proteins and can be visualised after a reduction step with chemical reagents. The location of the proteins bands are visualised as bands where the reduction occured.

The silver staining protocol described here was adapted from Mortz and colleagues (Mortz et al., 2001). 15 µl of each eluate obtained from the *Strep*-tag II pull-down assays mixed with sample buffer were ran on 12.5 or 15 % SDS-PAGE gels and the conditions for protein electrophoresis were the same as described in **Section 2.3.6**. At the end of each run, the gels were removed from the glass plates and washed in deionised water for 5 min. Each gel was soaked overnight in 100 ml l fixing solution (50 % ethanol, 12 % acetic acid and 0.0185 %, (v/v) 37 % formaldehyde) with gentle agitation on a shaker. The fixing solution was discarded and the gel was washed 3 times with 100 ml of 50 % ethanol for 20 min. The gel was pre-treated in 50 ml sensitisation solution (0.02 %, sodium thiosulfate pentahydrate) for 1 min. Washing was done 3 times with deionised water for 20 sec and this was followed by impregnating the gel with 50 ml silver nitrate solution (0.02775 %, (v/v) 37 % formaldehyde, 0.2 % silver nitrate) for 30 min with shaking to avoid unequal background. The silver nitrate solution was discarded and the gel was washed with deionised water 3 times for 20 sec. After washing with deionised water, the protein bands on the gel were developed by soaking the gel in 50 ml developing solution (6 % sodium carbonate, 0.0185 %, (v/v) 37 % formaldehyde and 0.0005 % sodium thiosulfate pentahydrate) for approximately 2 - 5 min until staining was sufficient. The developing solution was decanted and the reaction was quickly stopped by soaking the gel for 10 min in 50 ml stopping solution (50 % methanol and 12 % acetic acid). The gel was washed again in deionised water for 10 min and it was ready for scanning and stored in TIFF format at a resolution of 300 dpi.

Emphasis was made on the following:

1) All solutions were prepared fresh before use in clean glasswares using deionised water.
2) The protocol described above was used for the silver staining as depicted in **Fig. 3.13** and **Fig. 3.14**. This protocol differed with the silver staining that was compatible for mass spectrometry analyses. Under the supervision of Dr Barbara Sitek at *Medizinisches Proteom-Center* affiliated to the Ruhr University of Bochum, Germany, mass spectrometry compatible silver staining experiments were performed **(Fig. 3.15).**
3) Our protocols differed with that from the *Medizinisches Proteom-Center* in the composition of some of the solutions. For the differences refer to **Table 2.5**.

The chemicals that they used were of analytical grade and the gels were handled with powder-free gloves. These measures were done to minimise contamination with keratin since they could lead to false positives in protein identification by tandem mass spectrometry.

Table 2.5 Comparison of our in-house protocol with mass spectrometry compatible protocol used for identification of Par14/Par17 interaction partners

Solutions	In-House Protocol	Mass Spectrometry Compatible
Fixing solution	50 % ethanol, 12 % acetic acid, 0.0185 %, (v/v) 37 % formaldehyde	50 % Ethanol, 10 % acetic acid
Sentisation Solution	0.02 %, sodium thiosulfate	30 % ethanol, 500 mM sodium acetate, 8 mm sodium thiosulfate
Silver Nitrate Solution	0.02775 %, (v/v) 37 % formaldehyde, 0.2 % silver nitrate	0.01 % (v/v) 37 % formaldehyde, 6 mM silver nitrate
Developing Solution	6 % sodium carbonate, 0.0185 %, (v/v) 37 % formaldehyde and 0.0005 % sodium thiosulfate	236 mM sodium carbonate, 0.01 % (v/v) 37 % formaldehyde
Stopping Solution	50 % methanol and 12 % acetic acid	50 mM EDTA, pH 8.0

2.3.8 Tandem Mass Spectrometry Analysis

As already mentioned, mass spectrometric analyses were done at the *Medizinisches Proteom-Center* affiliated to the Ruhr University of Bochum, Germany under the direction of Dr Barbara Sitek and she provided us the following protocol.

Bands of interest were manually cut out of the preparative silver stained gels. The bands were digested with trypsin (Promega, Germany) in-gel, and later extracted from the gel. Protein-derived peptides were analysed by LC-MS/MS in an ESI-QTOF mass spectrometer (micrOTOF Q, Bruker Daltonics, Germany) connected online with a nanoflow HPLC (Ultimate 3000, Dionex, Germany). The reversed phase columns (75 µm ID, 150 mm length; Acclaim C18 PepMap Material) were ran at a flow rate of 300 nl/min after flow splitting. In order to improve reproducibility after 10 min preconcentration on a 2 cm pre-column (same specifications as analytical column ex-

cept 100 µm ID) gradient elution was applied from 12 % B to 85 % C (C=35 % ACN, 0.1 % FA) in 120 min followed by a ramp to 90 % B (B=84 % ACN, 0.1 % FA) over 25 min followed by column re-equilibration for 30 min.

The mass spectra were acquired in the 100-2000 m/z range with an online nanospray-source set to 1400 V capillary voltage and nitrogen dry gas flow to 6.0 l/min at 140°C. Each MS-scan was followed by MS/MS-experiments of the three most intense ions under varying collision RF values from 800 to 250 Vpp during fragmentation, with overall duty cycle times between 3.6 and 5.4 s depending on precursor ion intensity.

For protein identification, un-interpreted ESI-MS/MS-spectra were correlated with the IPI-protein sequence human sub-database (v3.41 Human, 72155 proteins) applying the Mascot (v.2.2.0) algorithm (Perkins et al., 1999). Proteins were considered as identified when either two peptides were explained by the spectra, with a Mascot Score higher than 22.5 or 1 peptide was explained by the spectra, with a Mascot Score higher than 70.

2.4 Par14/Par17 Gene Knock-Down Experiments

Over the last decade, RNA interference (RNAi) has been used as a powerful tool to study gene function. It is a phenomenon that small double-stranded RNA also known as small interfering RNA (siRNA) can post-transcriptionally prevent the expression of a gene product. Here, one of the double-stranded siRNAs is complementary to the target gene mRNA. Concomitant with the other cellular-based processes, the complementary strand will bind to the cognate mRNA that will lead to its cleavage and destruction, thus initiating a temporary knock-down of the gene and its cognate protein will not be expressed. Several authors have reviewed the mechanism of siRNAs and other small interfering RNA molecules, which can also initiate gene knock-down (Grimm, 2009; Scherr and Eder, 2007; Shabalina and Koonin, 2008).

We used two variations of the siRNA technology to induce gene knock-down of Par14/Par17. The first variation was the use of synthetic double-stranded siRNAs. We ordered four double-stranded synthetic siRNAs in a pool that were Par14/Par17-specific (Dharmacon, Germany). Their sequences can be seen on **Table 2.3** (siRNA-

1, siRNA-2, siRNA-3 and siRNA-4). A negative control non-targeting siRNA was also ordered. The sequence of the negative control siRNA was scrambled so that it had no homology to any human gene. Also ordered was a transfection indicator referred as siGLO green. It is a fluorophore with an absorption maximum at 488 nm and emission maximum at 518 nm. The siRNAs were re-suspended according to the protocol of the manufacturer and aliquots were stored at -80°C until use. For best results, we limited freeze thawing for each aliquot to five events and gloves were worn to maintain a nuclease-free working condition. Synthetic siRNAs are susceptible to enzymatic degradation by nucleases.

HeLa cells were grown and cultured as described in **Section 2.2.21**. They were co-transfected with the pool of Par14/Par17-specific siRNAs and the siGLO transfection indicator. They were transfected at a 1:1 ratio to a final concentration of 100 µM in 12-well plates. This was the highest concentration recommended by the manufacturer. Sterile cover slips (15 x 15 mm or 18 x 18 mm; Menzel-Gläser, Germany) were first placed on the wells before growth and transfection of HeLa cells. DharmaFECT siRNA transfection reagent (Dharmacon, Germany) was used for lipid-mediated delivery and the instructions of the manufacturer were followed. The duration of transfection lasted for 24 to 96 days. After transfection stop, the cells were washed 2 times with 1 ml of pre-warmed PBS, pH 7.4.

In order to check transfection efficiency and to visualise any morphological aberrations that cells might have incurred in the event of a Par14/Par17 knock-down, they were stained either with propidium iodide (PI) or DAPI as dyes that stain nuclear DNA. Stock solutions of either dye were made to 5 mg/ml and diluted with culture medium to a working solution of 200 nM. 300 µl of the pre-warmed DAPI or PI working solution was given to the each well and incubated for 1- 5 min at RT. Thereafter, the cells were washed 3 times with 1 ml of pre-warmed PBS, pH 7.4. Fixation was done with 0.5 ml PBS, pH 7.4 containing 3 % paraformaldehyde for 5 – 10 min at RT. Cells were washed again 3 times with PBS, pH 7.4. The cover slips-containing cells were semi-dried by exposing them in the air. They were carefully removed from the wells and embedded on a microscope slide on which 20 µl of mowiol (polyvinylalcohol) (Sigma, Germany) had been placed on. At this stage, the cover slips were

sealed to the microscope slides with nail polish and stored in darkness at 4 °C. Microscopic observations were done with an Olympus BX61 Fluorescence Microscope. Vector-based siRNA technology was the second variation of RNAi that we employed to elicit Par14/Par17 gene knock-down. Here, we designed 3 small DNA inserts which encoded short hairpin RNAs (shRNA) targeting Par14/Par17. The DNA inserts each of 76 bp were cloned into pRNTin-H1.2/Hygro vector with an inducible H1 promoter containing a tetracycline operator (TetO1). The cloning was done by GenScript, USA. The sequences of the shRNAs used have been listed on **Table 2.3** (shRNA-1, shRNA-2 and shRNA-3). A shRNA for luciferase was cloned into the vector pRNATin-H1.3/Hygro/siFluc and was used as non-targeting negative control. Both vectors embodied the GFP gene, whose gene product was used to test for transfection efficiency. The luciferase construct was referred to as shRNA-Luc. The sequence of siRNA-3 from the pool of the double-stranded siRNA overlapped with the sequence of shRNA-2. One of the advantages of using vector-based siRNA technology is that a stable cell line can be established and long-term effects of RNAi can be studied (Brummelkamp et al., 2002; Sui et al., 2002).

HeLa cells were grown and cultured as described in **Section 2.2.21**. The short hairpin constructs were propagated using NucleoBond^{R} Xtra Midi kit (Macherey-Nagel, Germany) and subsequently transfected using the transfection reagent, nanofectamin (PAA, Germany). The instructions of the manufacturers were strictly adhered too. Transfection was done in 12-well plates containing sterile cover slips. Transfection was stopped after 24 to 96 hrs. Before microscopic analyses, the cells were stained, fixed with 3 % paraformaldehyde and embedded in mowiol in the same way as was with the case with cells treated with Par14/Par17-specific synthetic siRNAs.

Par14/Par17 gene knock-down effects were not only verified on the basis of morphological phenotypes but also at the protein level. Transfected HeLa cellular lysates from both Par14/Par17-synthetic siRNAs and from Par14/Par17-short hair pins were processed for SDS-PAGE and western blot procedures in the same manner as described in **Section 2.3.6**. An antibody against the PPIase domain for Par14/Par17 (αPPIase) was used to detect the extent of knock-down of both proteins.

Also to investigate the level of knock-down, qRT-PCR was used. In this instance only the Par14/Par17-shRNAs were used and transfection was performed as described before in HCT116 cells. 12-wells plates were used and transfection was done for triplicates per shRNA. Duplicates of the C_t values were performed for each well. Quantitative RT-PCR could not be performed using the pool of Par14/Par17-synthetic double-stranded siRNAs because they ran out of stock and cost was a limiting factor for re-purchasing. The qRT-PCR procedure carried out has been elucidated in **Section 2.2.1.1**.

Calculation of the percentage knock-down (KD) for example for Par14 was done by comparing the expression of Par14 in the wells transfected with one of the shRNAs (e.g. shRNA-1) with the expression of Par14 in untreated cells after normalisation with the expression of the housekeeping genes (HKG) in both of the cells transfected with shRNA-1 and in untreated cells to account for any difference in cell number and transfection efficiency between the wells. The following formula was used:

$$\%\ KD\ Par14\ shRNA1\ = [1 - (Av\ of\ Av\ Ct\ Par14\ shRNA - 1)/(Av\ of\ Av\ HKGs\ shRNA1\ ) \times (Av\ of\ Av\ Ct\ HKGs\ untreated)/(Av\ of\ Av\ Ct\ Par14\ untreated)] * 100$$

Av of Av C_t Par14 shRNA-1: average of the average of the average of duplicate C_t values of the expression of Par14 from triplicates treated with shRNA-1
Av of Av HKGs shRNA-1: average of the average of the average of duplicate C_t values of the expression of GADPH and ribosomal protein L13A from triplicates treated with shRNA-1
Av of Av C_t HKGs untreated: average of the average of the average of duplicates C_t values of the expression of GAPDH and ribosomal protein L13A from untreated triplicates
Av of C_t Par14 untreated: average of the average of the average of duplicates C_t values of the expression of Par14 from untreated triplicates

The % KD for Par17 with the different shRNAs was calculated using the same formula and logic.

2.5 Microscopy Techniques

2.5.1 Immunostaining- and fluorescence of Polytene Chromosome Squashes

Slides on which polytene chromosomes have been embedded upon were taken out of 80 % ethanol and placed in 40 % ethanol for 10 min. Following this, the slides were immersed in 5 % anti-goat serum in buffer A (150 mM Tris-HCl, pH 7.4; 600 mM KCl, 150 mM NaCl, 5 mM Spermidin, 1.5 mM Spermin) for blocking purposes for a duration of 1 hr. The slides were then removed and immersed again 2 times in buffer A for 10 min. This step served as a washing procedure. Dilutions of 1:3000 (30 µl) of 5 % anti-goat serum in buffer A for preimmune serum of the PPIase domain of Par14/Par17, affinity chromatography purified final immune serum of αPPIase and αHistone H3 (Abcam, UK) were given to each slide respectively and incubated overnight at 4°C. Washing of the respective slides was done twice in buffer A after incubating them for 10 min. The slides were then labelled with 30 µl of anti-rabbit, Alexa Fluor 514 at 1:3000 (A31558 Invitrogen, Germany) using the same procedure as for the primary antibody labelling for 3 hrs at RT. This was followed by washing the slides twice for 10 min in buffer A. The slides were removed and immersed in 0.25 ml buffer A containing 0.1 µg/ml DAPI as a DNA counter stain for 5 - 10 min. Before embedding the slides in 87 % glycerol and 2 % propyl gallate, they were briefly washed in Buffer A again. Each slide was sealed with a cover slip using nail varnish before microscopic examination or storage at -20°C.

2.5.2 Indirect Immunofluorescence of Polytene Chromosome Squashes

The evaluation of the polytene chromosome squashes was carried out using Olympus BX61 fluorescence microscope having a F-View II camera and the Cell^P software (Olympus, Hamburg), a UPlanSApo 100x objective and a U-M41002b filter (excitation 545 +/- 30 nm, emission 610 +/- 35 nm for AlexaFluor 514 (PI) and excitation 480 +/- 10 nm, emission 520 +/- 20 nm for DAPI). The exposure time for AlexaFluor was 50-60 ms and 500-600 ms for DAPI.

2.5.3 Fluorescence of siRNA and shRNA treated HeLa Cells

The same Olympus microscope was used as in **Section 2.5.2** for the visualisation of siRNAs and shRNAs transfected HeLa and HCT116 cells. UPLAFL N 60x objective was used and the excitation and emission wavelengths for PI and DAPI were the

same as in **Section 2.5.2**. For GFP, we used an excitation of 480 nm and an emission of 510 nm.

3. Results

Here, the findings of the affinity purification of αPPIase and αPar17-Ext antisera will be presented. Also, the outcomes of the various biochemical fractionations, Chromatin Affinity Purification (ChAP) and indirect immunofluorescencence of polytene chromosomes experiments performed will be put into perspective. Furthermore, a critical look will be taken at the transcriptional/translational regulation of Par14/Par17 in the course of the cell cycle, and the data obtained from the search of potential interactors of Par14/Par17 by means of affinity purification coupled with mass spectrometry. Above all, an appraisal of the data generated from the Par14/Par17 knockdown experiments by means of siRNA-technology will be done.

3.1 Affinity Purification of Antibodies αPPIase and αPar17-Ext

In preparation of the cellular and sub-nuclear biochemical fractions, it was advisable to work with highly sensitive and specific antibodies for Par14 and Par17. After the production of the antisera of the PPIase domain of Par14/Par17 and the N-terminal extension of Par17, we affinity purified both antisera as described in Materials and Methods **(Section 2.3.1)**. Western blot analyses were done to validate the efficiency of the purification **(Fig. 3.1)**. Affinity-purified αPPIase was used on total cell extract (TCE) and recombinant Par14 (rhPar14) for immunoblotting **(Fig 3.1A)**. For αPar17-Ext, we used TCE and the lysate from recombinant Par17 *E. coli* expressing cells **(Fig. 3.1B).**

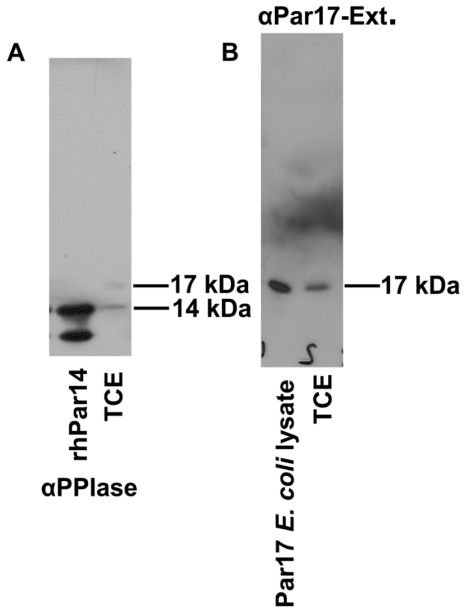

Fig 3.1 Affinity-purified αPPIase and αPar17-Ext

A) Recombinant Par14 (rhPar14) and total cell extract (TCE) from HeLa cells were used to determine the specificity of affinity-purified αPPIase. **B)** Cell lysate from *E. coli* expressing recombinant Par17 (Par17 E. coli Lysate) and total cell extract (TCE) from HeLa cells and were used to determine the specificity of affinity-purified αPar17-Ext 20 µg of TCE, 300 ng of Par17 *E. coli* lysate and 100 ng of rhPar14 were used respectively. Both affinity-purified antibodies were used at a 1:1000 dilution.

Affinity-purified αPPIase and αPar17-Ext were used at a final concentration of 1.74 ng/µl and 3 ng/µl respectively (1:1000 dilution). We acknowledged the presence of 14 and 17 kDa bands that corresponded to the molecular weights of Par14 and Par17 upon use with the αPPIase **(Fig. 3.1A)**. The band underneath rhPar14 was justified by proteolytic degradation suffered by the recombinant protein. We also saw a band of 17 kDa that reflected the molecular weight of Par17 when αPar17-Ext was used **(Fig. 3.1B)**. From the western blots using both affinity-purified antibodies, we saw only the signals of the proteins (Par14 and Par17 respectively) that they detected. This implied that the problem of unrelated proteins being detected was addressed.

In this work, we used the affinity-purified αPPIase antibody for western blot analyses for the fractions obtained from the sub-nuclear fractionation 2 **(Section 3.2.2**), the fractionation of nuclear and nucleic acid-binding proteins **(Section 3.2.3)** and lysates from the phases of the cell cycle for the detection of Par14 **(Section 3.3.2)**. The immunostainings of polytene chromosome squashes **(Section 3.2.4)** were also done with the purified αPPIase. The analyses of cell cycle phases lysates and the subse-

quent cellular fractionation of the respective phases of the cell cycle were performed with the purified αPar17-Ext for the detection of Par17 **(Section 3.3.3)**.

3.2 Par14, Chromatin and DNA-Binding *in vivo*

3.2.1 Sub-Nuclear Localisation 1 of Par14

One of the aims of this thesis was to characterise the sub-nuclear localisation of Par14. HeLa cells were employed for the biochemical fractionation procedures explained in Materials and Methods **(Section 2.3.2)**. Our first strategy was to fractionate the nucleus in a manner in which chromatin-nuclear matrix bound proteins will be isolated. For this goal, we adapted two nuclear fractionation protocols that served to address this question (Mendez and Stillman, 2000; Wysocka et al., 2001) as described in **Section 2.3.2.2**.

Fractions S2 (soluble cytosolic proteins), S3- (soluble nucleoplasmic proteins), S3+ (solubilised nuclear proteins with MNase), P3- (chromatin-nuclear matrix bound proteins) and P3+ (solubilised chromatin-nuclear matrix bound proteins with MNase) together with total cell extract (TCE) and recombinant Par14 (rhPar14) were ran on a 12.5 % SDS-PAGE gel **(Fig. 3.2A)**. TCE and rhPar14 were used as endogenous and exogenous positive controls for Par14. For fraction S3+, almost no nuclear proteins were retrieved when treated with MNase. This can be due to the fact that the treatment with MNase yielded no effect to release nuclear proteins. The gel also revealed that the loading was more or less constant although there was a slight discrepancy in the amount of protein found in P3+ as in P3- **(Fig. 3.2A)**. The samples analysed showed to an extent a non-homogenous protein separation pattern. We argue this on the grounds that these fractions contained proteins obtained from different cellular locations, thus the heterogeneity of the separation pattern. The lane for rhPar14 was virtually empty because only 50 ng was loaded but it was sufficient for the detection with the αPPIase antibody by western blotting.

When the SDS-PAGE was over, the gel was transferred to a nitrocelluse membrane for immunoblotting. We saw a Par14 signal for the recombinant Par14 sample. This is the upper band and not the lower band **(Fig. 3.2B)**. The upper band should be linearly viewed from right to left until we arrive at the band of the TCE as llustrated by

the red horizontal line. This is the convention we shall use in this section to determine whether or not Par14 band signals were present in the various isolated and analysed fractions. The lower band resulted from proteolytic degradation **(Fig. 3.1A)**.

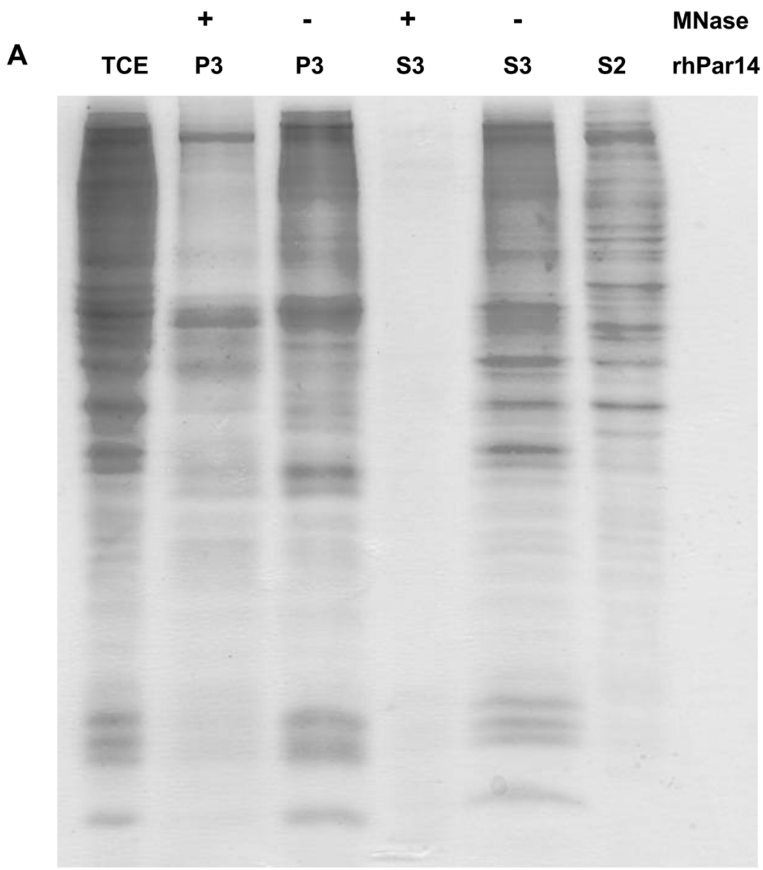

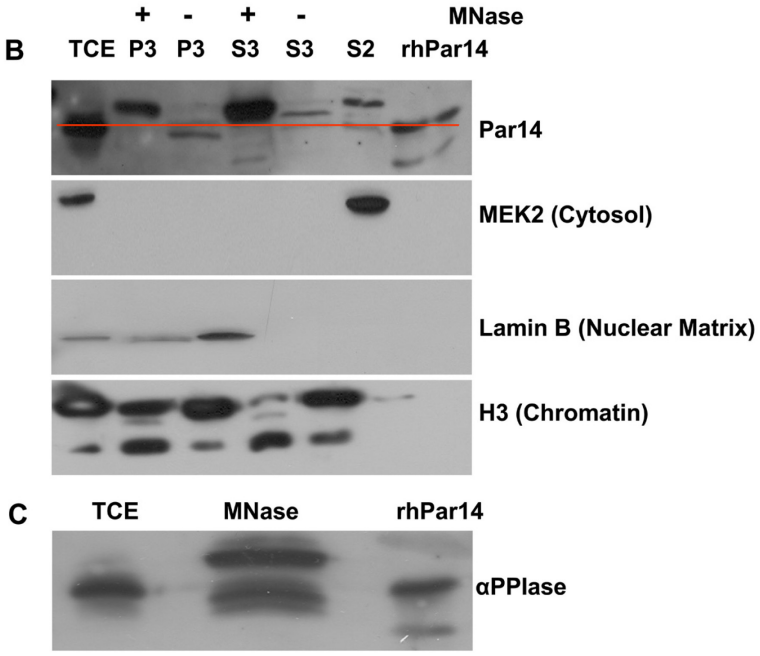

Fig 3.2 Par14 is present in chromatin-nuclear matrix bound fractions.

A) An asynchronous culture of HeLa cells was subjected to biochemical fractionation **(Section 2.3.2.2)**. After cell lysis, S2 (soluble cytosolic proteins) was obtained by centrifugation. The nuclei were divided in two equal aliquots. One of them was incubated for 1 hr at 28°C with 10 U of micrococcal nuclease (MNase), and the other one was incubated without MNase. After this treatment, nuclei were lysed and the following fractions were obtained S3- (soluble nucleoplasmic proteins), S3+ (solubilised nuclear proteins with MNase), P3- (chromatin-nuclear matrix bound proteins) and P3+ (solubilised chromatin-nuclear matrix bound proteins with MNase). Total cell extract (TCE) and recombinant Par14 (rhPar14) were used as endogenous and exogenous positive controls for Par14. Protein-equivalent amounts (30 µg) of the final fractions apart from fraction S3+ that contained virtually no protein were ran on a 12.5 % SDS-PAGE gel. 50 ng of rhPar14 was loaded **B)** After electrophoresis, the gel was transferred to a nitrocellulose membrane for immunoblotting with αPPIase, αMEK2, αLamin B1 and αHistone H3 antisera. Antibodies were used at a 1:1000 dilution. MEK2, lamin B1 and histone H3 were used to benchmark the different fractions. **C)** αPPIase was used for an analytical blot where TCE, MNase and rhPar14 had been probed on the membrane.

A western blot signal in fraction S2 containing soluble cytosolic proteins was seen for Par14 **(Fig. 3.2B)**. This confirmed the cytosolic localisation of Par14 as previously reported (Surmacz et al., 2002). The nuclei were divided in two equal amounts after the cytosolic fraction was isolated. P3- was the fraction that resulted after no treatment with MNase and P3+ was the fraction that resulted after MNase treatment. S3- and S3+ are the supernatants that were collected after centrifugation of P3- and P3+. The aim was to release with and without MNase soluble and solubilised chromatin-nuclear matrix bound proteins. S3- was believed to contain soluble nucleoplasmic

proteins and P3- was the chromatin-nuclear bound proteins fraction. The Par14 signal for the S3- fraction was weaker than the signal in the P3- fraction. Thus, we saw a trend that Par14 is associated with chromatin-nuclear matrix bound proteins.

S3+ and P3+ were referred to as solubilised nuclear proteins and solubilised chromatin-nuclear matrix bound proteins respectively. Taking a critical look at **Fig. 3.2B**, we saw no Par14 signals for both fractions. Instead, we saw a very strong protein band signals slightly above where a Par14 signal was expected for S3+ and P3+ respectively. We were interested in these bands and conducted western blot experiments using TCE, MNase, and rhPar14 as samples and applying the αPPIase antibody at a 1:1000 dilution. We saw that this antibody detected MNase **(Fig. 3.2C)**. Therefore, the question of the occurrence of the bands was addressed. Another striking revelation was a protein signal above the Par14 signal in fraction S2. This band was also seen in the different biochemical fractionation schemes so far described in the Materials and Methods. We will refer to them where necessary in the course of this result section. The fidelity of the sub-nuclear fractionation was confirmed by the use of antibodies against MEK2 for the cytosolic fraction, lamin B1 as a marker for the nuclear matrix fraction and histone H3, which characterised the chromatin fraction. We must also say that histone H3 was also found in the other fractions. This is because histones are abundantly highly expressend proteins and are ubiquitously present in various compartments of the cell. But it is a known fact that histones form an integral part of the chromatin structure.

3.2.2 Sub-Nuclear Localisation 2 of Par14

The sub-nuclear localisation 1 described above was ambiguous to characterise Par14 to chromatin or the nuclear matrix. For this reason, we adapted a sub-nuclear fractionation protocol used by Qiao and colleagues that could highly enrich chromatin and nuclear matrix proteins (Qiao et al., 2001). A small-scale biochemical fractionation procedure of an asynchronous culture of HeLa cells was performed as described in **Section 2.3.2.3**. From the scheme, we isolated cytosolic, chromatin and nuclear matrix proteins. Fractions S1 (soluble cytosolic proteins), S2+/S2- (chromatin proteins with and without DNase I), S3+/S3- (nuclear matrix proteins with and without DNase I), together with TCE and rhPar14 were ran on a 12.5 % SDS-PAGE gel **(Fig. 3.3A)**. TCE and rhPar14 were used as endogenous and exogenous positive

controls for Par14. We saw that an almost equal amount of protein was loaded for all the fractions. The samples analysed showed to an extent a non-homogenous protein separation pattern. The hetorogeneity of the separation patterns obtained is due to the fact that these were proteins obtained from different cellular localisations in the cell. 100 ng of rhPar14 was loaded and we could see a weak band of it on **Fig. 3.3B**.

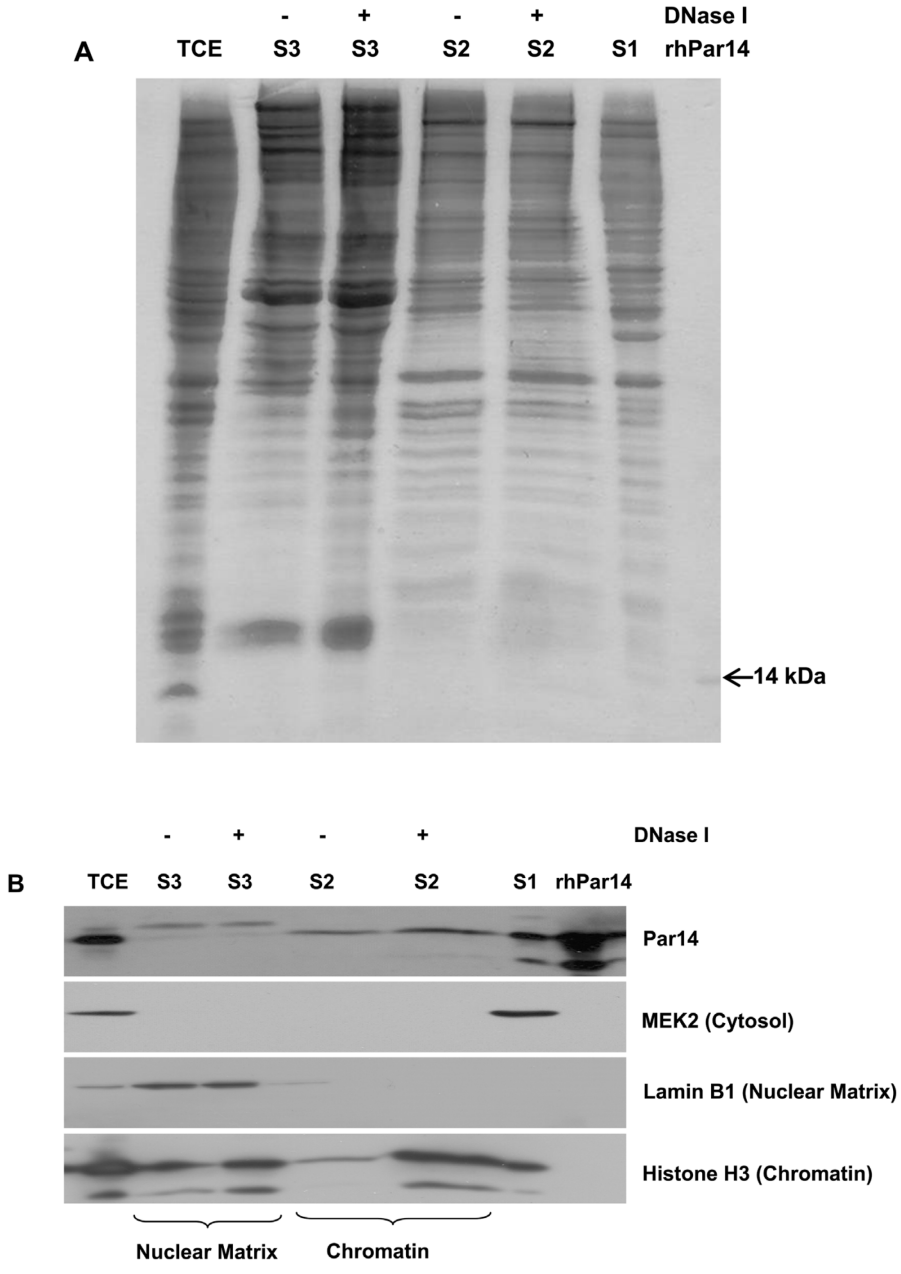

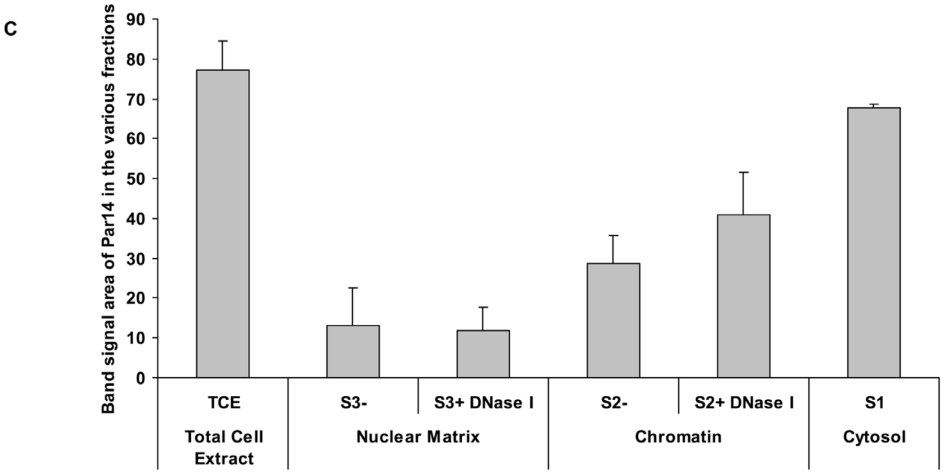

Fig 3.3 Par14 localises more to chromatin than to nuclear matrix

A) An asynchronous culture of HeLa cells was subjected to biochemical fractionation. Par14 was solubilised in the chromatin and nuclear matrix enriched fractions S2+ and S3+ respectively by treatment with DNase I as described in materials and methods **(Section 2.3.2.3)**. The distributions of different proteins in the TCE, S3+/- nuclear matrix fractions, S2+/- chromatin fractions and rhPar14 (as positive control for Par14) are shown. Protein-equivalent amounts (30 µg) of the final fractions were used for SDS-PAGE analysis. 100 ng of rhPar14 was laoded. **B)** After electrophoresis the gel was transferred to a nitrocellulose membrane for immunoblotting with αPPIase, αMEK2, αLamin B1 and αHistone H3 antisera. Antibodies were used at a 1:1000 dilution. MEK2, lamin B1 and histone H3 were used to benchmark the different fractions. **C)** Spatial distribution of Par14 in the various fractions quantified by densitometric analyses. The area of the band signals were measured and subtracted from the background signal on the blots. Multi Gauge densitometry software version 3.1 was used.

Comparing the western blot conducted and the densitogramm as shown on **Fig. 3.3B/C,** it was seen that the band area signals for Par14 in the chromatin fractions S2+ and S2- were 3- and 2-fold higher respectively than those of the nuclear matrix fractions S3+ and S3- respectively. The densitogramm shows the spatial distribution of Par14 in the various fractions **(Fig. 3.3C)**. The band signal areas were measured and corrected with the background signal on the blots using the Multiguage densitometry software. S2+ and S3+ were fractions that were solubilised with DNase I, while S2-/S3- did not undergo any nuclease treatment. Hence, we saw an appreciable enrichment of Par14 in the chromatin fractions than the nuclear matrix fractions.

To determine whether Par14 is bound to DNA, permeabilised HeLa cells were treated with DNase I for 1 hr. The first 30 mins of incubation was done at RT and the last 30 mins was conducted at 37°C. Par14 was 1.4-fold released from chromatin

when treated with DNase I as deduced from the Par14 band signal in S2+ on **Fig. 3.3B/C** as opposed to S2-. No appreciable difference of the release of Par14 could be inferred for the nuclear matrix fraction S3+ that underwent treatment with DNase I. These results indicated that Par14 was potentially chromatin-bound and was differentially released after DNase I treatment, suggesting an intimate association with DNA. Par14 has been shown to be present in the cytosol (Surmacz et al., 2002) and this we saw in S1 that reflected the proteome of the cytosol. TCE and rhPar14 were loaded to serve as endogenous and exogenous positive controls respectively for the detection of Par14 in the various fractions. The fidelity of the subnuclear fractionation was confirmed by the use of antibodies against MEK2 for the cytosolic fraction, lamin B1 as a marker for the nuclear matrix fraction and histone H3 that characterised the chromatin fraction. Histone H3 behaved in a similar way by occurring not only in the chromatin fractions as in **Fig. 3.2B**. To mention is also the fact that we saw protein band signals above the weak Par14 band signal in the nuclear matrix fractions S3+/S3-. This band was similar to what we saw in the Par14 signal in the S2 fraction in **Fig. 3.2B**.

3.2.3 Par14 binds to DNA *in vivo*

From DNA-cellulose binding assays and EMSA studies, it was demonstrated that Par14 bound to DNA *in vitro* (Kessler et al., 2007; Surmacz et al., 2002). In concert with our Par14 enrichment with chromatin and its release after treatment with DNase I as described in **Section 3.2.2**, it was mandatory to verify the *in vivo* binding of Par14 to DNA using a different biochemical fractionation approach. The Qproteome nuclear subfractionation kit from Qiagen, Germany was used whereby nuclear proteins are separated to allow for the enrichment detection of low-abundance proteins such as transcription factors. A small-scale biochemical fractionation procedure of HeLa cells was performed as described in **Section 2.3.2.4**.

From the fractionation scheme, we isolated cytosolic, nucleic-acid binding proteins and solublised nuclei. Fractions S1 (soluble cytosolic proteins), E1 - E3 (nucleic-acid binding proteins eluted with 0.1, 035 and 1 M NaCl), S4+ (nuclei solublised with bezonase) together with TCE and rhPar14 were ran on a 12.5 % SDS-PAGE gel **(Fig. 3.4A)**. TCE and rhPar14 were used as endogenous and exogenous positive controls for Par14. We saw a very little amount of proteins were eluted with

0.1 M NaCl. The band patterns of the protein samples obtained showed some discrepancies. For example, the bands on which the red lines are placed upon were a testimony of proteins that were conspicuously enriched in the S4+ fraction as opposed to the other fractions. No band was seen on the lane of rhPar14 because only 50 ng was loaded and this amount was sufficient for detection via immunoblotting.

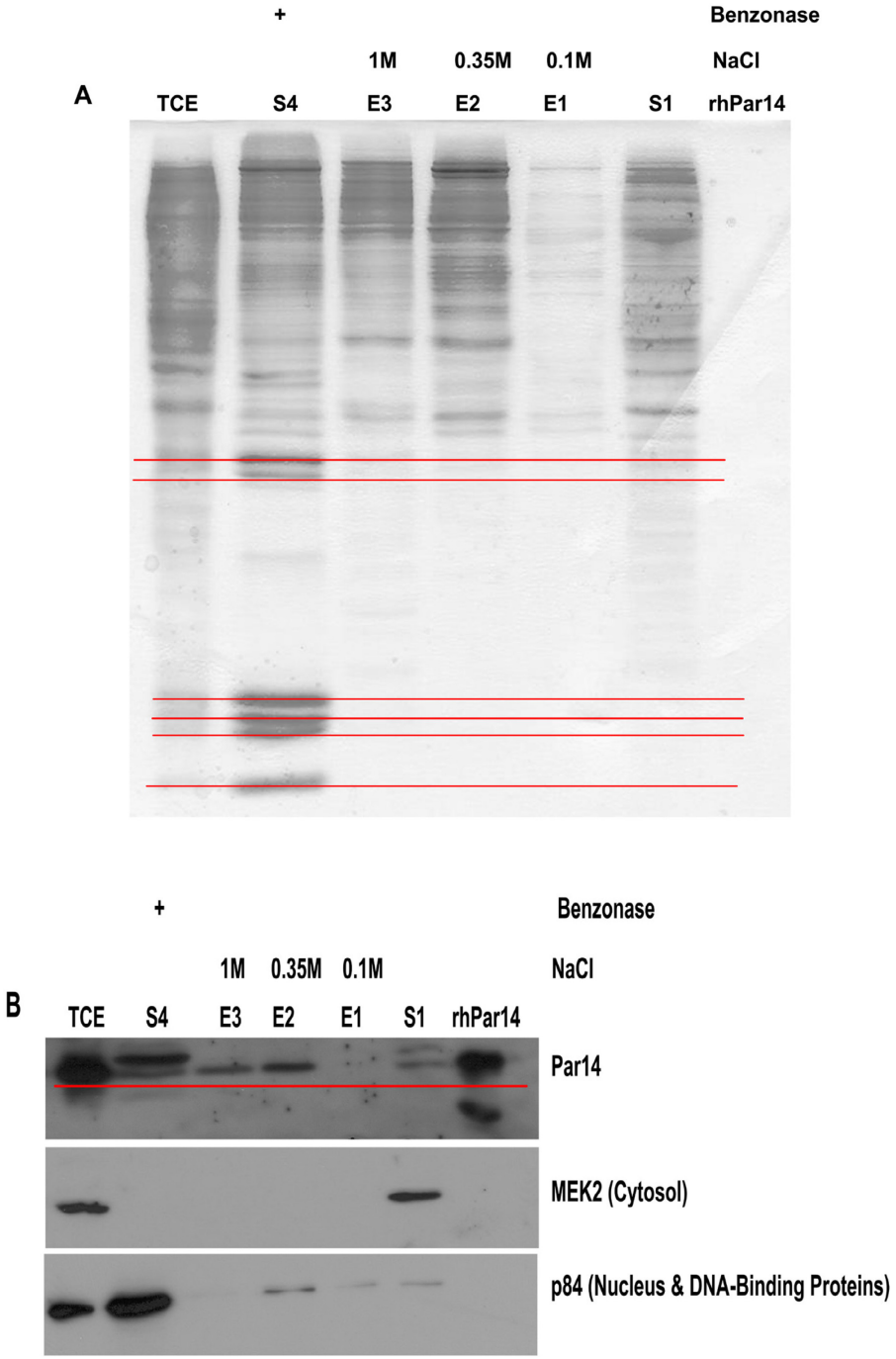

Fig 3.4 Par14 binds to DNA *in vivo* and elutes with increasing salt concentration

A) An asynchronous culture of HeLa cells was subjected to biochemical fractionation **(Section 2.3.2.4)**. The electrophorectic distributions of different proteins in the TCE, E1 - E3, nucleic acid-binding fractions; S4+, nuclei solubilised with benzonase and rhPar14 (as positive control for Par14) are shown. Protein-equivalent amounts (30 µg) of the final fractions were used for analysis. **B)** After SDS-PAGE, the gel was transferred to a nitrocellulose membrane for immunoblotting with the affinity-purified αPPIase, MEK2, and nuclear matrix protein p84 antisera. Antibodies were used at a 1:1000 dilution. MEK2 and nuclear matrix protein p84 were used as markers for the different fractions.

The nuclear and nucleic acid-binding protein fractionation scheme employed and the resulting fractions have been described in **Section 2.3.2.4**. Fraction S3 contained nucleic acid-binding proteins **(Fig. 2.4)** that was later bound on a phospho-cellulose column and eluates were collected using increasing salt concentrations (0.1, 0.35, and 1 M). Analysis of the eluates on an immunoblot showed that at 0.35 M (E2) and 1 M (E3) salt concentrations Par14 was eluted **(Fig. 3.4B)**. The red line is below of all Par14 band signals. This finding indicated that Par14 was part of the fraction termed nucleic acid-binding. Thus, Par14 bound to physiological DNA. S4+ was the supernatant of the nuclei pellet P4+ that was treated with benzonase, and it was referred to as the solubilised nuclei fraction. The presence of Par14 in S1 (cytosol) and S4+ (solubilised nuclei) went to validate previously published data that assigned Par14 to these compartments (Reimer et al., 2003). We also used an antibody against the transcription factor p84 as a marker to verify the fidelity of the eluates E1, E2 and E3 that resulted from S3, the nucleic acid-binding fraction. Transcription factors bind to DNA and this justified our use of p84, a transcription factor to characterise these eluates. We saw bands at E1 and E2 when the antiserum for p84 was probed on the membrane, although a band signal was also seen in the S1 fraction. TCE and rhPar14 were used as endogenous and exogenous positive controls for the identification of Par14. The protein band signal above the Par14 band signal reported in the S3+/S3- nuclear matrix fractions in **Fig 3.2B** and in the S2 cytosolic fraction **(Fig 3.3B)** was also recurrent in this fractionation procedure for the S4+ fraction **(Fig 3.4B)**.

3.2.4 Par14 and Polytene Chromosomes

We have shown with a certain body of evidence that Par14 is a chromatin protein and it binds to DNA *in vivo*. The next approach to validate this finding was to investigate if Par14 in *Drosophila melanogaster* is associated with polytene chromosomes. Human Par14, CCDS14417 shares 72.5 % sequence identity with its orthologue in *Drosophila melanogaster,* CG11858-RA (Wheeler et al., 2007). Within their PPIase domains, they share 81 % sequence identity **(Fig. 3.5A)**. Based on this fact, we decided to perform indirect immnolabeling on polytene chromosomes using the affinity-purified αPPIase to visualise polytene chromosomes. As mentioned earlier, Dr Corinna Schirling provided out of courtesy the polytene chromosome squashes. Alexa Fluor 514-conjugated goat anti-rabbit was used as a secondary antibody. Hence,

the orange colour we saw in **Fig 3.5B**. As a positive staining control for a chromatin protein, antiserum for histone H3 was also given onto the polytene chromosome squashes. The chromosomes were also stained with the preimmune serum for the αPPIase, which served as a negative staining control. **Fig. 3.5B** shows the detection of bands and interbands when the histone H3 antibody was used for staining. The detection of bands and interbands is also observed when the preimmune serum and the affinity-purified PPIase were applied. The pattern of staining was the same and to this effect, it reduced the credibility to acknowledge the fact that Par14 in *Drosophila melanogaster* was associated with polytene chromosomes.

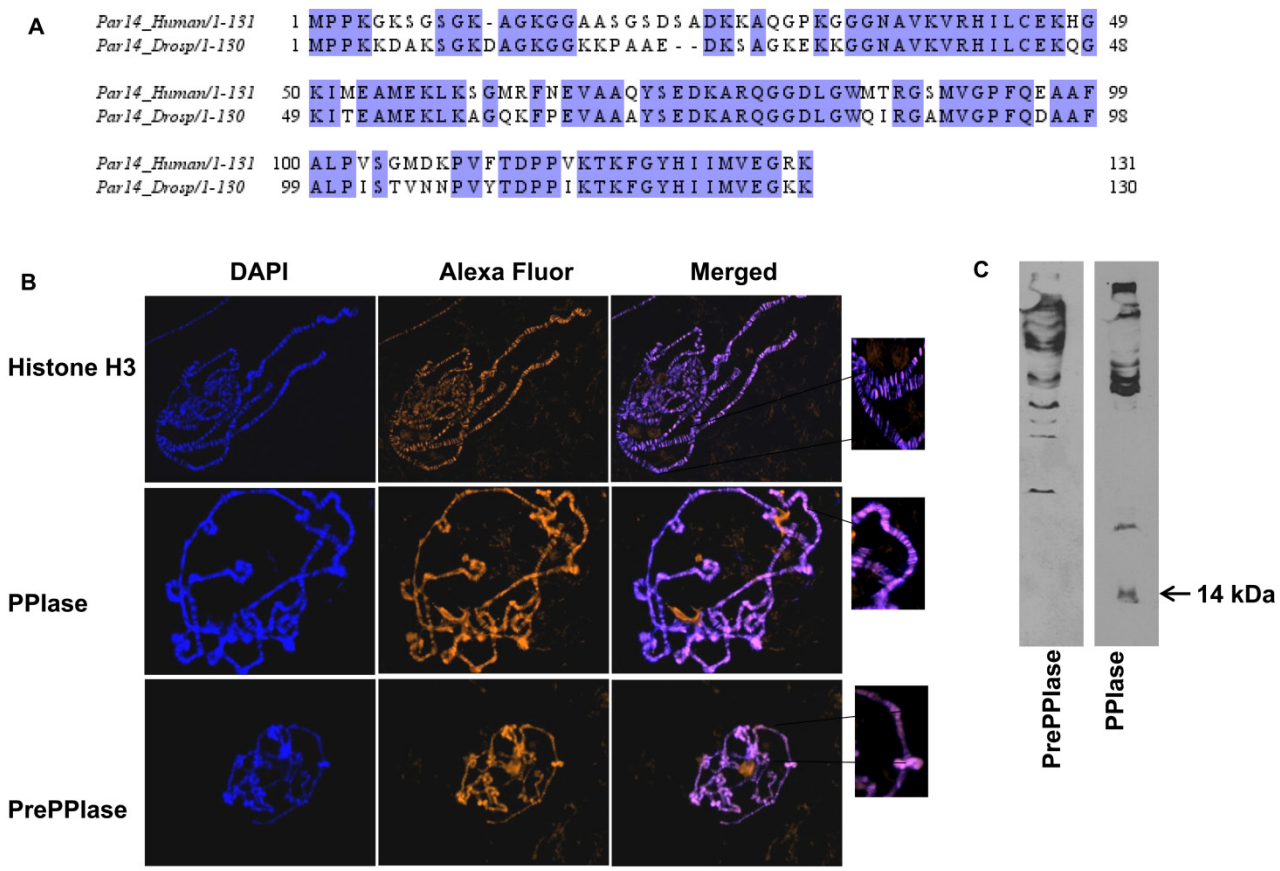

Fig 3.5 No clear-cut co-localisation of Par14 to either puffs or interbands on polytene chromosomes in *Drosophila melanogaster*

A) Sequence alignment of Par14 in humans and in *Drosophila melanogaster*. Identical residues are shown in blue. Multiple sequence alignment with the Clustal series of programs was used (Chenna et al., 2003). **B)** Immunodetection and distribution of Par14 on wild type polytene chromosomes. The left panel shows indirect immunofluorescence using antibodies against the PPIase domain of Par14/Par17, histone H3 and preimmune serum of PPIase domain of Par14/Par17 stained concomitantly with DAPI (blue, first column), Alexa Fluor 514 (orange, second column) and merged (third column). The right panel shows cutouts of the merged col-

umns on the left panel. **C)** Immunoblots of nuclear extracts from *Drosophila melanogaster* Kc cells. Left Lane: preimmune serum of PPIase domain of Par14/Par17; right Lane: affinity-purified serum of PPIase domain of Par14/Par17. A band of 14 kDa is observed on lane 2 and not on lane 1 corresponded to the molecular weight of Par14 in both organisms.

Western blots were carried out using the nuclear extracts of Kc cells from *Drosophila melanogaster.* A protein band of 14 kDa was detected when the αPPIase was used and this band was absent when the preimmune antiserum of αPPIase was applied **(Fig. 3.5C)**. 14 kDa is the molecular mass of Par14 in *Drosophila melanogaster* and in humans.

3.2.5 Chromatin Affinity Purification (ChAP)

From our sub-nuclear fractionation experiments, we observed the relatively enrichment of Par14 with chromatin than with the nuclear matrix. Besides, we saw the elution of Par14 at 0.35 and 1 M NaCl when nucleic acid-binding proteins were bound on a phospho-cellulose column. This knowledge paved the way for the search of potential DNA-binding motifs for not only Par14 but also for Par17. Par17 has been shown to bind to DNA *in vitro* (Kessler et al., 2007). We employed our home-made Chromatin Affinity Purification (ChAP) assay, which is a deviation from the conventional Chromatin Immunoprecipitation assay (ChIP), where large amounts of very specific and sensitive antibodies are required.

Before the transfection of HCT116 cells with Par17QR-*Strep*-GFP and Par17QR-GFP constructs, we first performed preliminary experiments to optimise the chromatin shearing efficiency. Sonification of untransfected cellular lysates previously fixed with 1 % formaldehyde at RT for 10 min was done at 4, 8, and 12 pulses with a 30 sec rest on ice at each pulse for lanes 2, 3 and 4 respectively **(Fig. 3.6)**. This was to avoid emulsification and overheating. An aliquot of un-sheared cellular lysate was also loaded on the 1 % agarose gel for comparison purposes. 100 bp ladder from New England Biolabs, Germany was used. DNA fragments of 200 – 1500 bp are desired for follow-up experiments (Chromatin Immunoprecipitation and Shearing Kits, Version E1, Active Motif, Belgium).

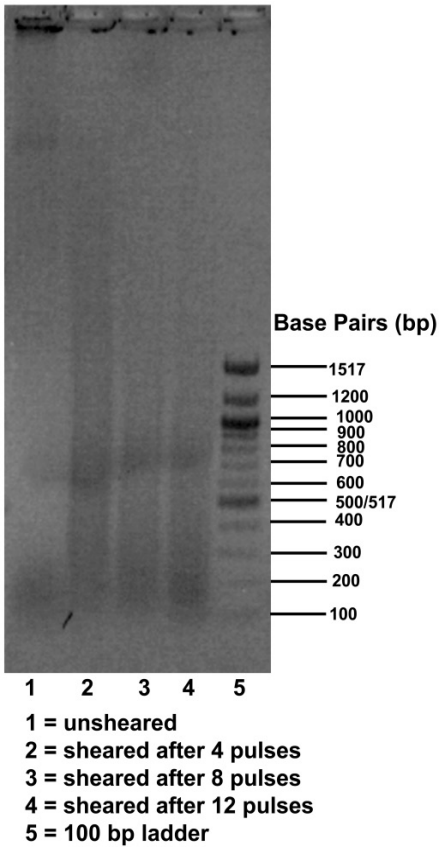

Fig 3.6 Analysis of DNA sheared

HCT116 cells were fixed for 10 mins with 1 % formaldehyde at RT and chromatin was prepared as described in Materials and Methods. Chromatin was sheared with 4, 8 and 12 pulses at 15 sec with a 30 sec rest on ice between each pulse at 17 - 20 % amplitude Bandelin Sonopuls HD 2200. The sheared and un-sheared chromatin samples were subjected to cross-link reversal, treated with 5 M NaCl, Proteinase K and purified with NucleoSpin® Extract II (Macherey-Nagel, Germany). Samples were separated by electrophoresis on a 1 % agarose gel.

Following the optimisation of shearing conditions, Par17QR-*Strep*-GFP and Par17QR-GFP constructs were transfected for 2 – 3 days in HCT116 cells. As described in Materials and Methods **(Section 2.3.4)**, the respective cellular lysates were fixed in formaldehyde, sheared, reversed cross-linked and pre-cleared. After DNA concentration measurement, the eluates obtained from Par17QR-*Strep*-GFP and Par17QR-GFP were sub-cloned into the HindIII and XhoI restriction sites on the pCR®2.1-TOPO® vector and transformed in *E. coli*.

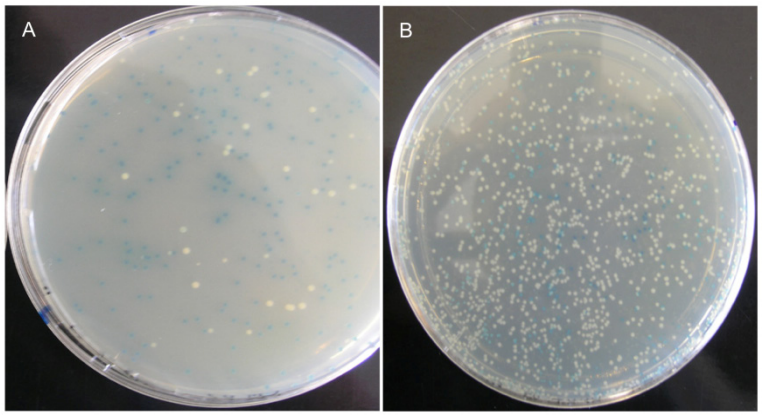

Fig 3.7 Blue and white colonies after cloning and transformation of DNA-fragments from Par17QR-*Strep*-GFP and Par17-GFP using pCR®2.1-TOPO® vector

A) Blue and white colonies from Par17-GFP construct and **B)** Blue and white colonies from Par17QR-Strep-GFP construct.

Blue and white colonies are seen on **Fig. 3.7**. The pCR®2.1-TOPO® vector contained the lacZ gene coding for α-galactosidase responsible for the hydrolysis of galactose. The presence of the LacZ gene on the vector allowed for blue/white screening after transformation. **Fig. 3.7A** showed colonies from DNA-fragments from Par17QR-GFP and **Fig. 3.7B** displayed colonies obtained after transformation with DNA-fragments from Par17QR-*Strep*-GFP.

9 and 3 white clones obtained from constructs Par17QR-*Strep*-GFP and Par17-GFP were picked respectively. Minipreps were made using NucleoSpin Plasmid Kit (Macherey-Nagel, Germany) and the the plasmids containing the DNA fragments were digested with HindIII and XhoI restriction enzymes. For unknown reasons, the restriction digestions did not work fully despite several repetitive attempts. Our goal was to verify the sizes of the inserted DNA fragments on a 1 % agarose gel. But since we were blocked by an unsuccessful restriction of the plasmids, we did not go further with sequencing.

3.3 Transcriptional and Translational Regulation of Par14/Par17 and the Cell Cycle

As stated in the **Section 1** of this work, we aimed to study the transcriptional and translational regulation of Par14/Par17 in the course of the cell cycle. Pin1, a paralogue to Par14/Par17 has been reported to play a role in cell cycle regulation.

Therefore, it was interesting to investigate the roles of Par14/Par17 within the cell cycle. For a brief overview of Pin1 refer to **Section 1.2.1**.

The transcriptional regulation experiments were conducted at the Department of Molecular Oncology affiliated to the *Frauenklinik* at the University of Leipzig by Dr Levin Böhlig. The working group of Dr Böhlig uses an established cell cycle synchronisation system by means of serum deprivation using human foreskin fibroblasts (HFF). We did not have this system in our laboratory at that time. In consequence, we came to the consensus that transcriptional experiments should first be carried out in Leipzig and if the outcome looks encouraging, the author of this work will go to their laboratory to learn this technique.

The findings of the transcriptional regulation experiments will be explained shortly in the coming paragraphs. These findings opened more questions and the author of this thesis made a 2-day research stay at the laboratory in Leipzig to learn cell cycle synchronisation by serum deprivation. During this time, the first translational regulation experiments were also carried out.

3.3.1 Transcriptional Regulation of Par14 and Par17 across the Cell Cycle

The transcriptional regulation of Par14 and Par17 across the cell cycle was studied with the aid of qRT-PCR technology (**Section 2.2.1.1**). Human foreskin fibroblasts (HFF) were suitable for cell cycle synchronisation by serum deprivation as described in Materials and Methods.

After 30 - 36 hrs of starvation by depriving cultured HFFs from FCS, an aliquot of 1.3 x 10^7 cells was obtained and termed G0 cells at t = 0. The rest of the cells were further cultured in medium containing 20 % FCS to re-stimulate them to enter the cell cycle. Normally, 10 % FCS in the culture medium of cells that have not been deprived from growth factors is sufficient. Aliquotes of 1.3 x 10^7 cells were collected within 14, 20, and 24 hrs after growth re-stimulation for G1, S and G2/M cells respectively (Tschop et al., 2006).

The determination of the cell cycle phases of harvested cells was determined by DNA staining and fluorescence-activated cell sorting (FACS) analysis. The distribu-

tion of the cells relative to their location during the cell cycle was represented with the help of a histogram **(Fig. 3.8A)**. The actual number of cells in the various cell cycle phases is shown on **Fig. 3.8B**. No cell cycle synchronisation method is known to date, which achieves a 100 % distribution of cells into the respective phases.

A

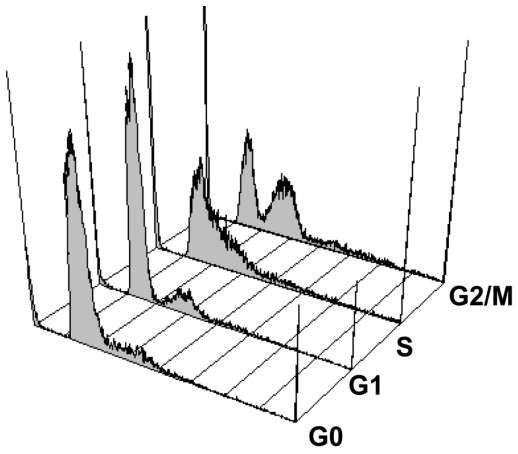

B

Time (hrs)	G0/G1 (%)	S (%)	G2/M (%)	X – Mean
0	86.62	4.09	4.89	202.03
14	89.72	7.49	2.79	214.05
20	43.87	36.54	16.82	309.53
24	32.62	22.74	38.63	391.65

Fig 3.8 Cell cycle distribution of synchronised human foreskin fibroblasts (HFF)

A) Histogram of the percentage of cells present in corresponding cell cycle phases. Cell cycle arrest at the respective phases was confirmed by flow cytometric analysis of cellular DNA content – FACSCalibur flow cytometer (BD) was used. **B)** The percentage of cells present in corresponding cell cycle phases is shown. The arithmetic X-Mean is a measure of the fluorescence intensity and a value of X-Mean = 200 +/- is a good indication how the fluorochrome (propidium iodide) bound to DNA.

Quantitative RT-PCR analyses were done using primers for Par14 and Par17 as previously described (Mueller et al., 2006). U6 splisosomal RNA (U6 snRNA) was used as an internal control since it is abundantly transcribed and highly conserved across species (Brow and Guthrie, 1988). Primers for cyclin B2 were employed and the transcription of cyclin B2 served as a marker gene for the G2/M phase (Wasner et

al., 2003). Transcriptional expression profiles for Par14, Par17, and cyclin B2 were normalised against the expression profile for snRNA U6. It was taken that cells in G0 are quiescent and the percentage mRNA expression was set at 100 for G0 cells harvested after serum deprivation. The percentage mRNA expression of Par14, Par17 and cyclin B2 at G1 was computed by calculating the difference of the exponential between the normalised C_t values of the respective genes at G0 and G1 and multiplying by 100:

$$\%\, mRNA\ expression = 2\text{^}(normalised\ Ct\ for\ gene\ A\ at\ G0 - normalised\ Ct\ for\ gene\ A\ at\ G1) \times 100$$

The same calculation and logic were used to obtain the percentage mRNA expressions at S and G2/M phases for Par14, Par17, and cyclin B2.

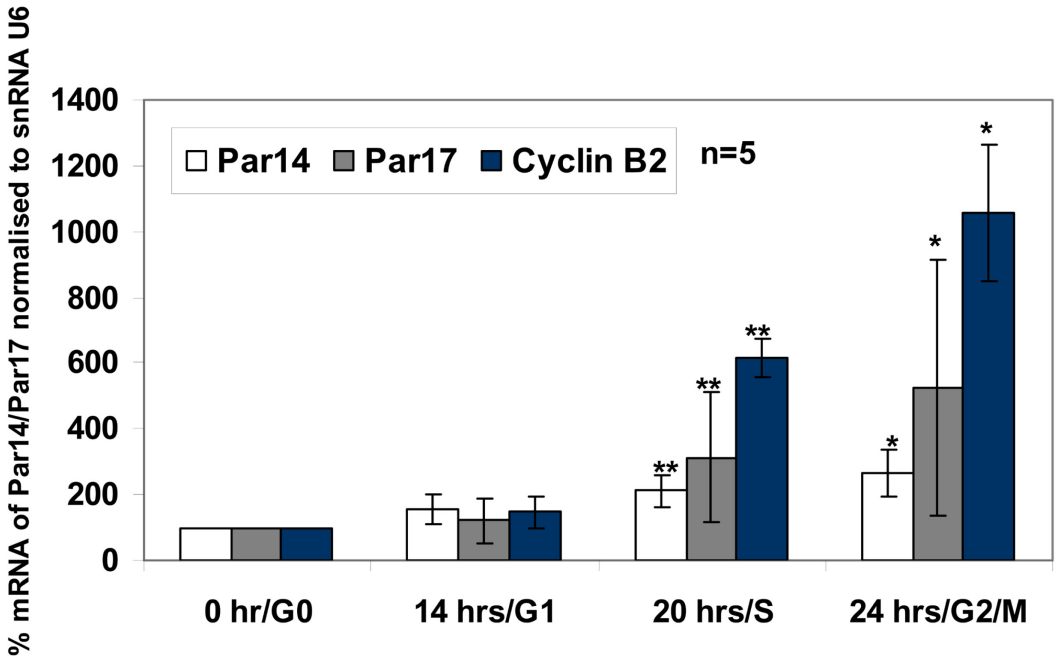

Fig 3.9 Slight but significant transcriptional up-regulation of Par17 than Par14 in the S and G2/M phases of the cell cycle

qRT-PCR analysis of Par14/Par17 across the cell cycle with synchronised human foreskin fibroblasts (HFF). Synchronisation was achieved by serum deprivation. After 30-36 hrs of serum deprivation, cells in G0 were arrested at t = 0 h. HFF cells were re-stimulated with 20 % FCS. G1 cells were harvested after t = 14 h; S phase cells harvested after t = 20 h and G2/M cells harvested after t = 24 hrs. mRNA levels of Par14/Par17 were normalised using snRNA U6. Cyclin B2 was used as a positive control for a gene highly expressed in the G2/M phase. One-way ANOVA was performed using R: A language and environment for statistical computing, R Development Core Team (2008). The bars are means (+/- SD) from five independent experiments. G0 = Gap 0

(quiescent), G1 = Gap 1, S = Synthesis, G2/M = Transition of Gap 2 and Mitosis; * = p α 0.05, ** = p α 0.01.

The white and grey columns represent the percentage mRNA expression for Par14 and Par17 across the cell cycle respectively. The dark blue column shows the percentage mRNA expression of cyclin B2 used as marker gene for the G2/M phase. The bars are an indication of the standard deviation between five independent experiments conducted. The asterisks on the bars are an indication of the statistical significance expressed in p-values. The probability of the observed event occurring by chance is less than one in one hundred (** = pα 0.01) or is less than one in 20 (* = p α 0.05). One-way analysis of variance (One-way ANOVA) was performed using R (A language and environment for statistical computing, R Development Core Team (2008), R Foundation for Statistical Computing, Vienna, Austria, and ISBN 3-900051-07-0). The semi-quantitative RT-PCR analyses were carried out for five independent experiments. One-way ANOVA compares the means of two more samples. The results showed that Par14 and Par17 are slightly up-regulated with expression of Par17 stronger than that of Par14 in the S and G2/M phases of the cell cycle.

3.3.2 Translational Regulation of Par14 and Par17 across the Cell Cycle

The slight but statistically significant transcriptional up-regulation of Par 14 and Par17 during the S and G2/M phases of the cell cycle warranted the investigation of the translational expression of both proteins. Cell cycle synchronisation, FACS and western blotting analyses were done as described in Materials and Methods during the 2-day research period in Leipzig by the author in collaboration with Dr Levin Böhlig. The distribution of the cells in the various phases of the cell cycle was the same to that used for the qRT-PCR experiments **(Fig. 3.8B)**. We used the lysates from the same cells from which the total RNA had been extracted for the transcriptional investigation experiments. For western blot analyses, the affinity-purified antibodies directed against the PPIase domain of Par14/Par17 and the N-terminal extension of Par17 were used to detect endogenous Par14 and Par17 respectively **(Section 3.1)**. An antibody for α-actin was applied to identify the cognate protein, which served as an internal loading control after stripping the membranes from the corresponding Par14 and Par17 antibodies.

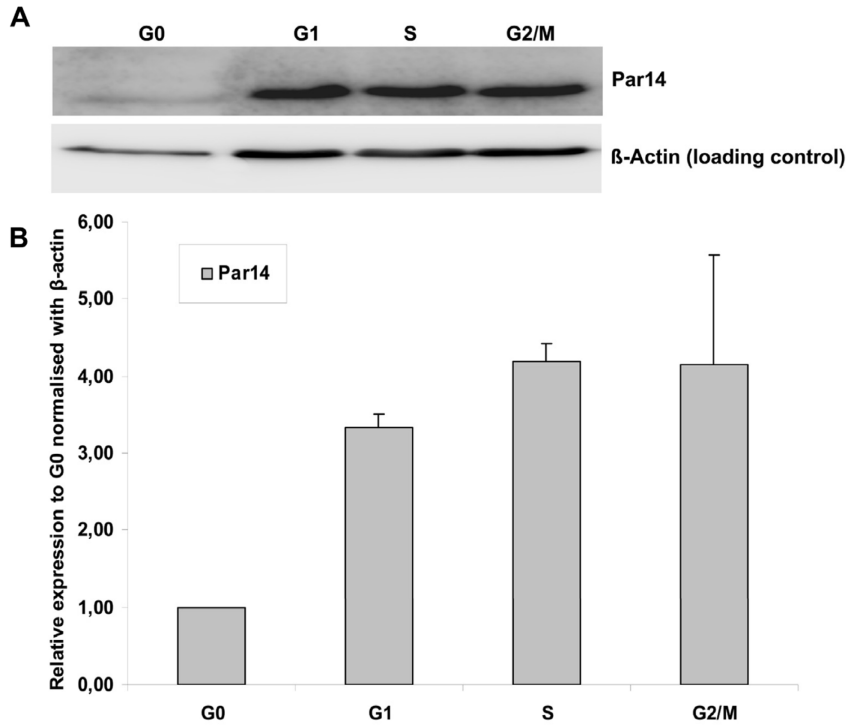

Fig 3.10 Translational up-regulation of Par14 in the course of the cell cycle

A) HFF cell lysates were prepared from the indicated cell cycle phases and processed for western blot analysis using αPPIase (1:1000) and α- actin (1:5000) antisera. 30 µg of protein for each cell lysate from the respective phase of the cell cycle was loaded. **B)** Densitometric analysis of Par14 band signals normalised with α- actin band signals in the respective phase of the cell cycle. Multi Gauge densitometry software version 3.1 was used.

We saw an up-regulation in the translational expression of Par14 in the course of the cell cycle (**Fig. 3.10**). There was a ~3-fold up-regulation of Par14 in G1 and a ~4-fold increase in both S and G2/M phases respectively (**Fig. 3.10B**). Normalisation of Par14 expression was done with α-actin. Firstly, the expression of α-actin at G0 was obtained by dividing the value of its band signal area by its self and a factor of 1 was obtained. This was done because we considered cells at G0 to be resting and thus no relative expression changes. Secondly, the relative expression of α-actin at G1, S and G2/M phases was calculated with respect to its expression at G0. This was done by dividing the values of the respective band signal areas at G1, S and G2/M by the value of the band signal area at G0. This can be explained by the following equation for the relative expression at G1:

$$Relative\ Expression\ of\ \beta - actin\ at\ G1\ = \frac{(Band\ signal\ area\ at\ G1 - Background\ signal)}{(Band\ signal\ area\ at\ G0 - Background\ signal)}$$

Thirdly, the normalisation of Par14 expression in the various phases of the cell cycle was computed by dividing the value of the band signal area of Par14 at the phase in question by the relative expression of α-actin during this phase. The equation below elucidates how the normalised expression of Par14 during G1 was obtained.

$$Normalisation\ of\ Par14\ at\ G1\ = \frac{(Band\ signal\ area\ of\ Par14\ at\ G1 - Background\ signal)}{Relative\ expression\ of\ \beta - actin\ at\ G1}$$

Fourthly and lastly, the fold changes of Par14 at G1, S and G2/M were done by dividing the normalised value of Par14 at the respective phase by its normalised value at G0. The equation below gives a visualisation of this calculation with respect to G1.

$$Relative\ expression\ of\ Par14\ at\ G1\ = \frac{Normalised\ value\ of\ Par14\ at\ G1}{Normalised\ value\ of\ Par14\ at\ G0}$$

After doing all these calculations, it was acknowledged that Par14 was translationally up-regulated in the course of the cell cycle and its expression in the S and G2/M was ~ 4-fold constant.

The translational regulation of Par17 within the cell cycle was also studied by western blotting. The densitometric analyses of the 17, 24 and 28 kDa bands were done in the same manner as described above for Par14.

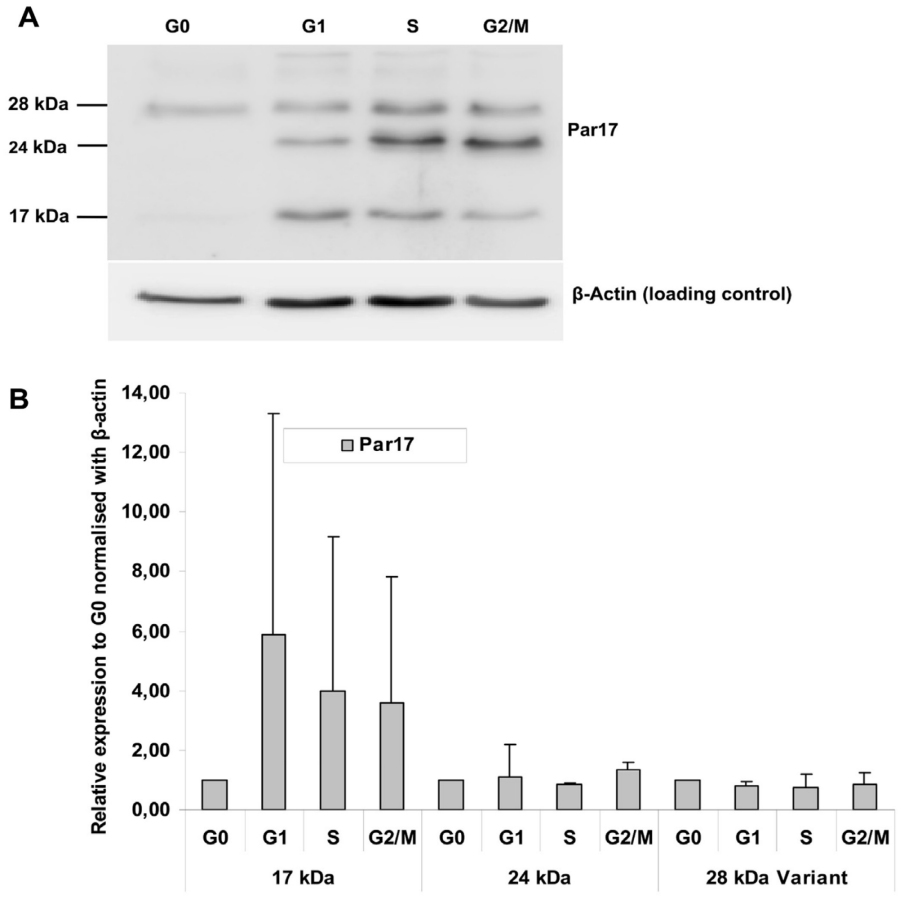

Fig 3.11 Translational down-regulation of Par17 at the S and G2/M phases of the cell cycle

A) HFF cell lysates were prepared from the indicated cell cycle phases and processed for western blot analysis using αPar17-Ext (1:1000) and anti α-actin (1:5000). α-actin was used as an internal loading control. 30 µg of protein for each cell lysate from the respective phase of the cell cycle was loaded. **B**) Densitometric analyses were done for the 17, 24, and 28 kDa bands. Multi Gauge densitometry software version 3.1 was used and α-actin was used for normalisation (internal control).

We saw three protein band signals (17, 24, and 28 kDa) after the use of αPar17-Ext on the cellular lysates from the different phases of the cell cycle **(Fig. 3.11A)**. Of interest was the presence of the 28 kDa band that had been previously observed when the same antibody was used (Mueller et al., 2006). Besides, the signal of the 28 kDa band was very strong as against the 17 kDa signal for Par17 at the G0 phase, which was almost absent. We performed densitometric analyses for all of the three bands

with the Multi Gauge densitometry software version 3.1 after normalising them with α-actin as an internal control. The grey columns stood for the quantitation of the relative fold changes for the 17, 24 and 28 kDa bands. Par17 was down-regulated at ~ 4 and 3.5-fold in the S and G2/M phases respectively while the fold changes of the 24 and 28 kDa bands were more or less constant throughout the cell cycle **(Fig. 3.11B)**.

3.3.3 Cellular Localisation - Translational Regulation Par17 across the Cell Cycle

This part of the study was carried out entirely in our laboratory after the successful establishment of the synchronisation of HFFs cells within the cell cycle by serum deprivation coupled with FACS analyses for verification. The expression of a 28 kDa Par17 variant when unfractionated cellular lysates were used pushed for the investigation of the expression this Par17 protein variant expression in different cellular compartments.

The percentage of cells found in the various phases of the cell cycle was determined by flow cytometry **(Fig. 3.12A).**

A

Time (hrs)	G0/G1 (%)	S (%)	G2/M (%)
0	75.81	6.35	17.99
14	76.93	13.32	9.75
20	29.34	42.15	28.51
24	46.59	16.11	37.30

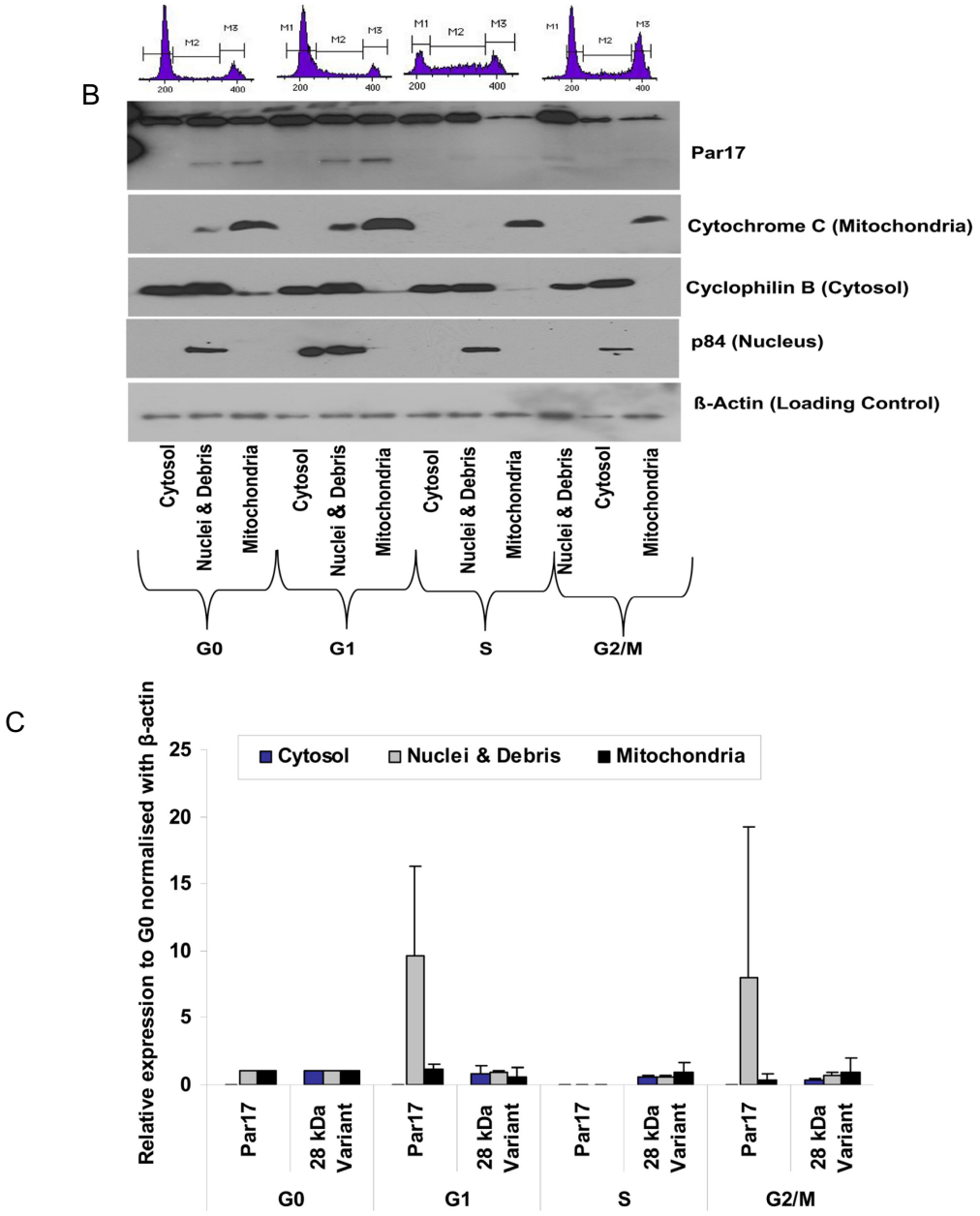

Fig 3.12 Translational down-regulation of Par17 during the S and G2/M phases of the cell cycle in the mitochondria

A) Percentage of cells present in corresponding cell cycle phases is shown. **B)** FACS and western blot analyses. The histograms above show the confirmation of cell cycle arrest at the respective phases by flow cytometric analysis of cellular DNA content of HFF cells. Synchronous cultures of G0, G1, S and G2/M HFF cells were subjected to biochemical cellular fractionation and equivalent amounts (30 µg) of the final fractions from each compartment in the respective cell cycle phase were used for analyses and probed by immunoblotting with αN-Terminal Par17 (1:1000), αCytochrome C (1:2000), αp84 (1:2000), αCyclophilin B (1:3000) and α-actin (1:5000). Antibodies against cytochrome C, cyclophilin B and p84 were used to benchmark the mitochondrial, cytosolic and nuclear fractions respectively. **C)** Densitometric analyses of the 17 and 28 kDa

bands using the Multi Gauge densitometry software version 3.1. α-actin was used as an internal control for normalisation.

Sub-cellular biochemical fractionation was done with the aid of Qproteome mitochondria isolation kit (Qiagen, Germany). The kit allows the separation of the cell into its cytosolic, mitochondrial, and nuclear constituents. In order to be sure that the isolated fractions for the respective cellular compartments where typical for the physiological state, different proteins specific for these compartments were used to characterise these fractions. An antibody against cytochrome C was used to benchmark the mitochondrial fraction. Antibodies against cyclophilin B and nuclear matrix protein p84 were used for the characterisation of the cytosolic and nuclear fractions respectively. α-actin was used as an internal control for equal loading and its constant expression in the respective compartments for each cell cycle phase is shown **(Fig. 3.12B)**.

We performed densitometric analyses with the Multi Gauge software version 3.1 to determine the relative expression of Par17 and the 28 kDa variant across the cell cycle in the respective cellular compartments **(Fig. 3.12C)**. The expressions of Par17 and the 28 kDa variant were normalised with respect to the expression of α-actin whose expression at G0 was kept constant. The equation underneath sheds light on how this was done for the expression of Par17 during the G2/M in the mitochondria:

$$Relative\ expression\ of\ Par17\ \ at\ G2M\ in\ Mitochondria$$
$$= \frac{(Band\ signal\ area\ of\ Par17\ at\ G2M\ in\ Mitochondria - Background\ signal)}{Normalised\ value\ of\ \beta - actin\ at\ G2M\ in\ Mitochondria} \times \frac{Normalised\ value\ of\ \beta - actin\ at\ G0\ in\ Mitochondria}{(Band\ signal\ area\ of\ Par17\ at\ G0\ in\ Mitochondria - Background\ signal)}$$

The normalised value of α-actin at G2/M in the mitochondria was done as follows:

$$Normalised\ value\ of\ \beta - actin\ at\ G2M\ in\ Mitochondria$$
$$= \frac{(Band\ signal\ area\ of\ \beta - actin\ at\ G2M\ Mitochondria - Background\ signal)}{(Band\ signal\ area\ of\ \beta - actin\ at\ G0\ Mitochondria - Background\ signal)}$$

To obtain the relative expression of Par17 and its 28 kDa variant at G0, G1 and S phases in the different celluar fractions, the equations above were adapted and used respectively. The dark blue columns revealed the relative expression of the 28 kDa variant across the cell cycle in the cytosol. The grey columns showed the relative expression of Par17 and the 28 kDa variant in the course of the cell cycle in the nucleus. The relative expression of Par17 and its 28 kDa variant within the cell cycle are shown by columns in black in the mitochondria. It is seen that Par17 was substantially down-regulated in the S and G2/M phases in the mitochondria **(Fig. 3.12B).** The band signal for Par17 was almost absent in the S phase and it was extremely weak in the G2/M phase (~ 3-fold decrease) in the mitochondria **(Fig. 3.12C)**.

After studying the transcriptional and translational expression of Par14/Par17 with respect to the cell cycle phases, we decided to search for potential interaction partners of both proteins. We were also interested to know if any of the potential interaction partners are cell cycle related proteins.

3.4 Protein-Protein Interactions of Par14/Par17

In our search of possible interaction partners for Par14/Par17, we used a Par17QR*Strep*-GFP construct, which had both *Strep* and *His* tags. We know that Par17 is the elongated isoform of Par14 since the only difference between both proteins is in the N-terminal 25-amino acid extension of Par17 (Kessler et al., 2007; Mueller et al., 2006). As a result, we reasoned that the potential binding partners for Par17 that we shall identify could as well be interaction partners for Par14. In the course of the results and discussion sections, we will make particular references if one of the potential binding partners found suits for Par14 or Par17 or for both.

3.4.1 Silver Staining of *Strep*-tag II Affinity Purified Par17 Fusion Protein

The transfection efficiency of HCT116 cells with constructs Par17QR*Strep*-GFP and Par17QR-GFP was evaluated by cell counting using a fluorescence microscope to be more than 60 %. The cellular lysates obtained after the transfection in HCT116 cells with Par17QR*Strep*-GFP and Par17QR-GFP constructs were ran on a 1 ml *Strep*-Trap HP column pre-packed with *Strep*-Tactin sepharose attached to an ÄKTApurifier 10/100 UPC-900 (GE Healthcare, Germany). The UV-absorption chromatogram at 280 nm on **Fig. 3.13A** depicts the run. UV-absoprtion was measured in milli-

absorbance-units (mAU) shown on the y-axis and the wash and eluted fractions (F) are shown as a measurement in volumes (ml) on the x-axis. Protein signals were seen as a measure of the peak area given by the absorption in mAU multiplied by the volume in ml. The chromatogram shows sub-peak areas of proteins eluted with 50, 150 and 500 mM NaCl and with 2.5 mM desthiobiotin. This was done with the aid of the Unicorn software (GE-Healthcare, Germany) that was part of the ÄKTApurifier 10/100 UPC-900 system. The aliquots of fractions in which we saw protein signals were collected and ran on a 12.5 % SDS-PAGE followed by silver staining. 2 ml of fractions of interest were collected and 15 µl for each were used for silver staining **(Fig. 3.13B).**

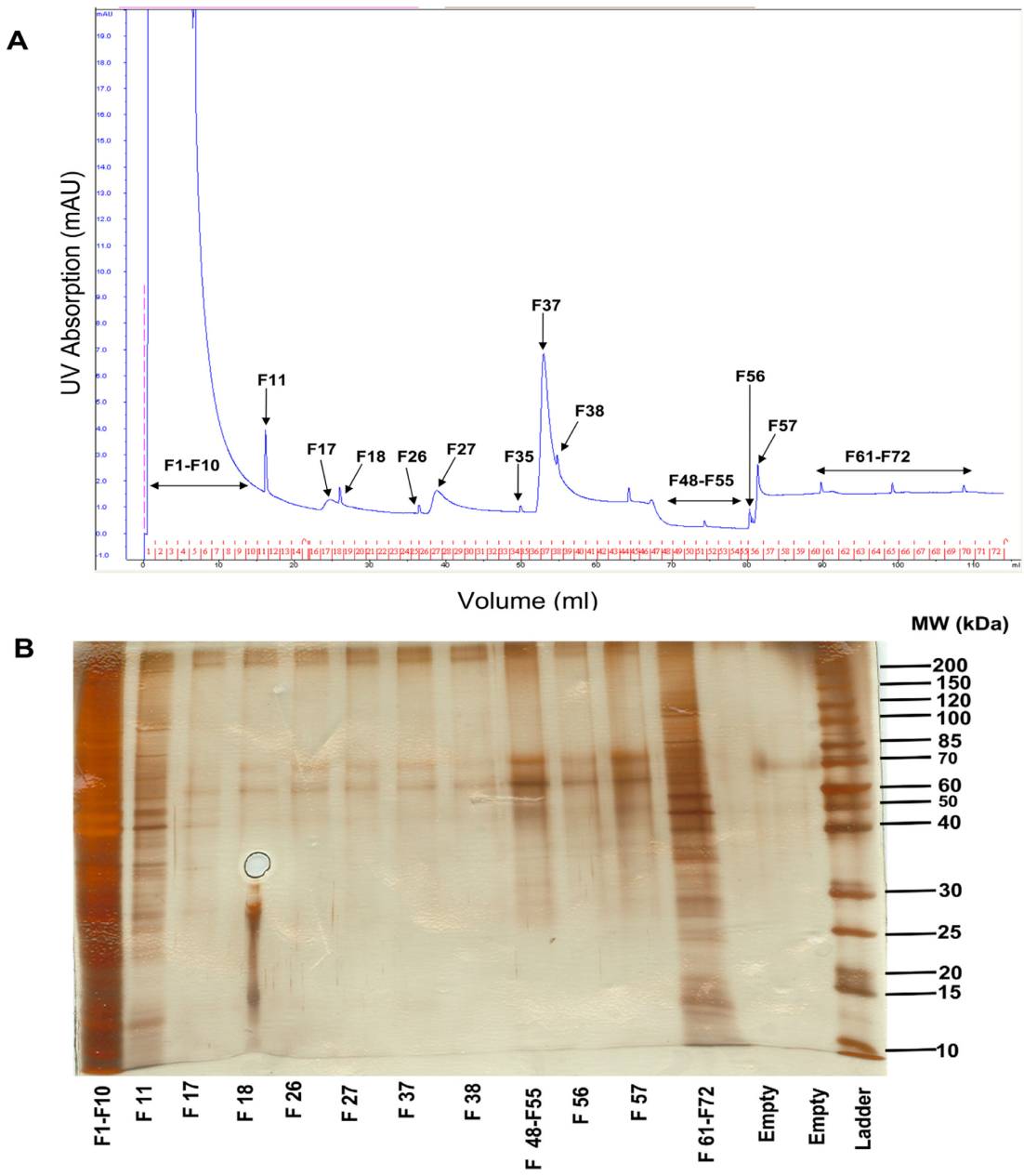

Fig 3.13 Chromatogram and Silver-stained Gel of Proteins pulled-down with Par17QR*Strep*-GFP construct

A) UV-absorption chromatogram at 280 nm. X-axis shows fractions (F) of wash and elution steps after the application of HCT116 cellular lysates transfected with Par17QRStrep-GFP on a *Strep*-Tactin column attached to an ÄKTApurifier 10/100 UPC-900. Y-axis shows the UV-absorption in milli-absorbance-units (mAU). **B)** Silver stain of the wash and eluted fractions. F1-F10: flow-through; F11: wash-through; F17 and F18: proteins eluted with 50 mM NaCl; F26 and F27: proteins eluted with 150 mM NaCl; F37 and F38 proteins eluted with 500 mM NaCl, F48-F55: wash-through with 0 mM NaCl and F56, F57 and F61-F72 pooled fractions of proteins eluted with 2.5 mM desthiobiotin.

Fraction F1-F10 contained unbound proteins that flew through the column **(Fig. 3.13B).** The column was washed with binding buffer and fraction F11 was col-

lected. A sharp difference in the amount of proteins present could be seen between the flow-through F1-F10 and wash-through F11 indicating a substantial amount of unspecific proteins flew through and were washed away during these steps. The first elution procedure that followed was done using an increasing salt gradient from 50, 150, to 500 nM NaCl since we reasoned that interactions between Par14/Par17 and its binding partners might be under electrostatic influence. Fraction F17 and fraction F18 showed samples that were obtained after elution with 50 mM NaCl, whereas fractions F26 and F27 were eluted with 150 mM NaCl. Fractions F37 and F38 **(Fig. 3.13B)** were samples obtained after the elution with 500 mM NaCl. **Fig. 3.13B** shows that no substantial amounts of proteins were pulled-down as a result from the salt gradient elutions.

The second elution procedure was performed with 2.5 mM desthiobiotin. Desthiobiotin binds to *Strep*-Tactin and elution with desthiobiotin served as a competitor to push away *Strep*-tag II bound proteins from the column. Before elution with desthiobiotin, the column was washed again with binding buffer, which was devoid of salt. Fractions F48-F55 were pooled from this washing step. Fractions F56, F57, and F61-F72 were pulled-down with 2.5 mM desthiobiotin. Fractions F61-F72 were pooled. The bands at about molecular weights of 75-85 kDa appeared to be procedural artefacts. They were redundant at the elution steps with NaCl, wash step with 0 NaCl and for fractions F56 and F57. A high density of proteins pulled-down in the fractions F61-F72 could be seen, which suggested that these were proteins that interacted with the heterologously expressed Par17 fusion protein.

The procedure explained in **Fig. 3.13A and B** was repeated for the control construct Par17QR-GFP, which was devoid of the *Strep*-tag II **(Fig. 3.14A and B)**. The numbering of the fractions were different as in **Fig. 3.13** but the logic was the same. Proteins were also eluted using 2.5 mM desthiobiotin with the pooled fraction F51-F67 of the control construct.

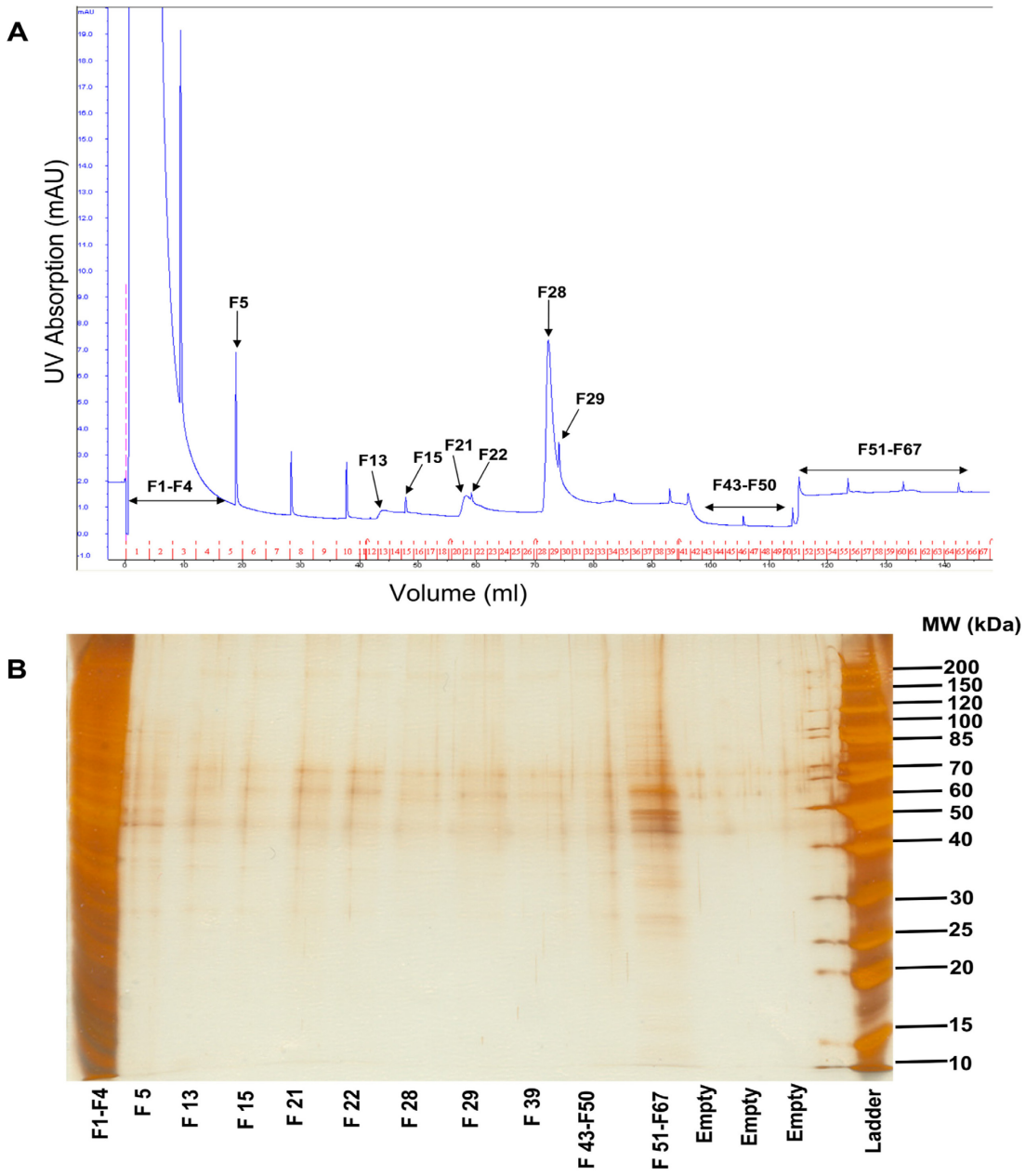

Fig 3.14 Chromatogram and Silver-stained Gel of Proteins pulled-down with Par17QR-GFP construct

A) UV-absorption chromatogram at 280 nm. X-axis shows fractions (F) of wash and elution steps after the application of HCT116 cellular lysates transfected with Par17QR-GFP on a Strep-Tactin column mounted to an ÄKTApurifier 10/100 UPC-900. Y-axis shows the UV-absorption in milli-absorbance-units (mAU). **B)** Silver stain of the wash and eluted fractions. F1-F4: flow-through; F5: wash-through; F13 and F15: proteins eluted with 50 mM NaCl; F21 and F22: proteins eluted with 150 mM NaCl; F28 and F29 proteins eluted with 500 mM NaCl; F43-F50: wash-through with 0 mM NaCl and F51-F67 pooled fraction of proteins eluted with 2.5 mM desthiobiotin.

Visual inspection acknowledged the fact that more proteins were eluted with the Par17QR*Strep*-GFP construct for fractions F61-F72 **(Fig 3.13B)** in comparison to the proteins obtained from the control construct Par17QR-GFP for fractions F51-F67

(Fig 3.14B). This acknowledgement edged us to identify proteins that were eluted in both pooled fractions by tandem mass spectrometry. Aliquots of eluted fractions F61-F72 and F51-F67 with 2.5 mM desthiobiotin were sent to the *Medizinisches Proteom-Center* affiliated to the Ruhr University of Bochum, Germany. Dr Barbara Sitek and her team performed an analytical silver gel as shown in **Fig. 3.15** that also reproduced our silver stainings in terms of the amount of the pulled-down proteins seen in the respective fractions. After this first analytical gel, they performed a second SDS-PAGE gel in which electrophoresis was paused immediately the proteins entered the resolving gel not allowing them to separate in their entirety. This was a measure to get the conglomerate of proteins in the respective samples before they got separated so that a differential protein determination via tandem mass spectrometry analysis could be done. We postulated that proteins identified in the test construct and absent in the control construct should be potential interaction partners to Par14/Par17 and proteins found from both constructs were considered to be unspecific binders.

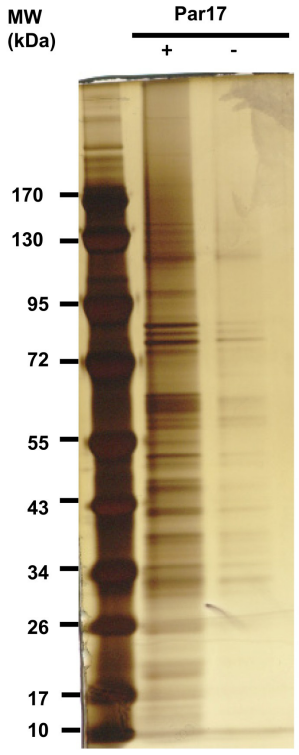

Fig 3.15 More proteins pulled-down with Par17QR*Strep*-GFP construct as compared to Par17QR-GFP construct

Silver stain compatible with mass spectrometry of 2.5 mM desthiobiotin eluted pooled fractions F61-F72 (Par17+) and (Par17-) for constructs Par17QR*Strep*-GFP and Par17QR-GFP respectively.

3.4.2 Identification of Par14/Par17 Affinity Purified Coupled with Mass Spectrometry Interactors

After the silver-stained protein bands for fractions F61-F72 (Par17QR*Strep*-GFP) and F51-F67 (Par17QR-GFP) were cut off from the gel, they were processed for tandem mass spectrometry as described in **Section 2.3.8**. The identification of proteins was done with the Mascot search engine that supports MS/MS ions data and the incorporation of a probability-based scoring (Perkins et al., 1999). The principle behind probability-based scoring is justified by the fact that the observed match between the experimental data set and each sequence database entry is a chance event. This implies that the best match is the match with the lowest probability (Perkins et al., 1999). As a rule of thumb to determine the significance of a match between an experimental data set and a database entry, the probability of the observed event occurring by chance should be less than one in twenty ($p < 0.05$).

Besides, the probability for a good match is usually a very small number, which must be expressed in scientific notation. This can be a bane for the analyses of MS/MS identified proteins. To circumvent this, Perkins and co-workers reported the convention often used in sequence similarity searches and report a score that is 10Log_{10} (P), where P is the probability (Perkins et al., 1999). This implies that the best match is the one with the highest score and a significant match should have a score of the order 70. In the evaluation of the proteins revealed by the Mascot search engine, we adopted the convention that for a protein to be accepted as identified a score of an order α 22.5 and at least 2 or more peptides or a score α 70 and at least 1 peptide of the identified protein must be present. **Table 3.1** shows Par14/Par17-associated identified proteins that met the conditions of the above convention.

Table 3.1 Identification of Par14/Par17-associated proteins by affinity purification coupled with mass spectrometry (AP-MS)

Proteins		Accession	Score	Peptides	MW (kDa)	Cellular Compartment
Protein translation						
TARS	Threonyl tRNA synthetase	IPI00910719	32.9	2	70.3	Cytoplasm
HARS	Histidyl-tRNA synthetase	IPI00909075	48.9	2	35.6	Cytoplasm
EEF1A2	Eukaryotic translation elongation factor 1 alpha 2	IPI00556204	73.8	2	36.9	Cytoplasm, nucleus

RNA processing						
SFRS1	Splicing factor, arginine/serine-rich 1	IPI00218592	70.8	1	70.8	Nucleus, cytoplasm
HNRNPA2B1	Heterogeneous nuclear ribonucleoprotein A2/B1	IPI00916517	87.0	2	34.2	Nucleus, cytoplasm
Ribosome biogenesis						
NCL	Nucleolin	IPI00444262	118.0	5	65.9	Nucleus, nucleolus
NPM1	Nucleophosmin	IPI00658013	29,8	1	28.4	Nucleus, nucleolus
Cell adhesion & cytoskeleton						
EZR	Ezrin	IPI00872684	388.8	14	69.3	Cytoskeleton, plasma membrane
ACTB	Actin, beta	IPI00894365	49.6	2	39.2	Cytoskeleton, cytoplasm
LMNA	Lamin A/C	IPI00655812	97.4	3	55.6	Cytoplasm, nucleus, plasma membrane
SHROOM4	Shroom family member 4	IPI00845416	32.3	2	152.7	Cytoskeleton, Cytoplasm, nucleus
SPTAN1	Spectrin	SHD00871535	47.3	2	284.9	Cytoskeleton, cytoplasm
Signal transduction						
CKB	Creatine kinase, brain	IPI00908811	53.8	2	38.7	Cytoplasm, mitochondrion
YWHAE	14-3-3 protein epsilon	IPI00000816	102.2	4	29.2	Cytoplasm, mitochondrion
Metabolism						
GOT2	Aspartate aminotransferase 2 (mitochondrial)	IPI00910267	59.4	2	43	Mitochondrion
TKT	Transketolase	IPI00792641	104.8	3	58,9	Cytoplasm
Annexin						
ANXA1	Annexin A1	IPI00549413	79.3	3	22.7	Plasma membrane, cytoplasm, nucleus
ANXA2	Annexin A2	IPI00455315	114.0	4	38.6	Plasma membrane, cytoplasm, nucleus
ANXA5	Annexin A5	IPI00872379	50.2	2	35.8	Plasma membrane, cytoplasm, nucleus
Peptidyl prolyl isomerases						
PPIA	Cyclophilin B	IPI00925411	36.6	2	13	Cytoplasm, nucleus
PPIB	Cyclophilin A	IPI00646304	58.3	2	23.7	endoplasmic reticulum
Chaperone proteins						
HSP90AA1	Heat shock protein 90kDa alpha, class A member 1	IPI00784295	223.5	7	84.6	Cytoplasm
HSP90AB1	Heat shock protein 90kDa alpha, class B member 1	IPI00414676	242.5	7	83.2	Cytoplasm
HSPA4	Heat shock 70kDa protein 4	IPI00002966	108.6	3	94.3	Cytoplasm, nucleus
HSPA5	Heat shock 70kDa protein 5	IPI00003362	252.0	6	72.4	endoplasmic reticulum, nucleus
HSPA9	Heat shock 70kDa protein 9	IPI00922694	50.1	2	69.9	Mitochondrion, cytoplasm
Protein disulfide isomerases						
P4HB	Prolyl 4-hydroxylase,	IPI00010796	103.3	2	57.1	endoplasmic

	beta polypeptide					reticulum,plasma membrane
PDIA3	Protein disulfide isomerase family A, member 3	IPI00025252	201.3	7	56.7	endoplasmic reticulum
PDIA4	Protein disulfide isomerase family A, member 4	IPI00009904	61.0	2	72.9	endoplasmic reticulum
Unclassified						
PRDX1	Peroxiredoxin 1	IPI00640741	126.2	4	19	Cytoplasm, nuleus
NCAPG2	Isoform 1 of Condensin-2 complex subunit G2	SHD00797030	31.0	2	130.9	Nucleus
NOMO1	NOMO1;NOMO3 139 kDa protein	SHD00413732	44.2	2	139.3	Plasma membrane

The proteins on **Table 3.1** that met our criteria for identification have been classified in various groups based on a functional property that they might share in common. Proteins involved in the translational apparatus, RNA-processing, ribosome biogenesis, cell adhesion and the cytoskeletal network, signal transduction, metabolism, chaperones and peptidyl-prolyl and protein disulfide isomerases were found. Cellular compartments and molecular masses of the identified proteins are also listed on **Table 3.1**. The highest score of 388.8 is seen for EZR, a protein that is part of the cytoskeletal network.

After identifying some potential interaction partners of Par14/Par17, it was mandatory to investigate the up- and down-regulation of some of these proteins in the case that Par14/Par17 was absent.

3.5 Par14/Par17 Gene Knock-Down Experiments

Two approaches of siRNA technology were used to knock-down Par14/Par17. We first used synthetic double-stranded siRNAs in a pool consisting of 4 siRNAs specific for Par14/Par17. After transfection, fixation and staining were done as described in Materials and Methods. Cells were visualised using an Olympus BX61 fluorescence microscope (**Fig. 3.16A;** first column; top and bottom rows). The second column depicted cells treated with scrambled siRNA with no known sequence homology to any human gene, and the third column represented cells that were not treated with any form of siRNA. Transfection was stopped for cells treated with Par14/Par17 specific siRNA pool and scrambled siRNA after 72 hrs **(Fig. 3.16A)**.

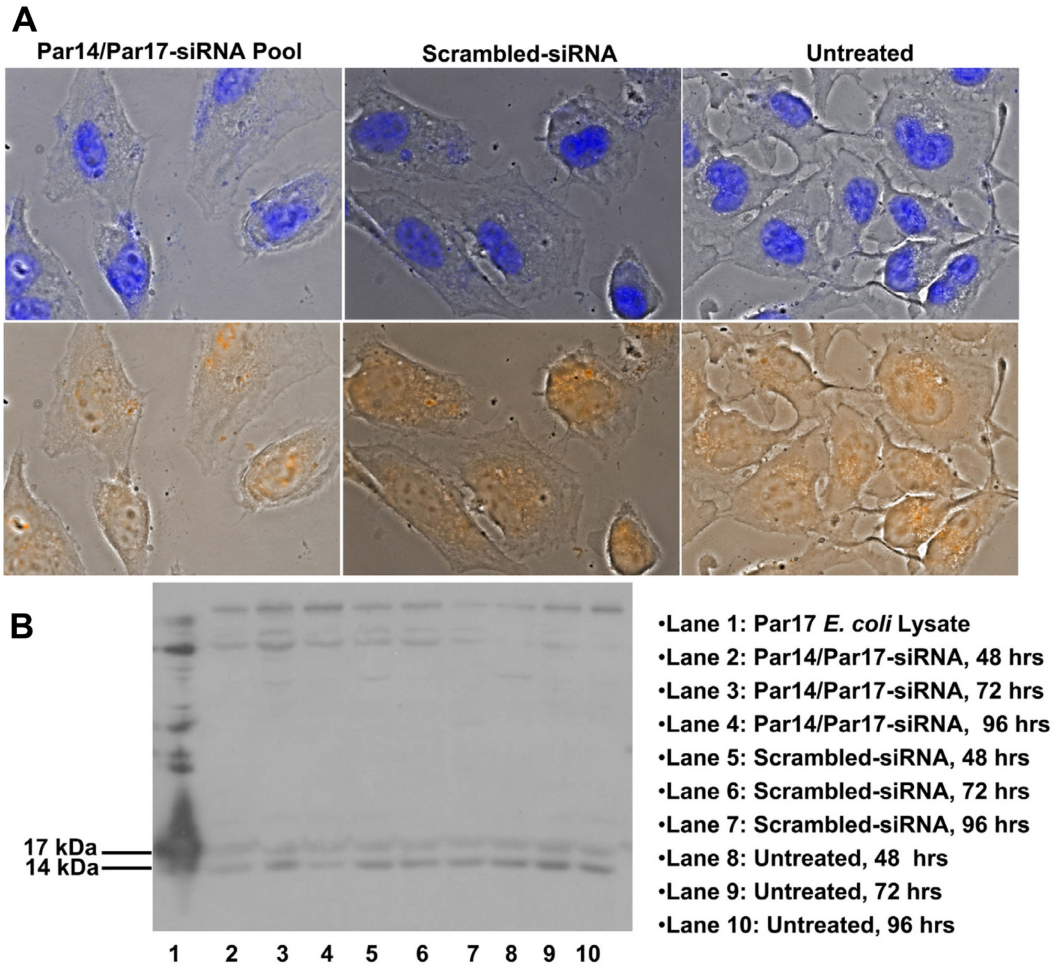

Fig 3.16 Study of morphological changes and protein knock-down levels with siRNAs in a pool specific to Par14/Par17

A) 4 Par14/Par17 siRNAs in a pool were transfected in HeLa cells for 72 hrs. A scrambled siRNA sequence with no homology to any human gene was co-transfected. Transfected cells where stained with DAPI and PI and observed under a fluorescence microscope in bright field. **B)** HeLa lysates were prepared for western blot analyses with Par14/Par17 siRNAs in a pool after 48, 72, and 96 hrs of transfection.

For western blot analyses, lysates of HeLa cells were used after being treated with Par14/Par17 siRNAs in a pool and the scrambled siRNA. Lane 1 was the lysate of *E. coli* over-expressing Par17 and was used as a positive control for the αPPIase antiserum for the detection of Par14 or Par17 **(Fig. 3.16B)**. This antibody was the un-purified final bleeding of αPPIase. Lanes 2, 3, and 4 were from lysates obtained after the transfection with Par14/Par17 siRNAs for 48, 72, and 96 hours respectively. Lanes 5 – 7 and lanes 8 – 10 were lysates from the treatment with the scrambled siRNA for 48, 72, and 96 hrs and from untreated cells cultured also for 48, 72, and 96 hrs respectively. Since we could not achieve an appreciable knock-down at the pro-

tein level and no observable morphological changes of the cells could be appreiciated, we then moved to the second approach to the elicit knock-down.

Our second strategy with siRNA technology was the use of shRNAs cloned in to a plasmid. Three Par14/Par17 shRNAs and one shRNA for luciferase were cloned by GenScript, USA into pRNTin-H1.2/Hygro and pRNATin-H1.3/Hygro/siFluc vectors respectively. After a 72-hour transfection with all three Par14/Par17 shRNAs and the luciferase shRNA, HeLa cells were fixed and stained with DAPI. Fluorescence microscopic observations were performed as was the case with double-stranded synthetic siRNAs in a pool. shRNA-1, shRNA-2 and shRNA-3 are shown on the upper row from left to right respectively **(Fig. 3.17A)**. Cells treated with siRNA-Luc are on the bottom row.

HeLa lysates from shRNAs 1 - 3, siRNA-Luc, and that from untreated cells were used for western blot analyses. The lysates were prepared after 48, 72, and 96 hrs of transfection with the respective shRNAs **(Fig. 3.17B)**. αPPIase (not affinity-purified) was used for detection of endogenous Par14/Par17 and rhPar14 was employed to verify the efficiency of the antibody.

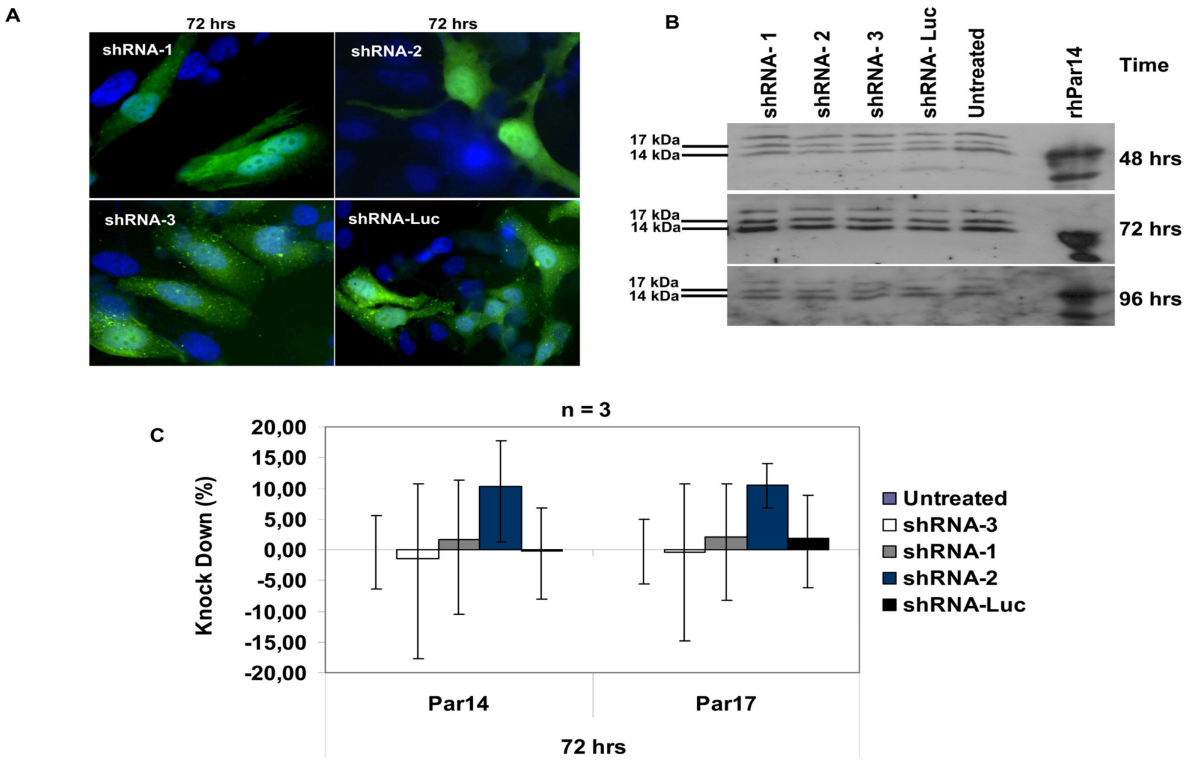

Fig 3.17 Study of morphological changes, mRNA and protein knock-down levels with shRNAs specific to Par14/Par17

A) 3 shRNAs specific to Par14/Par17 were cloned into pRNTin-H1.2/Hygro vector and transfected in HeLa cells for 72 hrs. The shRNA for luciferase in pRNATin-H1.3/Hygro/siFluc vector was also transfected for 72 hrs. Both vectors coded for the reporter gene GFP that was used as a transfection indicator. The transfected cells were stained with DAPI and observed under a fluorescence microscope. **B)** HeLa lysates were prepared for western blot analyses with Par14/Par17 shRNAs and luciferase shRNA after 72 hrs of transfection. **C)** qRT-PCR was performed from HCT116 cells transfected with Par14/Par17 shRNAs and luciferase shRNA after 72 hrs of transfection. The white column shows the % KD of Par14 and Par17 with shRNA-3, the gray columns display the % KD for shRNA-1 for both genes and the blue columns depicts the % KD for shRNA-2 for both genes. The black columns stand for the % KD of the control shRNA-Luc in Par14 and Par17. For western blot and qRT-PCR analyses, lysates of untransfected cells were also used.

To look at the mRNA levels of Par14/Par17 with the Par14/Par17 shRNAs used, we performed qRT-PCR experiments **(Materials and Methods)**. Here, HCT116 cells were used instead of HeLa cells because they had higher transfection efficiencies of more than 60 % and this was not the case with HeLa cells where transfection efficiencies stood at 30 %. For each shRNA, transfection was done for 72 hrs in triplicates in 12-well plates and for the RNA isolated from each well duplicates of the crossing point (C_t) values were measured. The percentage knock-down was calculated as explained in **Section 2.4** and as shown on **Fig. 3.17C**. The columns in white

represented the % KD of Par14/Par17 with the shRNA-3 construct. The gray and blue columns showed the % KD achieved by construchts shRNA-1 and shRNA-2 for Par14/Par17 respectively. The % KD for the shRNA-Luc is shown on the black columns for Par14/Par17. The bars on the columns were a reflection of the standard deviations in the three independent experiments carried out with the respective shRNAs constructs. A 10 % KD is seen for Par14/Par17 when shRNA-2 was used. The other shRNA constructs achieved a knock-down of Par14/Par17 mRNA in a magnitude of α 2 %.

4. Discussion

4.1 Par14, Chromatin and DNA-Binding *in vivo*

Given the enrichment of Par14 in the nucleus and its structural and sequence identity to HMGB and HMGN proteins, it was pivotal to investigate the sub-nuclear localisation of Par14 so that clues to its cellular function could be obtained. Two biochemical fractionations were performed that fractionated the nucleus. In the sub-nuclear fractionation 1, we obtained fractions S3- (soluble nucleoplasmic proteins) and P3- (chromatin-nuclear matrix bound proteins). We saw a trend that the Par14 signal in the P3- was stronger than the signal in the S3- fraction. The use of MNase to release DNA-bound proteins was less effective as seen for fractions S3+ (solubilised nuclear proteins) and P3+ (solubilised chromatin-nuclear matrix bound proteins). The purity of the fractions was monitored with the use of marker proteins characterising these fractions. The indications showed that Par14 probably associated with chromatin-nuclear matrix bound proteins and this paved the way for the next sub-nuclear fractionation scheme.

The sub-nuclear fractionation 2 was particular in being able to discriminate between chromatin and nuclear matrix proteins. We acknowledged strong Par14 signals (3- and 2-fold) in the S2+ and S2- chromatin fractions respectively as opposed to the signals that were seen in the S3+ and S3- nuclear matrix fractions. The chromatin fraction S2+, which was treated with DNase I, showed a stronger band signal for Par14 (1.4-fold) than the fraction S2-, which was not treated with the nuclease. This suggested that Par14 preferably bound to DNA on chromatin. DNase I treatment of nuclear matrix fraction S3+ showed no difference to the fraction S3- that was not treated with the nuclease. Our results suggest that Par14 is a chromatin protein since it was enriched in the chromatin fractions than in the nuclear matrix fractions and was also released with DNA following DNase I treatment.

Furthermore, we saw in the fractionation of nuclear and nucleic acid-binding proteins that Par14 was eluted with increasing salt concentrations from the fraction that was termed nucleic acid-binding. Par14 band signals could be seen for eluates E2 and E3 that were eluted with 0.35 and 1 M NaCl. The manufacturers of the kit (Qiagen, Germany) that was used to perform the fractionation procedure claimed that the proteins

contained in the nucleic acid-binding fraction are low-abundant nuclear proteins such as transcription factors. We validated our fractionation scheme **(Fig 3.4B)** by using nuclear matrix protein p84, a transcription factor that was detected in the eluate E1 and E2 that was eluted with 0.1 and 0.35 M NaCl respectively. In DNA cellulose affinity experiments, total cell extracts and recombinant Par14 were used to show that Par14 bound to DNA *in vitro* (Surmacz et al., 2002).

To mention, ASCC2 was reported to interact with Par14/Par17 in a yeast two-hybrid assay (Stelzl et al., 2005) and it was found to be a member of a novel transcription co-activator complex (Jung et al., 2002). In the same yeast two-hybrid screen, polycomb group (PcG) protein EZH2 (Enhancer of Zeste homologue 2), a histone methyltransferase associated with transcriptional repression, was reported as an interactor to Par14/Par17. Fujiyama and colleagues demonstrated that nucleolin interacted with Par14 (Fujiyama et al., 2002; Fujiyama-Nakamura et al., 2009) and in our protein-protein interaction studies **(Section 3.4.2)**, we shortlisted nucleolin to be a potential interaction partner to Par14/Par17. In co-immunoprecipitation experiments, Rickards and co-authors confirmed nucleolin to be associated with chromatin-containing rRNA genes transcriped by RNA polymerase I and not with genes transcribed by RNA polymerase II or III (Rickards et al., 2007). They proposed that the function of nucleolin is to permit the transcription of nucleolar chromatin by RNA polymerase I. Furthermore, nucleolin was reported as a nuclear protein with a histone chaperone function (Angelov et al., 2006). Its histone chaperone activity enhanced the activity of chromatin remodelling machineries such as SWI/SNF and ACF. All these lines of evidence show Par14/Par17, more likely Par14, to interact with the aforementioned proteins that play a role in transcription.

Other proline isomerases have also been shown to be associated with chromatin. The nuclear FKBP, SpFkbp39p from *Schizosaccharomyces pombe* was reported to be a histone chaperone regulating rDNA silencing and it influenced chromatin organisation both *in vivo* and *in vitro* (Kuzuhara and Horikoshi, 2004). Still in yeast, Fpr4, a member of the FKBPs in *Saccharomyces cerevisiae* was shown to bind the amino-terminal tail of histones H3 and H4 and catalyses the isomerisation of histone H3 proline P30 and P38 *in vitro* (Nelson et al., 2006). In the same work, they also showed that the abrogation of Fpr4 catalytic activity *in vivo* resulted in increasing lev-

els of H3K36 methylation and delayed transcriptional induction kinetics of yeast-specific genes. The work summarises proline isomerisation as a novel non-covalent histone modification that regulates transcription and provides evidence for crosstalk between histone lysine methylation and proline isomerisation. Above all, Pin1 and its orthologue Ess1, haven been demonstrated to modulate the C-terminal domain (CTD) of RNA polymerase II (Pol II) during the transcriptional cycle (Krishnamurthy et al., 2009; Xu and Manley, 2007). The CTD is the largest subunit of Pol II and contains repeatedly the heptad sequence (Tyr1-Ser2-Pro3-Thr4-Ser5-Pro6-Ser7) that plays a key role in the transcription cycle, coordinating the exchange of transcription and RNA processing factors. CTD has a structurally flexible structure that undergoes conformational changes in the advent of serine phosphorylation and proline isomerisation by Pin1/Ess1, which then have an effect on the transcription of genes. However, the role of Par14 in transcription remains to be proven experimentally.

4.1.1 Par14 and Polytene Chromosomes

It was experimentally difficult to establish an unequivocal association of Par14 with polytene chromosomes by indirect immunostainings. In an effort to circumvent the not so successful immunostainings of polytene chromosome squashes, we performed a complementary experiment. Immunoblots were conducted using the nuclear extracts of Kc cells from *Drosophila melanogaster,* which *per se* embodies polytene chromosomes. A protein band of 14 kDa was detected when the αPPIase-was used as opposed to the use of the preimmune antisera of αPPIase **(Fig. 3.5C)**. 14 kDa is the molecular weight for endogenous Par14 in both organisms. Nevertheless, Par14 was reported in immunofluorence studies to have apparently accumulated around chromosomes during mitosis (Fujiyama-Nakamura et al., 2009). This line of evidence adds weight to our findings that Par14 is a chromatin and DNA-binding protein.

4.1.2 Chromatin Affinity Purification (ChAP)

One of the questions to be addressed in the course of this thesis was the search DNA-binding motifs of Par14/Par17. We used sheared cellular lysates after the transfection of HCT 116 cells with Par17QR-GFP and Par17QR-*Strep*-GFP constructs. The use of transfection to characterise DNA binding sites using formaldehyde cross-linking has previously been reported (Wells and Farnham, 2002). Before this step, we

had to optimise the shearing conditions. We agreed on shearing the transfected cellular lysates at 8 pulses for 15 sec with a 30 sec rest on ice between each pulse **(Fig. 3.6)**. At this pulse rate, we could see DNA smears in the range of about 700 – 800 bp. This was in line with shearing efficiency to obtain DNA fragments for subsequent use that should be in the range of 200 – 1500 bp. 4 and 12 pulses were also tried and smears were also in this range. In effect, any of the pulse rates tried could have been used.

The sheared chromatin from both constructs were further processed and sub-cloned in the pCR®2.1-TOPO® vector and transformed in *E. coli.* Blue and white screening was used to discriminate between clones that contained DNA fragments. White clones will test positive and blue clones will not. We observed in **Fig. 3.7A** that there were far less white clones than in **Fig. 3.7B.** The presence of more clones from Pa17QR-*Strep*-GFP was an indication that more DNA was pulled-down with this construct than with the Par17QR-GFP construct. Minipreps were made for clones from the respective constructs. We performed restriction digestions with HindIII and XhoI in order to very the sizes of the inserts. After several attempts, we could not get successful digestions and this hindered the processing of the clones for sequencing. Following careful trouble-shooting, the entire experiment will be repeated. Par14 shows sequence and structural similarity to HMGN and HMGB proteins and was shown by fluorescence titration and electromobility shift assays to bind to AT-rich DNA oligonucleotides (Surmacz et al., 2002). AT-rich sequences of DNA are suggested to dictate nucleosome positioning and play a role in the initiation of transcription (Mueller and Bayer, 2008). The basic domain of Par14, which is also embodied in Par17, has sequence similarity to the chromatin-unfolding domain (CHUD) in HMGN proteins. This basic domain was indispensible for high affinity DNA-binding. Moreover, Par17 was demonstrated to bind to DNA *in vitro* at physiological salt concentrations (Kessler et al., 2007). Based on these arguments and with the data presented here so far, it is of paramount interest to investigate the DNA-binding motifs of both proteins *in vivo*.

4.2 Transcriptional and Translational Regulation of Par14/Par17 across the Cell Cycle

The data from our qRT-PCR analyses showed to a certain degree that Par17 was more up-regulated during the S and G2/M phases as compared to its isoform Par14 **(Fig. 3.9)**. Minimal fold changes were observed for the mRNA expression of Par14, Par17, and cycline B2 at G1. Par14 and Par17 showed a 2- and 3-fold increase in expression at the S phase respectively. 3 and 5-fold increments in the expression for Par14 and Par17 at the G2/M phase were observed respectively. The expression of cyclin B2 in the S-phase was 6-fold as compared to a 10-fold increase in expression during G2/M phase. Cyclin B2 is a marker protein for the G2/M phase (Tschop et al., 2006).

Western blot analyses investigating the expression of Par14 showed an up-regulation during the cell cycle **(Fig. 3.10)**. The signal for Par14 at G0 was very faint and this was also reflected in the weak signal of α-actin in the same phase. We argue that this observation was a result of an unequal amount of protein that was loaded. The anti-serum for α-actin was applied after stripping the same membrane on which the αPPIase was applied. α-actin was used for the normalisation of Par14 expression. The 2 and 3-fold transcriptional increase of Par14 in the S and G2/M phases **(Fig. 3.9)** corrolated with a 4-fold translational up-regulation of Par14 in these phases **(Fig. 3.10)**.

We saw ~ 5-fold increase in the translational expression of Par17 during the G1 phase and ~ 4- and 5-folds increases at the S and G2/M phases respectively **(Fig. 3.11)**. The expressions of the 24 and 28 kDa species were almost constant throughout G1, S and G2/M phases. The increase of Par17 protein expression is directly proportional to the transcriptional increase of its mRNA during the S and G2/M phases of the cell cycle **(Fig. 3.9)**. The occurrence of the 28 kDa species made us to investigate if the same scenario will occur when HFF cells were fractionated into cytosol, nuclei and mitochondria.

The nucleus is not the physiological compartment of Par17 but the mitochondria (Kessler et al., 2007). The observation of protein expression in the nuclear fraction can be justified by the fact that this fraction was impure and did not only contain nu-

clear proteins but also contained cell debris and unbroken cells. This should explain the presence of Par17, which was seen in the nuclear fractions during G1 and G2/M phases. The expression of Par17 in the mitochondria during the G0 and G1 phases was approximately constant but an almost null expression was observed during the S and an almost constant expression in the G2/M phases in the mitochondria. We also saw the almost constant expression of the 28 kDa variant throughout the phases of the cell cycle in the cytosol, nuclei and mitochondria in a similar manner observed when unfractionated cellular lysates were used.

At the time when our group was characterising Par17 as a novel isoform of Par14, they acknowledged the occurrence of the 28 kDa band in cellular lysates (Mueller et al., 2006). They purported a potential SUMOylation or ubiquitylation as possible post-translational modifications. They argued this because of the 11 kDa difference in the molecular weights of endogenous Par17 and this putative modified varaint weighing 28 kDa. Western blot analyses with antibodies for SUMO und ubiquitin failed to detect this 28 kDa in cellular lysates. We observed this 28 kDa variant of Par17 in our cell cycle experiments. We also saw an increase in the transcriptional up-regulation of Par17 in the S and G2/M phases, which was proportional to the amount of the protein expressed in these phases when the cells were not fractionated into cytosol, nucleus, and mitochondria. Upon cellular fractionation, we saw a tendential down-regulation of Par17 in the S and G2/M phases in the mitochondria. The mitochondrion is the physiological compartment of Par17. Therefore, we can speculate that total Par17 mRNA is expressed as the sum of Par17 protein plus Par17 protein variant of 28 kDa.

$$|Par17\ mRNA| = |Par17\ Protein| + |Par17\ Protein\ variant\ of\ 28\ kDa|$$

4.3 Protein-Protein Interactions of Par14/Par17

A considerable body of caution should be exercised when analysing data obtained from affinity purification combine with mass spectrometry (AP-MS) experiments. One reason for this is the presence of false positive interactors and the absence of real interactors (false negatives).

4.3.1 Filtering out Spurious and Non-specific Interactors of Par14/Par17

Table 3.1 shows chaperone proteins and α-actin that were identified. Ribosomal proteins, tubulin, actin, and chaperones exhibit a relative high abundance in the cell (Gingras et al., 2007). Thus, they are often considered as false positives or promiscuous proteins. Moreover, chaperones and heat-shock proteins bind to unfolded peptides, as it might be the case for misfolded bait proteins that are usually overexpressed as compared to their endogenous counterparts (Berggard et al., 2007). Therefore, we excluded all the chaperone proteins identified.

With reservation, the protein disulfide isomerases listed on **Table 3.1** could be biological contaminants. We argue this because the physiological cellular localisation of Par14 is the cytosol and nucleus (Reimer et al., 2003; Surmacz et al., 2002) and Par17 has been shown to be predominantly targeted to the mitochondrial matrix and to a lesser extend to the cytoplasm (Kessler et al., 2007). Protein disulfide isomerases are enzymes present in the endoplasmic reticulum that catalyse the formation and breakage of disulfide bonds between cysteine residues within proteins as they fold (Gruber et al., 2006). Based on this sub-cellular localisation difference, it is presumable to say that they are non-physiological targets to Par14 or to Par17 and probably must have associated with them during cell lysis, hence, their identification. In addition, P4HA2 (prolyl 4-hydroxylase, alpha polypeptide II) has been found as a contaminant in an affinity purification combined with mass spectrometry experiment (Glatter et al., 2009). This gives more weight to our argument to exclude the protein disulfide isomerases from our list of potential interactors to Par14/Par17. The peptidyl-prolyl isomerases PPIA and PPIB identified are potential biological false positives because they show chaperone-like activity and are abundantly present. In addition, PPIB is localised to the endoplasmic reticulum justifying them not to be physiological interactors to Par14 or Par17.

A decoy database is incorporated into the Mascot search engine. A decoy (false) is used to test the null hypothesis. This will determine whether a peptide was not identified in mass spectrometry (Bianco et al., 2009). It is useful in filtering off incorrect identifications found in the target search and hence eliminating false positives. In doing this, all the amino acids of the source sequence are shuffled by arranging them randomly or the protein sequence of the source database is simply reversed. In consequence hereof, we elimated the following proteins from being potential

Par14/Par17 interactors as listed on **Table 3.1**: SPTAN1 (SHD00871535), NCAPG2 (SHD00797030) and NOMO1 (SHD00413732). SDH stands for decoy shuffled proteins and it is the identifier used to search for such proteins in IPI (Internation Protein Index) databases. However, SPTAN1 (spectrin) was identified in a yeast two-hybrid screen as an interaction partner to Par14/Par17 (Stelzl et al., 2005). Based on these two contracding findings, we are in quandary on how to deal with SPTAN1.

The exclusion of biological-based false positives is not sufficient in shortlisting potential interactors of Par14/Par17 without looking at the possibility of the presence of technique-dependent contaminants. The proteins reported on **Table 3.1** are only those, which agreed with our probability-based scoring model and where not present in the negative control. Moreover, since a differential protein determination was done, proteins identified in the pull-downs with the Par17QR*Strep*-GFP construct, and the Par17QR-GFP construct (negative control) were not considered **(Table 4.1)**. These proteins were classified into two main groups. One group contained proteins of keratin cytoskeletal origin. These proteins were considered to be technical contaminants. The other group embodied non-specific binders, which were believed to have probably interacted with the *Strep*-Tactin affinity column.

Table 4.1 Proteins identified in both Par17-tagged and non-tagged Par17

Protein	Accession	Scores	Peptides	MW (kDa)
Technical contaminants				
Keratin, type II cytoskeletal 1	IPI00220327	591.0	12	66.0
Keratin, type I cytoskeletal 10	IPI00009865	436.1	12	58.8
Keratin, type I cytoskeletal 9	IPI00019359	406.0	11	62.0
Keratin, type II cytoskeletal 2 epidermal	IPI00021304	257.4	7	65.8
Non-specific binders				
Fructose-bisphosphate aldolase A	IPI00465439	117.8	3	39.4
cDNA FLJ53060, moderately similar to PPIA	IPI00910407	64.1	2	14.0
Histone H4	IPI00453473	115.5	3	11.4
PA2G4 41 kDa protein	IPI00794875	107.4	3	41.2
SET translocation	IPI00917753	109.4	2	31.0

The differential protein determination approach applied herein had also been successfully used in an integrated workflow for charting the human interaction proteome that gave insights into the PP2A system (Glatter et al., 2009). Glatter and co-workers excluded potential binders to GFP or to the modified streptavidin column in their tandem affinity purification experiments (SH-tag consisting of a streptavidin-binding peptide and hemagglutinin epitope). Protein IDs were filtered against a contaminant database obtained from a total of eight independent SH-eGFP control purifications ana-

lysed by 16 LC-MS/MS experiments and mapped to non-redundant entrez gene IDs (Glatter et al., 2009). Inspecting their supplementary table 2, which contains a list of contaminant proteins observed in SH-eGFP control purifications, we took into account the following proteins: ACTB (IPI00021439), EEF1A2 (IPI00014424), HSPA9 (IPI00007765) and NCAPG2. We double-checked this with our data and we found corresponding proteins or proteins that were highly similar for them. ACTB corresponded to our protein IPI00894365 described as highly similar to cytoplasmic actin. EEF1A2 matched to our IPI00556204 defined as eukaryotic elongation translation factor 1 alpha 2 and HSPA9 fitted to our IPI00922694 termed as highly similar mitochondrial Stress-70 protein. NCAPG2 was the same found in our experiment and in the data of Glatter and co-workers. NCAPG2 is for the second time herein mentioned as a potential false positive. In this vain, we excluded ACTB, EEF1A2, HSPA9, and NCAPG2 from our list of potential interaction partners of Par14/Par17. We speculate that they are either abundantly present or sticky proteins, which most likely interacted with the *Strep*-Tactin column (Gravel and Narang, 2005).

4.3.2 Par14/Par17 Interactors

After the exclusion of possible false interactors of Par14/Par17 as described in **Section 4.3.1**, we were left with 17 proteins that could be possible physiological interactors to both parvulins proteins **(Fig. 4.1)**. We will not deal with all of these proteins since their validation is still pending if indeed they are *bona fide* interacting partners of Par14/Par17. We will make mention of a few that suggest Par14/Par17 involvement in the cytoskeletal network.

The high score of 388.8 for EZR seen in our affinity purification and mass spectrometric analyses suggests a possible interaction with Par14/Par17. This implied that the probability that the 14 identified peptides for EZR occurring by chance was less than one in twenty; $p < 0.05$ (Perkins et al., 1999). EZR was first isolated and identified as a protein located under the plasma membrane of chicken intestinal microvilli (Bretscher et al., 2002). Moreover, EZR has also been shown to be mostly associated with various membrane and cytoskeletal components such as CD44, EPB50 and of F-actin (Bretscher et al., 1997). The ERM (ezrin, radixin, and merlin) domain is common to both ERZ and protein 4.1 (EPB41). EPB41 was reported in a high-throughput co-immunoprecipitation and mass spectrometry screen to interact with

Par14/Par17 (Ewing et al., 2007). This 97 kDa protein, which is essential for normal cell shape and integrity, provides connections between the cytoskeleton and the plasma membrane in erythrocytes, but also plays an important role in a variety of functions in many tissues/organs, including the bone marrow, cerebellum, lungs, testes and thymus (Taylor-Harris et al., 2005). EPB41 and EZR belong to the protein 4.1 superfamily. All the members of the protein 4.1 superfamily contain the ERM domain at the N-terminus (Diakowski et al., 2006). Following the line of thinking that EPB41 is an interactor to Par14/Par17 and we have reported in this study a potential interaction between EZR and Par14/Par17, it is intriguing to purport that the ERM domain might serve as a binding site for Par14/Par17 and thus justifying the herein observed interactions. Others have also reported that the ERM domain is responsible for the binding of EPB41 to other proteins such as glycophorin C (Gascard and Cohen, 1994; Hemmings et al., 1996), protein p55 (Manno et al., 2005; Marfatia et al., 1994) and calmodulin (Nunomura et al., 2000).

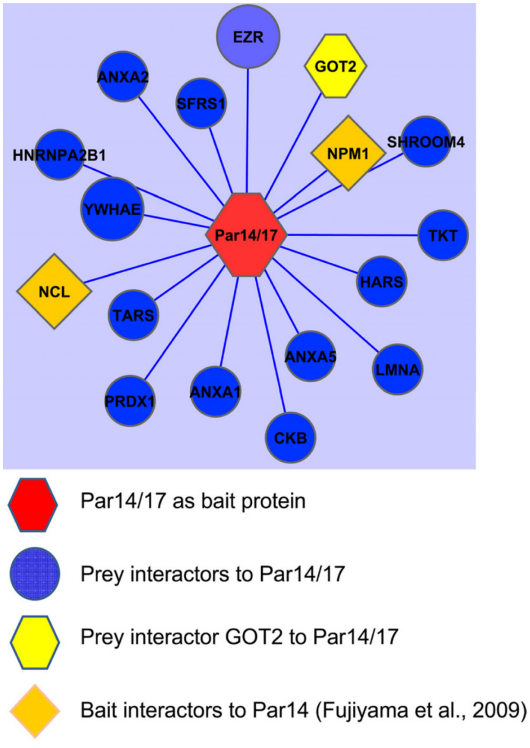

Fig 4.1 Protein-protein interactions of Par14/Par17

Map of Par14/Par17 depicting its physical association with affinity-purified proteins detected by tandem mass spectrometry. The hexagonal node in red, Par14/Par17 served as the bait protein and the ellipse nodes in blue were the captured prey proteins. GOT2 as a node in the yellow hexagon was identified as a prey protein, which interacted with Par14/Par17 in this study and has been shown to interact with MPG and EPB41 (Ewing et al., 2007). The

diamond node in orange are prey proteins found in this study and have been previously found in a GST-Pull-down screen (Fujiyama-Nakamura et al., 2009). The edges in blue depict the link between the nodes of the bait and prey proteins. The line between two nodes is described as an edge. The visualisation was done using the software Cytoscape-v2.6.3 (Cline et al., 2007).

In this study, we showed that cDNA FLJ55705 highly similar to threonyl-tRNA synthetase (IPI00910719, TARS), and cDNA FLJ59476 highly similar to histidyl-tRNA synthetase (IPI00909075, HARS) co-purified with Par14/Par17 **(Table 3.1 and Fig. 4.1)**. In the light of this, the binding of EPB41 to eIF3-p44 suggested an interaction between the cytoskeletal network and the translation apparatus (Hou et al., 2000). eIF3-p84 represents a subunit of the eukaryotic translation initiation factor 3 (eIF3) complex (Block et al., 1998). The eIF3 is a large translation initiation complex that contains at least 10 subunits. It plays an essential role in the binding of the initiator methionyl-tRNA and mRNA to the 40S ribosomal subunit to form the 40S initiation complex (Hershey et al., 1996). Large body of evidences have pointed to the fact that EZR and EPB41 are cytoskeletal proteins with their roles in cell shape, adhesion, motility et cetera (Sylvain et al. 2009). The potential association of Par14/Par17 with EZR, EPB41, TARS, and HARS may suggest that Par14/Par17 acts as an anchor protein that links the cytoskeleton network to the translation apparatus. However, this suggestion stills remains to be validated.

4.3.3 The Par14/Par17 Interactome

We now have a list of 17 potential interaction partners of Par14/Par17 as revealed from our affinity purification coupled with mass spectrometric analysis. With this knowledge, we reasoned that it would be worthwhile to combine our data with all experimentally proven interactors of Par14/Par17. For this purpose, we used the protein-interaction IntAct-database (Aranda et al., 2010), iHOP (Information Hyperlinked over Proteins) database (Hoffmann and Valencia, 2004; Hoffmann and Valencia, 2005) and the Entrez Gene database (Maglott et al., 2005) to identify previously reported interactors of Par14/Par17.

Fig. 4.2 shows all these reported interactions of Par14/Par17 with other proteins. MPG (N-methylpurine-DNA glycosylase) and EPB41 have been shown to interact with Par14/Par17 (Ewing et al., 2007). The white parallelogram nodes for HSPE1

heat shock 10 kDa protein 1 (chaperonin 10), IARS (isoleucyl-tRNA synthetase), CACYBP (calcyclin binding protein), PSMA1 (proteasome macropain subunit, alpha type 1) and MIF (macrophage migration inhibitory factor) are interactors common both to MPG and EPB41 (Ewing et al., 2007). Ewing and co-workers also demonstrated that Pin1 (white parallelogram) interacted with EPB41. Since Pin1 is a paralogue to Par14/Par17 (Mueller and Bayer, 2008), it was interesting to acknowledge the fact that it also interacts with EPB41. In a yeast two-hybrid assay, Stelzl and co-authors reported that DNM1 (dynamin), EZH2 (enhancer of zeste homolog 2), ASCC2 (activating signal cointegrator 1 complex subunit 2), and SPTAN1 interacted with Par14/Par17 (Stelzl et al., 2005). FBL (fibrillarin), NPM1 (nucleophosmin) and NCL (nucleolin) were reported in a GST-Pull-down study to be interactors of Par14 (Fujiyama-Nakamura et al., 2009). We also identified NPM1 and NCL in this study.

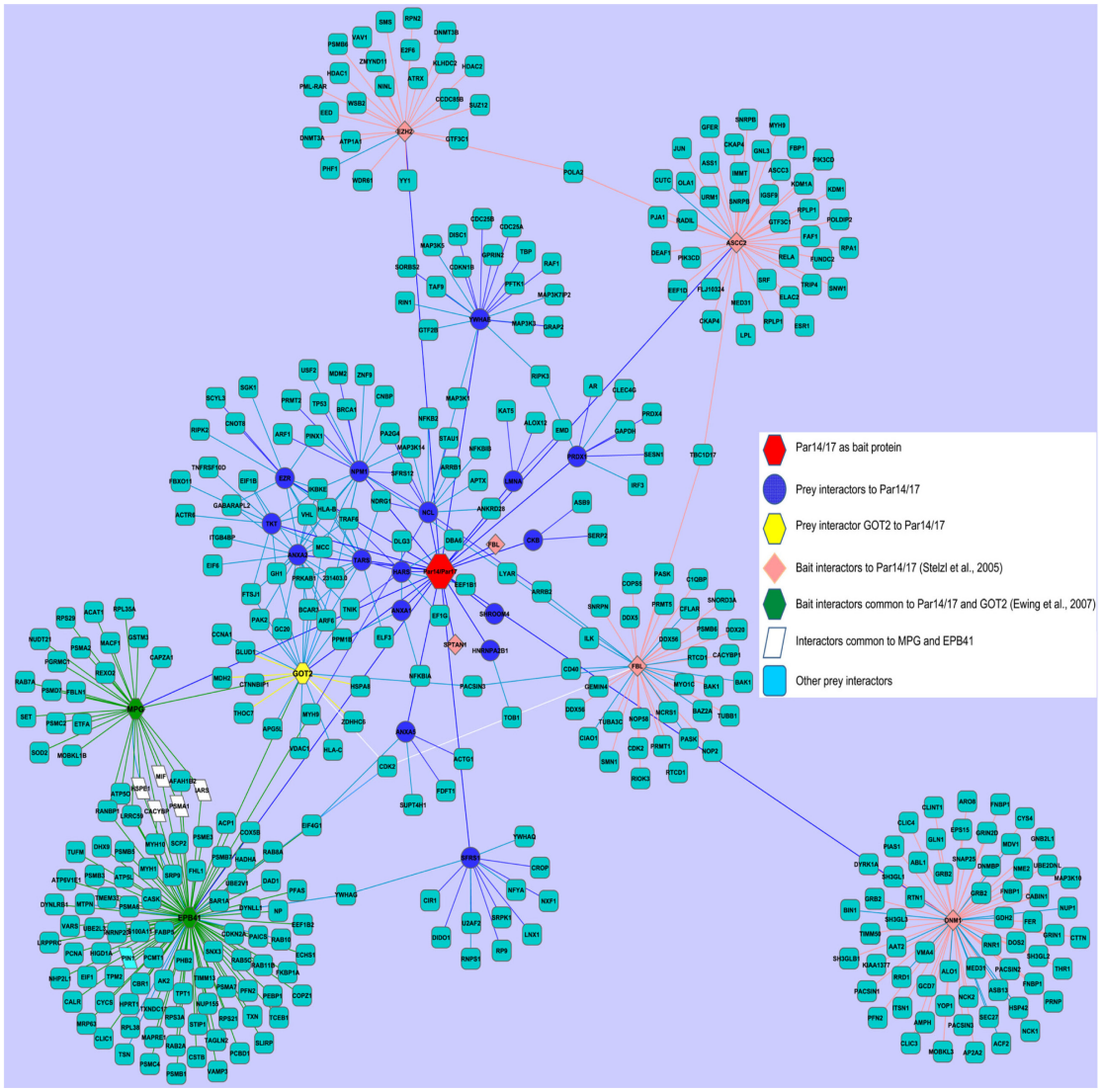

Fig 4.2 The Par14/Par17 interactome map

The network involves 408 proteins (nodes) linked via 480 interactions (edges). The line between two nodes is described as an edge. Par14/Par17 is the node in the red hexagon. Ellipse blue nodes are prey interactors to Par14/Par17 found in this study and pink diamond nodes are bait proteins that directly interacted with Par14/Par17 in a yeast two-hybrid system (Stelzl et al., 2005). Nodes in the green hexagon are proteins that co-immunoprecipitated with Par14/Par17 (Ewing et al., 2007). GOT2 as a node in the yellow hexagon was identified as a prey protein, which interacted with Par14/Par17, MPG and EPB41 indicating an interesting interaction complex. The white parallelogram nodes are proteins, which interacted with both MPG and EPB41. Other prey interactors are depicted as roundrect nodes in light green. The visualisations were done using the software Cytoscape-v2.6.3 (Cline et al., 2007).

Table 4.2 Par14/Par17 interactors independently identified by other methods and found in this study.

Common interactors identified in one or more approaches are represented as shaded blocks in light yellow, pale and sky blue respectively.

Bait	Prey	Method of Detection	Reference
Par14/Par17	NCL	AP-MS	This study
Par14	NCL	GST-Pull-Down	Fujiyama et al. (2002; 2009)
Par14/Par17	NPM1	AP-MS	This study
Par14	NPM1	GST-Pull-Down	Fujiyama et al. (2002; 2009)
Par14/Par17	YWHAE	AP-MS	This study
Par14	YWHAE	GST-Pull-Down and Co-IP	Doctoral Thesis Tatiana Reimer
Par14/Par17	GOT2	AP-MS	This study
EPB41	Par14/Par17	Co-IP-MS	Ewing et al. (2007)
MPG	Par14/Par17	Co-IP-MS	Ewing et al. (2007)

From the interactome map of Par14/Par17 **(Fig. 4.2 and Table 4.2)**, three sub-networks can be deduced. One of them is the ASCC2, POLA2 polymerase (DNA directed, alpha 2 70kD subunit), EZH2 and Par14/Par17 network. NCL, NPM1, and Par14 also show reciprocal interactions. We also acknowledge a Par14/Par17-EPB41-GOT2-MPG network.

4.3.4 Par14/Par17 Sub-Interactome Networks

4.3.4.1 The ASCC2-POLA2-EZH2-Par14/Par17 Network

As a bait protein, ASCC2 interacted with the prey protein POLA2 in a yeast two-hybrid screen (Stelzl et al., 2005). In the same study, EZH2 as a bait served to catch the prey protein POLA2. Noteworthy was the fact that these two bait proteins ASCC2 and EZH2 captured Par14/Par17 as a prey in the said study (Stelzl et al., 2005). The mutual interaction between Par14/Par17 with ASCC2 and EZH2 and the interaction of POLA2 to ASCC2 and EZH2 lead to the speculation that Par14, Par17, or both could as well have interacted with POLA2 within the framework of a complex.

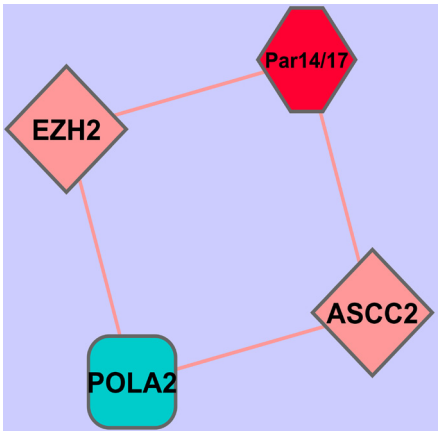

Fig 4.3 The ASCC2-POLA2-EZH2-Par14/Par17 network

ASCC2 was shown to be part of a novel transcriptional co-activator complex (Jung et al., 2002). Histone-lysine N-methyltransferase EZH2 is a member of the Polycomb-group (PcG) family and members form multimeric protein complexes, which are involved in maintaining the transcriptional repressive state of genes over successive cell generations (van, V and Otte, 1999). Evidence has also been provided that POLA2 is required for the initiation of SV40 DNA replication *in vitro* and was suggested to play a similar role in cellular DNA replication (Collins et al., 1993; Weinberg et al., 1990). Up to now, nothing is known if Par17 is a nuclear protein but its isoform Par14 has been reported to be located in the nucleus (Surmacz et al., 2002). However, both of them are reported to bind DNA (Kessler et al., 2007; Surmacz et al., 2002). ASCC2, EZH2, and POLA2 are nuclear proteins and this warrants the speculation that in this scenario Par14 could have been the interactor instead of Par17. Nevertheless, experimental data will be mandatory to validate this assertion.

4.3.4.2 The NCL-NPM1-Par14 Network

In our affinity purification followed by mass spectrometry experiments, we observed that NCL and NPM1 associated with Par14/Par17 **(Table 4.2)**. Comprehensive proteomic-scale analyses with the aid of LC/MS/MS showed that Par14 is an interactor to both NCL and NPM1 (Fujiyama et al., 2002; Fujiyama-Nakamura et al., 2009). In the same study, they also reported that Par14 was localised to the nucleolus. Furthermore, NCL and NPM1 were shown in a yeast-two-hybrid screen to interact with each other (Li et al., 1996).

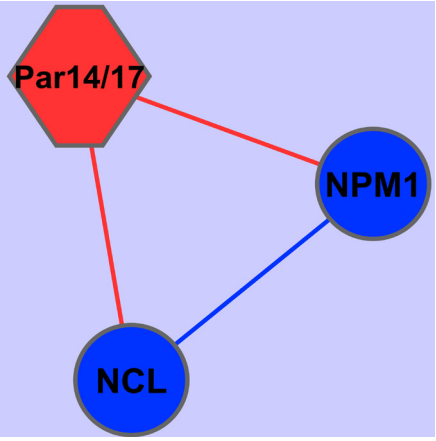

Fig 4.4 The NCL-NPM1-Par14 network

NCL is a nucleolar phosphoprotein involved in the regulation of cell proliferation, cytokenesis, replication, embryogenesis, and nucleogenesis (Jordan, 1987; Srivastava and Pollard, 1999). NCL is expressed on the cell surface and has been demonstrated to associate with actin cytoskeleton (Hovanessian et al., 2000). NMP1 on its part is also a nucleolar phosphoprotein constantly shuttling between the nucleolus and the cytoplasm (Borer et al., 1989). The main function of NPM1 is in ribosome biogenesis. NMP1 associated with large RNA-ribonucleoprotein complexes containing nucleolin, fibrillarin, and several ribosomal proteins (Pinol-Roma, 1999). Based on the lines of evidence presented above and the nucleolar localisation of NCL and NPM1, it is acceptable to speculate they are interactors to Par14 and not Par17.

4.3.4.3 The Par14/Par17-EPB41-GOT2-MPG Network

We showed in this work that mitochondrial GOT2 possibly associated with Par14/Par17. Co-immunoprecipitation coupled with high-throughput mass spectrometry revealed that GOT2 interacted with EPB41 and MPG (Ewing et al., 2007). In the same high-throughput analysis, EPB41 and MPG were observed to have interacted with Par14/Par17 respectively. This cross-interaction between EPB41 and MPG each interacting with Par14/Par17 and GOT2 respectively and the association of Par14/Par17 and GOT2 proposes a large body of evidence that EPB41, MPG, GOT2 and Par14/Par17 display a socio-affinity (physical proximity). This proposition should be assimilated with a pinch of salt. We say this because GOT2 plays a role in amino acid metabolism and the urea and tricarboxylic acid cycles. Berggard and co-authors mentioned that metabolic enzymes could be a source of contaminating pro-

teins in protein-protein interaction studies because they are often present in large amounts in the cell (Berggard et al., 2007). This might also imply that GOT2 is a potential false positive that has been observed in these two independent approaches.

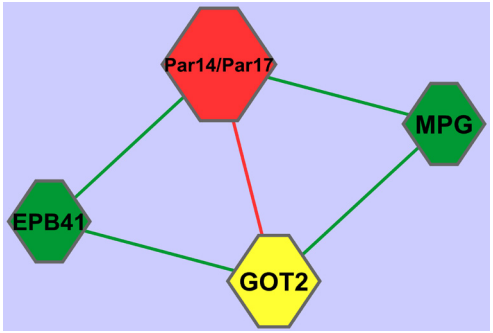

Fig 4.5 The Par14/Par17-EPB41-GOT2-MPG network

N-methylpurine DNA glycosylase (MPG) is an initiator glycosylase in base excision repair (BER) and it is the principal mechanism by which mammalian cells repair alkylation damage in DNA (Krokan et al., 2000). BER appears to be the predominant DNA repair system in the mitochondria (Fishel et al., 2003; Harrison et al., 2007). MPG is a glycosylase that cleaves the N-glycosylic bond between the deoxyribose sugar moiety and the DNA base that is damaged but does not nick the DNA backbone (Fishel et al., 2003). Repair of mitochondrial DNA (mtDNA) is crucial because it suffers more damage than nuclear DNA after treatment with oxidative or alkylating agents (Fishel et al., 2003). In addition to being subjected to more damage, the mutation rate is also 5 – 10 times higher in mtDNA (Fishel et al., 2003). We now know that GOT2 and MPG are of mitochondrial origin. Kessler and co-workers demonstrated that Par17 is targeted to the mitochondrial matrix (Kessler et al., 2007). Our current knowledge does not allow us to assign EPB41 as a mitochondrial protein. However, with the lines of arguments herein presented, we could presume that the interactions of GOT2, MPG, EPB41, if true, within the framework of a complex was with Par17 and not Par14.

We have gone to a certain length in analysing some of the possible interaction partners of Par14/Par17 identified in this work. We also explored the Par14/Par17 interactome und its embodied sub-networks. Now, we will look at a common thread that some members of the Par14/Par17 interactome share in common.

4.3.5 Par14/Par17 Interactors and the Lysine Acetylome

The lysine acetylome describes the conglomerate of proteins in the cell that have been acetylated on one or more lysine residues. In a high-resolution mass spectrometry approach, Choudhary and co-workers reported 3600 lysine acetylation sites on 1750 proteins and quantified acetylation changes in response to the deacetylase inhibitors suberoylanilide hydroxamic and MS-275 (Choudhary et al., 2009). Par14/Par17 was reported in the mentioned approach to be acetylated on lysine K32 and K57 with respect to Par14 and Par17 respectively. The acetylation site (_AQGPK (ac) GGGNAVK_) is four amino acids less in front of the NMR resolved catalytic (PPIase) domain structure (Sekerina et al., 2000; Terada et al., 2001) of Par14/Par17. The PPIase domain is characterised by four-stranded α-sheets and three α-helices and it has been reported that acetylation sites were frequently located in regions with ordered secondary structure (Kim et al., 2006).

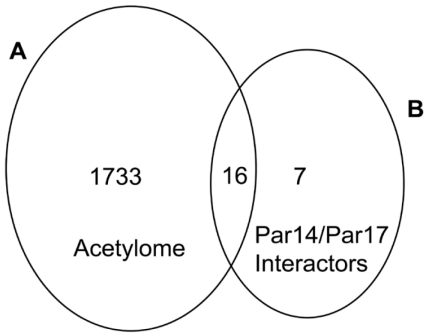

Fig 4.6 Venn diagram of Par14/Par17 interactors and the lysine acetylome

Showing 16 proteins (point of intersection) found in our affinity purification coupled with mass spectrometry studies and from the yeast-two hybrid screen and co-immunoprecipitation experiments of Stelzl and colleagues (Stelzl et al., 2005) and Ewing and co-authors (Ewing et al., 2007) respectively. These 16 proteins were also found to be acetylated in the study of Choudhary and co-workers (Choudhary et al., 2009). **A)** 1750 acetylated proteins found in the Choudhary study **B)** 23 Par14/Par17 interactors found in this study and in previously reported data. The list of the 17 proteins is found on Supplementary Table 2.

Looking at the Par14/Par17 interactome in a nutshell, 16 of its interacting proteins are acetylated (13 of them from **Fig. 4.1**), DMN1 and SPTAN1 from the two-hybrid-screen of (Stelzl et al., 2005) and EPB41 from the co-immunoprecipitation studies of (Ewing et al., 2007). No reported acetylation of MPG is known to our knowledge but a

similar repair protein UDG (Uracil-DNA glycosylase) was reported to be acetylated (Choudhary et al., 2009). For this reason, we added MPG to the list on the **Supplementary Table 2**. The acetylation of lysines can create new docking sites for protein–protein interactions, for example via recognition by the bromo-domain containing proteins (Spange et al., 2009). Moreover, a striking feature of lysine acetylation is that it tends to occur in large macromolecular complexes involved in diverse cellular processes, such as chromatin remodelling, cell cycle, splicing, nuclear transport, and actin nucleation (Choudhary et al., 2009). Based on this line of argument, we can speculate that Par14/Par17 and its acetylated interactors might exist as a complex with bromo-domain-containing proteins in the cell. However, experimental evidence will be paramount to prove this claim.

The search of interaction partners of Par14/Par17 were followed by knock-down experiments. The aim behind these knock-down trials was to verify any phenotypic changes like morphological aberrations in cells in the advent of the absence of Par14/Par17. Moreover, it was intended to check if the potential physiological partners found in this study might be up- or down-regulated in the case of a Par14/Par17 knock-down. This was to be verified by DNA microarray analyses.

4.4 Par14/Par17 Gene Knock-Down Experiments

To elicit knock-down, we first used double-stranded Par14/Par17 siRNAs in a pool. As it can be seen on **Fig. 3.16A**. HeLa cells treated with Par14/Par17 siRNAs looked the same as cells treated with scrambled siRNA with no known homology to any human gene. This was also the case when untreated HeLa cells were compared. The treatment with scrambled siRNA and non-treatment served as negative controls. We next checked the level of knock-down at the protein level by performing western blots. Transfections with these siRNAs were done for 48, 72, 96 hrs, and still no appreciable reduction of Par14/Par17 could be recorded when compared with the controls samples **(Fig. 3.16B)**.

After seeing no morphological abnormalities and no reduction at the protein levels in cells treated with Par14/Par17 double-stranded siRNAs, we employed plasmid-based siRNA technology as a second strategy. Nevertheless, we had similar observations that we experienced with the synthetic double-stranded Par14/Par17 siRNAs.

Fig. 3.17A revealed minor or no morphological changes in HeLa cells treated with shRNA-1-3 and cells treated with shRNA-Luc that served as negative control. However, what struck our attention was the presence of granule-like structures in both treated and untreated HeLa cells. The protein expression of Par14/Pa417 did not suffer any changes when comparing the experimental samples with the control samples **(Fig. 3.17B)**.

After observing no knock-down at the protein level with the use of two different strategies of siRNA technology, we aimed at looking at the efficiency of knock-down at the mRNA level. We used qRT-PCR and the calculation of percentage knock-down has been elucidated in **Section 3.5**. We observed a 10 % KD for shRNA-2 **(Fig. 3.17C**). This was the only knock-down worth mentioning when comparing the knock-down seen with shRNA-1 and shRNA-3. The knock-down with shRNA-Luc for Par14 and Par17 approached null and two respectively. siRNA-Luc was used as a negative control and no knock-down was to be expected. A knock-down of 10 % is not enough to evaluate the effects of the absence of a gene. Follow-up experiments of at least $\geq 80\,\%$ gene knock-down are usually recommended. A more than 80 % knock-down of Par14 mRNA and protein has been reported (Fujiyama-Nakamura et al., 2009). The authors demonstrated that Par14 knock-down decelerated the processing of pre-rRNAs to 18S and 28S rRNAs and had a diminishing effect on cell growth.

5. Conclusion

Using different biochemical fractionation schemes, we showed that Par14 is 3 and 2-fold enriched in chromatin fractions (S2+/S2-) than in nuclear matrix fractions (S2+/S2-) respectively. The binding of Par14 to DNA *in vivo* was investigated. By means of the fractionation of nucleic-acid binding proteins and their elution with increasing salt concentrations from a phospho-cellulose column, we demonstrated that Par14 bound to DNA in the nucleus. We went further to search for the DNA-binding motifs of Par14 and Par17. For this purpose, we used a Par17QR-*Strep*-GFP and Par17QR-GFP construct, the latter serving as a negative control. A substaintial amount of DNA fragments were pulled-down with the Par17QR-*Strep*-GFP construct than with the control construct but we did not determine the sequences of the inserted DNA fragments.

We also investigated the transcriptional and translational regulation of Par14/Par17 in synchronised HFF cells. With the use of qRT-PCR, we acknowledged a 3- and 5-fold increase in the mRNA of Par17 during the S and G2/M phases in correlation with a tendential 4- and 3-fold up-regulation of the Par17 protein in these phases as seen in western blot experiments and in subsequent dentitiometric analyses. There was the occurrence of a 28 kDa variant of Par17 in both unfractionated and fractionated cellular lysates in G0, G1, S and G2/M phases of the cell cycle. We hypothesise that the amount of mRNA expressed is mirrored by the sum of Par17 and the 28 kDa variant post-transcriptionally expressed. As for Par14, there was a 2- and 3-fold increase of Par14 mRNA in the S and G2/M phases of the cell cycle. This transcriptional up-regulation of Par14 was reciprocated by a 4-fold translational up-regulation in the S and G2/M phases when unfractionated cellular lysates were used.

Our protein-protein interaction studies using affinity purification combined with mass spectrometry revealed 17 potential interaction partners to Par14/Par17. Some of these proteins are involved in translation, RNA processing, ribosome biogenesis, cell adhesion, signal transduction and metabolism. GOT2 and EZR were of interest. GOT2 was reported to interact with Par14/Pa17 in a co-immunoprecipitation study (Ewing et al., 2007). EZR had a score of 388.8 with 14 of its peptides found and it shares a common homology domain ERM with EPB41. EPB41 was found to interact

with Par14/Par17 in a co-immunoprecipitation combined with mass spectrometry high-througput experiment (Ewing et al., 2007). NCL and NMP1 previously reported to interact with Par14 (Fujiyama et al., 2002; Fujiyama-Nakamura et al., 2009) were also found in our AP-MS screens. Besides, we reported the interaction of YWHAE and Par14/Par17. This same interaction had been demonstrated in GST-Pull-downs and Co-IP studies (Doctoral thesis of Tatiana Reimer).

The use of double-stranded siRNAs and shRNAs did not invoke the knock-down of Par14/Pa17 either at the mRNA or protein levels. We observed only a 10 % knock-down at the transcriptional level when shRNA-2 was used in HCT116 cells.

6. Future Perspectives

We suggest that the ChAP experiment used to search for DNA-binding motifs for Par14/Par17 to be repeated after a thorough trouble shooting analysis. As a complementary experiment, not only Par17QR-*Strep*-GFP construct but also a Par14-*Strep*-GFP construct should be used in order to achieve a clean discrimination of the DNA-binding motifs for both proteins. In this light, nuclear and mitochondrial extracts should be used for Par14 and Par17 respectively.

The fractionation of the cellular lysates from the phases of the cell cycle into cytosol and nucleus was absent for Par14. The expression of Par14 after cellular fractionation will be interesting to investigate if it is also up-regulated when cellular lysates were used. Moreover, the identification and charaterisation of the 28 kDa variant of Par17 that was present in all the phases of the cell cycle will be mandatory.

The 17 potential interaction partners to Par14/Par17 need to be validated by other techniques. EZR and GOT2 are favourites for reasons mentioned in **Section 5**. Based on the fact that we used a tagging approach, EZR-*Strep*-GFP or GOT2 *Strep* GFP constructs could be used for affinity purification and mass spectrometry experiments. If we find Par17 or Par14 in the pull-down data, this will add credit to their physiological interaction. Co-immunoprecipitation (Co-IP) is another method to verify the protein-protein interactions. The antibodies for EZR or GOT2 could be employed in Co-IP experiments and the eluates should be probed in western blotting with antibodies specific to both Par14/Par17 (αPPIase) or to Par17 (αPar17-Ext). If we find their respective signals in the eluates, this will give additional evidence that their interaction to Par14/Par17 was *bona fide*.

We could also use spectrometric approaches to validate our protein-protein interaction data. The prerequisite is that the two interacting proteins should exhibit a difference relative to the free individual proteins in any spectrometer (for instance, the fluorescence intensity, wave length maximum or polarisation, fluorescence resonance energy transfer efficiency, circular dichroism, or NMR chemical shift or intensity) (Berggard et al., 2007). Confocal microscopy (Miyashita, 2004) and surface plasmon resonance (Huber and Mueller, 2006) techniques have been reported in the verifica-

tion of protein-protein interaction data. Protein-protein interactions have also been validated with the use of isothermal titration calirometry (Liang, 2008; Velazquez-Campoy et al., 2004). Nevertheless, after the validation of these interactions, distinguishing the interaction partners that belong only to Par14 and to Par17 must be addressed. We propose that mitochondrial lysate obtained after transfection with Par17QR-*Strep*-GFP construct should be used to find Par17 interactors. The same should also be done with nuclear lysates obtained after transfection with Par14-*Strep*-GFP construct to search for Par14 interactors.

Knock-down of Par14/Par17 is still a prerequisite to characterise any associated phenotypic changes. We have ordered three stealth siRNAs (Invitrogen, Germany) to perform new RNAi experiments. Stealth siRNAs are double-stranded siRNAs sequences with a chemical modification that enhances specificity and stability and thus, the half-lives of the siRNA *in vitro* and *in vivo* could be extended. Two of the stealth siRNA sequences have been successfully used by Fujiyama and colleagues in Par14 knock-down studies (Fujiyama-Nakamura et al., 2009) and the sequence of the third stealth siRNA correspond to that with shRNA-2 since it was the only shRNA that showed a reasonable but not enough 10 % KD at the mRNA level. We hope that this time an unequivocal knock-down of Par14/Par17 can be achieved. With a Par14/Par17 knock-down, whole genome microarray analyses can be conducted to determine which genes are up- and down-regulated in the absence of Par14/Par17. The transcriptional status of genes whose gene products we identified to be potential interactors to Par14/Par17 will be worthwhile to verify. If any changes are observed, this will serve as another source of validation of our protein-protein interaction data. The generation of a stable transfection line in DT40 cells in which both Par14/Par17 alleles have been knocked-out by means of Cre-Lox recombination will be an alternative to carry out the planned experiments in the advent of the absence of Par14/Par17.

7. Reference List

Literature Cited

Angelov, D., Bondarenko, V. A., Almagro, S., Menoni, H., Mongelard, F., Hans, F., Mietton, F., Studitsky, V. M., Hamiche, A., Dimitrov, S. et al. (2006). Nucleolin is a histone chaperone with FACT-like activity and assists remodeling of nucleosomes. *EMBO J.* 25, 1669-1679.

Aranda, B., Achuthan, P., am-Faruque, Y., Armean, I., Bridge, A., Derow, C., Feuermann, M., Ghanbarian, A. T., Kerrien, S., Khadake, J. et al. (2010). The IntAct molecular interaction database in 2010. *Nucleic Acids Res.* 38, D525-D531.

Atchison, F. W. and Means, A. R. (2003). Spermatogonial depletion in adult Pin1-deficient mice. *Biol. Reprod.* 69, 1989-1997.

Bayer, E., Goettsch, S., Mueller, J. W., Griewel, B., Guiberman, E., Mayr, L. M. and Bayer, P. (2003). Structural analysis of the mitotic regulator hPin1 in solution: insights into domain architecture and substrate binding. *J. Biol. Chem.* 278, 26183-26193.

Bayer, E., Thutewohl, M., Christner, C., Tradler, T., Osterkamp, F., Waldmann, H. and Bayer, P. (2005). Identification of hPin1 inhibitors that induce apoptosis in a mammalian Ras transformed cell line. *Chem. Commun. (Camb.)*, 516-518.

Berggard, T., Linse, S. and James, P. (2007). Methods for the detection and analysis of protein-protein interactions. *Proteomics.* 7, 2833-2842.

Bianco, L., Mead, J. and Bessant, C. (2009). Comparison of novel decoy database designs for optimizing protein identification searches using ABRF sPRG2006 standard MS/MS datasets. *J. Proteome. Res.*

Block, K. L., Vornlocher, H. P. and Hershey, J. W. (1998). Characterization of cDNAs encoding the p44 and p35 subunits of human translation initiation factor eIF3. *J. Biol. Chem.* 273, 31901-31908.

Borer, R. A., Lehner, C. F., Eppenberger, H. M. and Nigg, E. A. (1989). Major nucleolar proteins shuttle between nucleus and cytoplasm. *Cell* 56, 379-390.

Bretscher, A., Edwards, K. and Fehon, R. G. (2002). ERM proteins and merlin: integrators at the cell cortex. *Nat. Rev. Mol. Cell Biol.* 3, 586-599.

Bretscher, A., Reczek, D. and Berryman, M. (1997). Ezrin: a protein requiring conformational activation to link microfilaments to the plasma membrane in the assembly of cell surface structures. *J. Cell Sci.* 110 (Pt 24), 3011-3018.

Brow, D. A. and Guthrie, C. (1988). Spliceosomal RNA U6 is remarkably conserved from yeast to mammals. *Nature* 334, 213-218.

Brummelkamp, T. R., Bernards, R. and Agami, R. (2002). A system for stable expression of short interfering RNAs in mammalian cells. *Science* 296, 550-553.

Bustin, M. (2001). Chromatin unfolding and activation by HMGN(*) chromosomal proteins. *Trends Biochem. Sci.* 26, 431-437.

Chao, S. H., Greenleaf, A. L. and Price, D. H. (2001). Juglone, an inhibitor of the peptidyl-prolyl isomerase Pin1, also directly blocks transcription. *Nucleic Acids Res.* 29, 767-773.

Chenna, R., Sugawara, H., Koike, T., Lopez, R., Gibson, T. J., Higgins, D. G. and Thompson, J. D. (2003). Multiple sequence alignment with the Clustal series of programs. *Nucleic Acids Res.* 31, 3497-3500.

Choudhary, C., Kumar, C., Gnad, F., Nielsen, M. L., Rehman, M., Walther, T. C., Olsen, J. V. and Mann, M. (2009). Lysine acetylation targets protein complexes and co-regulates major cellular functions. *Science* 325, 834-840.

Cline, M. S., Smoot, M., Cerami, E., Kuchinsky, A., Landys, N., Workman, C., Christmas, R., vila-Campilo, I., Creech, M., Gross, B. et al. (2007). Integration of biological networks and gene expression data using Cytoscape. *Nat. Protoc.* 2, 2366-2382.

Collins, K. L., Russo, A. A., Tseng, B. Y. and Kelly, T. J. (1993). The role of the 70 kDa subunit of human DNA polymerase alpha in DNA replication. *EMBO J.* 12, 4555-4566.

Crenshaw, D. G., Yang, J., Means, A. R. and Kornbluth, S. (1998). The mitotic peptidyl-prolyl isomerase, Pin1, interacts with Cdc25 and Plx1. *EMBO J.* 17, 1315-1327.

Davis, P. K., Ho, A. and Dowdy, S. F. (2001). Biological methods for cell-cycle synchronization of mammalian cells. *Biotechniques* 30, 1322-1.

Diakowski, W., Grzybek, M. and Sikorski, A. F. (2006). Protein 4.1, a component of the erythrocyte membrane skeleton and its related homologue proteins forming the protein 4.1/FERM superfamily. *Folia Histochem. Cytobiol.* 44, 231-248.

Esnault, S., Shen, Z. J., Whitesel, E. and Malter, J. S. (2006). The peptidyl-prolyl isomerase Pin1 regulates granulocyte-macrophage colony-stimulating factor mRNA stability in T lymphocytes. *J. Immunol.* 177, 6999-7006.

Ewing, R. M., Chu, P., Elisma, F., Li, H., Taylor, P., Climie, S., Broom-Cerajewski, L., Robinson, M. D., O'Connor, L., Li, M. et al. (2007). Large-scale mapping of human protein-protein interactions by mass spectrometry. *Mol. Syst. Biol.* 3, 89.

Fanghanel, J. and Fischer, G. (2004). Insights into the catalytic mechanism of peptidyl prolyl cis/trans isomerases. *Front Biosci.* 9, 3453-3478.

Fila, C., Metz, C. and van der, S. P. (2008). Juglone inactivates cysteine-rich proteins required for progression through mitosis. *J. Biol. Chem.* 283, 21714-21724.

Fischer, G., Bang, H. and Mech, C. (1984). [Determination of enzymatic catalysis for the cis-trans-isomerization of peptide binding in proline-containing peptides]. *Biomed. Biochim. Acta* 43, 1101-1111.

Fischer, G., Wittmann-Liebold, B., Lang, K., Kiefhaber, T. and Schmid, F. X. (1989). Cyclophilin and peptidyl-prolyl cis-trans isomerase are probably identical proteins. *Nature* 337, 476-478.

Fishel, M. L., Seo, Y. R., Smith, M. L. and Kelley, M. R. (2003). Imbalancing the DNA base excision repair pathway in the mitochondria; targeting and overexpressing N-methylpurine DNA glycosylase in mitochondria leads to enhanced cell killing. *Cancer Res.* 63, 608-615.

Fujimori, F., Takahashi, K., Uchida, C. and Uchida, T. (1999). Mice lacking Pin1 develop normally, but are defective in entering cell cycle from G(0) arrest. *Biochem. Biophys. Res. Commun.* 265, 658-663.

Fujiyama, S., Yanagida, M., Hayano, T., Miura, Y., Isobe, T., Fujimori, F., Uchida, T. and Takahashi, N. (2002). Isolation and proteomic characterization of human Parvulin-associating preribosomal ribonucleoprotein complexes. *J. Biol. Chem.* 277, 23773-23780.

Fujiyama-Nakamura, S., Yoshikawa, H., Homma, K., Hayano, T., Tsujimura-Takahashi, T., Izumikawa, K., Ishikawa, H., Miyazawa, N., Yanagida, M., Miura, Y. et al. (2009). Parvulin (Par14), a peptidyl-prolyl cis-trans isomerase, is a novel rRNA processing factor that evolved in the metazoan lineage. *Mol. Cell Proteomics.* 8, 1552-1565.

Gascard, P. and Cohen, C. M. (1994). Absence of high-affinity band 4.1 binding sites from membranes of glycophorin C- and D-deficient (Leach phenotype) erythrocytes. *Blood* 83, 1102-1108.

Gemmill, T. R., Wu, X. and Hanes, S. D. (2005). Vanishingly low levels of Ess1 prolyl-isomerase activity are sufficient for growth in Saccharomyces cerevisiae. *J. Biol. Chem.* 280, 15510-15517.

Gingras, A. C., Gstaiger, M., Raught, B. and Aebersold, R. (2007). Analysis of protein complexes using mass spectrometry. *Nat. Rev. Mol. Cell Biol.* 8, 645-654.

Glatter, T., Wepf, A., Aebersold, R. and Gstaiger, M. (2009). An integrated workflow for charting the human interaction proteome: insights into the PP2A system. *Mol. Syst. Biol.* 5, 237.

Goodwin, G. H., Sanders, C. and Johns, E. W. (1973). A new group of chromatin-associated proteins with a high content of acidic and basic amino acids. *Eur. J. Biochem.* 38, 14-19.

Gothel, S. F. and Marahiel, M. A. (1999). Peptidyl-prolyl cis-trans isomerases, a superfamily of ubiquitous folding catalysts. *Cell Mol. Life Sci.* 55, 423-436.

Gravel, R. A. and Narang, M. A. (2005). Molecular genetics of biotin metabolism: old vitamin, new science. *J. Nutr. Biochem.* 16, 428-431.

Grimm, D. (2009). Small silencing RNAs: state-of-the-art. *Adv. Drug Deliv. Rev.* 61, 672-703.

Gruber, C. W., Cemazar, M., Heras, B., Martin, J. L. and Craik, D. J. (2006). Protein disulfide isomerase: the structure of oxidative folding. *Trends Biochem. Sci.* 31, 455-464.

Grum, D., Boom, J. V., Neumann, D., Matena, A., Link, N. M. and Mueller, J. W. (2010). A heterodimer of human 3'-phospho-adenosine-5'-phosphosulphate (PAPS) synthases is a new sulphate activating complex. *Biochem. Biophys. Res. Commun.*

Hanes, S. D., Shank, P. R. and Bostian, K. A. (1989). Sequence and mutational analysis of ESS1, a gene essential for growth in Saccharomyces cerevisiae. *Yeast* 5, 55-72.

Harding, M. W., Galat, A., Uehling, D. E. and Schreiber, S. L. (1989). A receptor for the immunosuppressant FK506 is a cis-trans peptidyl-prolyl isomerase. *Nature* 341, 758-760.

Harrison, J. F., Rinne, M. L., Kelley, M. R., Druzhyna, N. M., Wilson, G. L. and LeDoux, S. P. (2007). Altering DNA base excision repair: use of nuclear and mitochondrial-targeted N-methylpurine DNA glycosylase to sensitize astroglia to chemotherapeutic agents. *Glia* 55, 1416-1425.

Heikkinen, O., Seppala, R., Tossavainen, H., Heikkinen, S., Koskela, H., Permi, P. and Kilpelainen, I. (2009). Solution structure of the parvulin-type PPIase domain of Staphylococcus aureus PrsA--implications for the catalytic mechanism of parvulins. *BMC. Struct. Biol.* 9, 17.

Hemmings, L., Rees, D. J., Ohanian, V., Bolton, S. J., Gilmore, A. P., Patel, B., Priddle, H., Trevithick, J. E., Hynes, R. O. and Critchley, D. R. (1996). Talin contains three actin-binding sites each of which is adjacent to a vinculin-binding site. *J. Cell Sci.* 109 (Pt 11), 2715-2726.

Hennecke, G., Nolte, J., Volkmer-Engert, R., Schneider-Mergener, J. and Behrens, S. (2005). The periplasmic chaperone SurA exploits two features characteristic of integral outer membrane proteins for selective substrate recognition. *J. Biol. Chem.* 280, 23540-23548.

Hennig, L., Christner, C., Kipping, M., Schelbert, B., Rucknagel, K. P., Grabley, S., Kullertz, G. and Fischer, G. (1998). Selective inactivation of parvulin-like peptidyl-prolyl cis/trans isomerases by juglone. *Biochemistry* 37, 5953-5960.

Hershey, J. W., Asano, K., Naranda, T., Vornlocher, H. P., Hanachi, P. and Merrick, W. C. (1996). Conservation and diversity in the structure of translation initiation factor EIF3 from humans and yeast. *Biochimie* 78, 903-907.

Hock, R., Furusawa, T., Ueda, T. and Bustin, M. (2007). HMG chromosomal proteins in development and disease. *Trends Cell Biol.* 17, 72-79.

Hodak, H., Wohlkonig, A., Smet-Nocca, C., Drobecq, H., Wieruszeski, J. M., Senechal, M., Landrieu, I., Locht, C., Jamin, M. and Jacob-Dubuisson, F. (2008). The peptidyl-prolyl isomerase and chaperone Par27 of Bordetella pertussis as the prototype for a new group of parvulins. *J. Mol. Biol.* 376, 414-426.

Hoffmann, R. and Valencia, A. (2004). A gene network for navigating the literature. *Nat. Genet.* 36, 664.

Hoffmann, R. and Valencia, A. (2005). Implementing the iHOP concept for navigation of biomedical literature. *Bioinformatics.* 21 Suppl 2, ii252-ii258.

Horikoshi, M., Himukai, R. and Kuzuhara, T. (2004). [Mechanisms of gene regulation centered on peptidyl prolyl cis-trans isomerase]. *Tanpakushitsu Kakusan Koso* 49, 1195-1203.

Hou, C. L., Tang, C., Roffler, S. R. and Tang, T. K. (2000). Protein 4.1R binding to eIF3-p44 suggests an interaction between the cytoskeletal network and the translation apparatus. *Blood* 96, 747-753.

Hovanessian, A. G., Puvion-Dutilleul, F., Nisole, S., Svab, J., Perret, E., Deng, J. S. and Krust, B. (2000). The cell-surface-expressed nucleolin is associated with the actin cytoskeleton. *Exp. Cell Res.* 261, 312-328.

Hsu, T., McRackan, D., Vincent, T. S. and Gert de, C. H. (2001). Drosophila Pin1 prolyl isomerase Dodo is a MAP kinase signal responder during oogenesis. *Nat. Cell Biol.* 3, 538-543.

Huber, W. and Mueller, F. (2006). Biomolecular interaction analysis in drug discovery using surface plasmon resonance technology. *Curr. Pharm. Des* 12, 3999-4021.

Jordan, G. (1987). At the heart of the nucleolus. *Nature* 329, 489-490.

Jordens, J., Janssens, V., Longin, S., Stevens, I., Martens, E., Bultynck, G., Engelborghs, Y., Lescrinier, E., Waelkens, E., Goris, J. et al. (2006). The protein phosphatase 2A phosphatase activator is a novel peptidyl-prolyl cis/trans-isomerase. *J. Biol. Chem.* 281, 6349-6357.

Jung, D. J., Sung, H. S., Goo, Y. W., Lee, H. M., Park, O. K., Jung, S. Y., Lim, J., Kim, H. J., Lee, S. K., Kim, T. S. et al. (2002). Novel transcription coactivator complex containing activating signal cointegrator 1. *Mol. Cell Biol.* 22, 5203-5211.

Junttila, M. R., Saarinen, S., Schmidt, T., Kast, J. and Westermarck, J. (2005). Single-step Strep-tag purification for the isolation and identification of protein complexes from mammalian cells. *Proteomics.* 5, 1199-1203.

Kessler, D., Papatheodorou, P., Stratmann, T., Dian, E. A., Hartmann-Fatu, C., Rassow, J., Bayer, P. and Mueller, J. W. (2007). The DNA binding parvulin Par17 is targeted to the mitochondrial matrix by a recently evolved prepeptide uniquely present in Hominidae. *BMC. Biol.* 5, 37.

Kim, C. J., Cho, Y. G., Park, Y. G., Nam, S. W., Kim, S. Y., Lee, S. H., Yoo, N. J., Lee, J. Y. and Park, W. S. (2005). Pin1 overexpression in colorectal cancer and its correlation with aberrant beta-catenin expression. *World J. Gastroenterol.* 11, 5006-5009.

Kim, S. C., Sprung, R., Chen, Y., Xu, Y., Ball, H., Pei, J., Cheng, T., Kho, Y., Xiao, H., Xiao, L. et al. (2006). Substrate and functional diversity of lysine acetylation revealed by a proteomics survey. *Mol. Cell* 23, 607-618.

Krishnamurthy, S., Ghazy, M. A., Moore, C. and Hampsey, M. (2009). Functional interaction of the Ess1 prolyl isomerase with components of the RNA polymerase II initiation and termination machineries. *Mol. Cell Biol.* 29, 2925-2934.

Krokan, H. E., Nilsen, H., Skorpen, F., Otterlei, M. and Slupphaug, G. (2000). Base excision repair of DNA in mammalian cells. *FEBS Lett.* 476, 73-77.

Kruse, M., Brunke, M., Escher, A., Szalay, A. A., Tropschug, M. and Zimmermann, R. (1995). Enzyme assembly after de novo synthesis in rabbit reticulocyte lysate involves molecular chaperones and immunophilins. *J. Biol. Chem.* 270, 2588-2594.

Kuzuhara, T. and Horikoshi, M. (2004). A nuclear FK506-binding protein is a histone chaperone regulating rDNA silencing. *Nat. Struct. Mol. Biol.* 11, 275-283.

Laemmli, U. K. (1970). Cleavage of structural proteins during the assembly of the head of bacteriophage T4. *Nature* 227, 680-685.

Leulliot, N., Vicentini, G., Jordens, J., Quevillon-Cheruel, S., Schiltz, M., Barford, D., van, T. H. and Goris, J. (2006). Crystal structure of the PP2A phosphatase activator: implications for its PP2A-specific PPIase activity. *Mol. Cell* 23, 413-424.

Li, H. Y., Xu, Q., Zhu, T., Zhou, J. H., Deng, D. R., Wang, S. X., Lu, Y. P. and Ma, D. (2006). [Expression and clinical significance of Pin1 and Cyclin D1 in cervical cancer cell lines and cervical epithelial tissues]. *Ai. Zheng.* 25, 367-372.

Li, Y. P., Busch, R. K., Valdez, B. C. and Busch, H. (1996). C23 interacts with B23, a putative nucleolar-localization-signal-binding protein. *Eur. J. Biochem.* 237, 153-158.

Liang, Y. (2008). Applications of isothermal titration calorimetry in protein science. *Acta Biochim. Biophys. Sin. (Shanghai)* 40, 565-576.

Liou, Y. C., Ryo, A., Huang, H. K., Lu, P. J., Bronson, R., Fujimori, F., Uchida, T., Hunter, T. and Lu, K. P. (2002). Loss of Pin1 function in the mouse causes phenotypes resembling cyclin D1-null phenotypes. *Proc. Natl. Acad. Sci. U. S. A* 99, 1335-1340.

Livak, K. J. and Schmittgen, T. D. (2001). Analysis of relative gene expression data using real-time quantitative PCR and the 2(-Delta Delta C(T)) Method. *Methods* 25, 402-408.

Lu, K. P. (2004). Pinning down cell signaling, cancer and Alzheimer's disease. *Trends Biochem. Sci.* 29, 200-209.

Lu, K. P., Hanes, S. D. and Hunter, T. (1996). A human peptidyl-prolyl isomerase essential for regulation of mitosis. *Nature* 380, 544-547.

Lu, P. J., Wulf, G., Zhou, X. Z., Davies, P. and Lu, K. P. (1999). The prolyl isomerase Pin1 restores the function of Alzheimer-associated phosphorylated tau protein. *Nature* 399, 784-788.

Maglott, D., Ostell, J., Pruitt, K. D. and Tatusova, T. (2005). Entrez Gene: gene-centered information at NCBI. *Nucleic Acids Res.* 33, D54-D58.

Maleszka, R., Hanes, S. D., Hackett, R. L., de Couet, H. G. and Miklos, G. L. (1996). The Drosophila melanogaster dodo (dod) gene, conserved in humans, is functionally interchangeable with the ESS1 cell division gene of Saccharomyces cerevisiae. *Proc. Natl. Acad. Sci. U. S. A* 93, 447-451.

Mamane, Y., Heylbroeck, C., Genin, P., Algarte, M., Servant, M. J., LePage, C., DeLuca, C., Kwon, H., Lin, R. and Hiscott, J. (1999). Interferon regulatory factors: the next generation. *Gene* 237, 1-14.

Mamane, Y., Sharma, S., Petropoulos, L., Lin, R. and Hiscott, J. (2000). Posttranslational regulation of IRF-4 activity by the immunophilin FKBP52. *Immunity.* 12, 129-140.

Manno, S., Takakuwa, Y. and Mohandas, N. (2005). Modulation of erythrocyte membrane mechanical function by protein 4.1 phosphorylation. *J. Biol. Chem.* 280, 7581-7587.

Marfatia, S. M., Lue, R. A., Branton, D. and Chishti, A. H. (1994). In vitro binding studies suggest a membrane-associated complex between erythroid p55, protein 4.1, and glycophorin C. *J. Biol. Chem.* 269, 8631-8634.

Maruyama, T., Suzuki, R. and Furutani, M. (2004). Archaeal peptidyl prolyl cis-trans isomerases (PPIases) update 2004. *Front Biosci.* 9, 1680-1720.

Mendez, J. and Stillman, B. (2000). Chromatin association of human origin recognition complex, cdc6, and minichromosome maintenance proteins during the cell cycle: assembly of prereplication complexes in late mitosis. *Mol. Cell Biol.* 20, 8602-8612.

Merrill, G. F. (1998). Cell synchronization. *Methods Cell Biol.* 57, 229-249.

Metzner, M., Stoller, G., Rucknagel, K. P., Lu, K. P., Fischer, G., Luckner, M. and Kullertz, G. (2001). Functional replacement of the essential ESS1 in yeast by the plant parvulin DlPar13. *J. Biol. Chem.* 276, 13524-13529.

Miyashita, H., Mori, S., Motegi, K., Fukumoto, M. and Uchida, T. (2003). Pin1 is overexpressed in oral squamous cell carcinoma and its levels correlate with cyclin D1 overexpression. *Oncol. Rep.* 10, 455-461.

Miyashita, T. (2004). Confocal microscopy for intracellular co-localization of proteins. *Methods Mol. Biol.* 261, 399-410.

Model, K., Prinz, T., Ruiz, T., Radermacher, M., Krimmer, T., Kuhlbrandt, W., Pfanner, N. and Meisinger, C. (2002). Protein translocase of the outer mitochondrial membrane: role of import receptors in the structural organization of the TOM complex. *J. Mol. Biol.* 316, 657-666.

Mortz, E., Krogh, T. N., Vorum, H. and Gorg, A. (2001). Improved silver staining protocols for high sensitivity protein identification using matrix-assisted laser desorption/ionization-time of flight analysis. *Proteomics.* 1, 1359-1363.

Mueller, J. W. and Bayer, P. (2008). Small family with key contacts: par14 and par17 parvulin proteins, relatives of pin1, now emerge in biomedical research. *Perspect. Medicin. Chem.* 2, 11-20.

Mueller, J. W., Kessler, D., Neumann, D., Stratmann, T., Papatheodorou, P., Hartmann-Fatu, C. and Bayer, P. (2006). Characterization of novel elongated Parvulin isoforms that are ubiquitously expressed in human tissues and originate from alternative transcription initiation. *BMC. Mol. Biol.* 7, 9.

Nakashima, M., Meirmanov, S., Naruke, Y., Kondo, H., Saenko, V., Rogounovitch, T., Shimizu-Yoshida, Y., Takamura, N., Namba, H., Ito, M. et al. (2004). Cyclin D1 overexpression in thyroid tumours from a radiocontaminated area and its correlation with Pin1 and aberrant beta-catenin expression. *J. Pathol.* 202, 446-455.

Nelson, C. J., Santos-Rosa, H. and Kouzarides, T. (2006). Proline isomerization of histone H3 regulates lysine methylation and gene expression. *Cell* 126, 905-916.

Neve, R. L. and McPhie, D. L. (2006). The cell cycle as a therapeutic target for Alzheimer's disease. *Pharmacol. Ther.* 111, 99-113.

Nunomura, W., Takakuwa, Y., Parra, M., Conboy, J. G. and Mohandas, N. (2000). Ca(2+)-dependent and Ca(2+)-independent calmodulin binding sites in erythrocyte protein 4.1. Implications for regulation of protein 4.1 interactions with transmembrane proteins. *J. Biol. Chem.* 275, 6360-6367.

Perkins, D. N., Pappin, D. J., Creasy, D. M. and Cottrell, J. S. (1999). Probability-based protein identification by searching sequence databases using mass spectrometry data. *Electrophoresis* 20, 3551-3567.

Pinol-Roma, S. (1999). Association of nonribosomal nucleolar proteins in ribonucleoprotein complexes during interphase and mitosis. *Mol. Biol. Cell* 10, 77-90.

Potter, A. J., Ray, S., Gueritz, L., Nunns, C. L., Bryant, C. J., Scrace, S. F., Matassova, N., Baker, L., Dokurno, P., Robinson, D. A. et al. (2010). Structure-guided design of alpha-amino acid-derived Pin1 inhibitors. *Bioorg. Med. Chem. Lett.* 20, 586-590.

Qiao, F., Moss, A. and Kupfer, G. M. (2001). Fanconi anemia proteins localize to chromatin and the nuclear matrix in a DNA damage- and cell cycle-regulated manner. *J. Biol. Chem.* 276, 23391-23396.

Rahfeld, J. U., Rucknagel, K. P., Schelbert, B., Ludwig, B., Hacker, J., Mann, K. and Fischer, G. (1994a). Confirmation of the existence of a third family among peptidyl-prolyl cis/trans isomerases. Amino acid sequence and recombinant production of parvulin. *FEBS Lett.* 352, 180-184.

Rahfeld, J. U., Schierhorn, A., Mann, K. and Fischer, G. (1994b). A novel peptidyl-prolyl cis/trans isomerase from Escherichia coli. *FEBS Lett.* 343, 65-69.

Reimer, T., Weiwad, M., Schierhorn, A., Ruecknagel, P. K., Rahfeld, J. U., Bayer, P. and Fischer, G. (2003). Phosphorylation of the N-terminal domain regulates subcellular localization and DNA binding properties of the peptidyl-prolyl cis/trans isomerase hPar14. *J. Mol. Biol.* 330, 955-966.

revalo-Rodriguez, M., Cardenas, M. E., Wu, X., Hanes, S. D. and Heitman, J. (2000). Cyclophilin A and Ess1 interact with and regulate silencing by the Sin3-Rpd3 histone deacetylase. *EMBO J.* 19, 3739-3749.

Rickards, B., Flint, S. J., Cole, M. D. and LeRoy, G. (2007). Nucleolin is required for RNA polymerase I transcription in vivo. *Mol. Cell Biol.* 27, 937-948.

Riva, A. and Kohane, I. S. (2002). SNPper: retrieval and analysis of human SNPs. *Bioinformatics.* 18, 1681-1685.

Scherr, M. and Eder, M. (2007). Gene silencing by small regulatory RNAs in mammalian cells. *Cell Cycle* 6, 444-449.

Schirling, C., Heseding, C., Heise, F., Kesper, D., Klebes, A., Klein-Hitpass, L., Vortkamp, A., Hoffmann, D., Saumweber, H. and Ehrenhofer-Murray, A. E. (2010). Widespread regulation of gene expression in the Drosophila genome by the histone acetyltransferase dTip60. *Chromosoma* 119, 99-113.

Schmid, F. X. (1995). Protein folding. Prolyl isomerases join the fold. *Curr. Biol.* 5, 993-994.

Schmidt, T. G. and Skerra, A. (2007). The Strep-tag system for one-step purification and high-affinity detection or capturing of proteins. *Nat. Protoc.* 2, 1528-1535.

Schmittgen, T. D. and Livak, K. J. (2008). Analyzing real-time PCR data by the comparative C(T) method. *Nat. Protoc.* 3, 1101-1108.

Schouten, S., Hopmans, E. C., Baas, M., Boumann, H., Standfest, S., Konneke, M., Stahl, D. A. and Sinninghe Damste, J. S. (2008). Intact membrane lipids of "Candidatus Nitrosopumilus maritimus," a cultivated representative of the cosmopolitan mesophilic group I Crenarchaeota. *Appl. Environ. Microbiol.* 74, 2433-2440.

Schreiber, S. L. and Crabtree, G. R. (1992). The mechanism of action of cyclosporin A and FK506. *Immunol. Today* 13, 136-142.

Segal, E., Fondufe-Mittendorf, Y., Chen, L., Thastrom, A., Field, Y., Moore, I. K., Wang, J. P. and Widom, J. (2006). A genomic code for nucleosome positioning. *Nature* 442, 772-778.

Sekerina, E., Rahfeld, J. U., Muller, J., Fanghanel, J., Rascher, C., Fischer, G. and Bayer, P. (2000). NMR solution structure of hPar14 reveals similarity to the peptidyl prolyl cis/trans isomerase domain of the mitotic regulator hPin1 but indicates a different functionality of the protein. *J. Mol. Biol.* 301, 1003-1017.

Shabalina, S. A. and Koonin, E. V. (2008). Origins and evolution of eukaryotic RNA interference. *Trends Ecol. Evol.* 23, 578-587.

Shaw, P. E. (2007). Peptidyl-prolyl cis/trans isomerases and transcription: is there a twist in the tail? *EMBO Rep.* 8, 40-45.

Shen, M., Stukenberg, P. T., Kirschner, M. W. and Lu, K. P. (1998). The essential mitotic peptidyl-prolyl isomerase Pin1 binds and regulates mitosis-specific phosphoproteins. *Genes Dev.* 12, 706-720.

Shen, Z. J., Esnault, S. and Malter, J. S. (2005). The peptidyl-prolyl isomerase Pin1 regulates the stability of granulocyte-macrophage colony-stimulating factor mRNA in activated eosinophils. *Nat. Immunol.* 6, 1280-1287.

Siekierka, J. J., Hung, S. H., Poe, M., Lin, C. S. and Sigal, N. H. (1989). A cytosolic binding protein for the immunosuppressant FK506 has peptidyl-prolyl isomerase activity but is distinct from cyclophilin. *Nature* 341, 755-757.

Siepe, D. and Jentsch, S. (2009). Prolyl isomerase Pin1 acts as a switch to control the degree of substrate ubiquitylation. *Nat. Cell Biol.* 11, 967-972.

Spange, S., Wagner, T., Heinzel, T. and Kramer, O. H. (2009). Acetylation of non-histone proteins modulates cellular signalling at multiple levels. *Int. J. Biochem. Cell Biol.* 41, 185-198.

Srivastava, M. and Pollard, H. B. (1999). Molecular dissection of nucleolin's role in growth and cell proliferation: new insights. *FASEB J.* 13, 1911-1922.

Stelzl, U., Worm, U., Lalowski, M., Haenig, C., Brembeck, F. H., Goehler, H., Stroedicke, M., Zenkner, M., Schoenherr, A., Koeppen, S. et al. (2005). A human protein-protein interaction network: a resource for annotating the proteome. *Cell* 122, 957-968.

Stros, M. (2010). HMGB proteins: Interactions with DNA and chromatin. *Biochim. Biophys. Acta* 1799, 101-113.

Stros, M., Launholt, D. and Grasser, K. D. (2007). The HMG-box: a versatile protein domain occurring in a wide variety of DNA-binding proteins. *Cell Mol. Life Sci.* 64, 2590-2606.

Struhl, K. (1998). Histone acetylation and transcriptional regulatory mechanisms. *Genes Dev.* 12, 599-606.

Stukenberg, P. T. and Kirschner, M. W. (2001). Pin1 acts catalytically to promote a conformational change in Cdc25. *Mol. Cell* 7, 1071-1083.

Stymest, K. H. and Klappa, P. (2008). The periplasmic peptidyl prolyl cis-trans isomerases PpiD and SurA have partially overlapping substrate specificities. *FEBS J.* 275, 3470-3479.

Sui, G., Soohoo, C., Affar, e. B., Gay, F., Shi, Y., Forrester, W. C. and Shi, Y. (2002). A DNA vector-based RNAi technology to suppress gene expression in mammalian cells. *Proc. Natl. Acad. Sci. U. S. A* 99, 5515-5520.

Surmacz, T. A., Bayer, E., Rahfeld, J. U., Fischer, G. and Bayer, P. (2002). The N-terminal basic domain of human parvulin hPar14 is responsible for the entry to the nucleus and high-affinity DNA-binding. *J. Mol. Biol.* 321, 235-247.

Switzer, R. C., III, Merril, C. R. and Shifrin, S. (1979). A highly sensitive silver stain for detecting proteins and peptides in polyacrylamide gels. *Anal. Biochem.* 98, 231-237.

Takahashi, N., Hayano, T. and Suzuki, M. (1989). Peptidyl-prolyl cis-trans isomerase is the cyclosporin A-binding protein cyclophilin. *Nature* 337, 473-475.

Taylor-Harris, P. M., Felkin, L. E., Birks, E. J., Franklin, R. C., Yacoub, M. H., Baines, A. J., Barton, P. J. and Pinder, J. C. (2005). Expression of human membrane skeleton protein genes for protein 4.1 and betaIISigma2-spectrin assayed by real-time RT-PCR. *Cell Mol. Biol. Lett.* 10, 135-149.

Terada, T., Shirouzu, M., Fukumori, Y., Fujimori, F., Ito, Y., Kigawa, T., Yokoyama, S. and Uchida, T. (2001). Solution structure of the human parvulin-like peptidyl prolyl cis/trans isomerase, hPar14. *J. Mol. Biol.* 305, 917-926.

Thorpe, J. R., Rulten, S. L. and Kay, J. E. (1999). Binding of a putative and a known chaperone protein revealed by immunogold labeling transmission electron microscopy: A suggested use of chaperones as probes for the distribution of their target proteins. *J. Histochem. Cytochem.* 47, 1633-1640.

Tossavainen, H., Permi, P., Purhonen, S. L., Sarvas, M., Kilpelainen, I. and Seppala, R. (2006). NMR solution structure and characterization of substrate binding site of the PPIase domain of PrsA protein from Bacillus subtilis. *FEBS Lett.* 580, 1822-1826.

Tschop, K., Muller, G. A., Grosche, J. and Engeland, K. (2006). Human cyclin B3. mRNA expression during the cell cycle and identification of three novel non-classical nuclear localization signals. *FEBS J.* 273, 1681-1695.

Uchida, T., Fujimori, F., Tradler, T., Fischer, G. and Rahfeld, J. U. (1999b). Identification and characterization of a 14 kDa human protein as a novel parvulin-like peptidyl prolyl cis/trans isomerase. *FEBS Lett.* 446, 278-282.

Uchida, T., Fujimori, F., Tradler, T., Fischer, G. and Rahfeld, J. U. (1999a). Identification and characterization of a 14 kDa human protein as a novel parvulin-like peptidyl prolyl cis/trans isomerase. *FEBS Lett.* 446, 278-282.

Uchida, T., Takamiya, M., Takahashi, M., Miyashita, H., Ikeda, H., Terada, T., Matsuo, Y., Shirouzu, M., Yokoyama, S., Fujimori, F. et al. (2003). Pin1 and Par14 peptidyl prolyl isomerase inhibitors block cell proliferation. *Chem. Biol.* 10, 15-24.

Ueda, T. and Yoshida, M. (2010). HMGB proteins and transcriptional regulation. *Biochim. Biophys. Acta* 1799, 114-118.

van, d., V and Otte, A. P. (1999). Transcriptional repression mediated by the human polycomb-group protein EED involves histone deacetylation. *Nat. Genet.* 23, 474-478.

Velazquez-Campoy, A., Leavitt, S. A. and Freire, E. (2004). Characterization of protein-protein interactions by isothermal titration calorimetry. *Methods Mol. Biol.* 261, 35-54.

Wasner, M., Haugwitz, U., Reinhard, W., Tschop, K., Spiesbach, K., Lorenz, J., Mossner, J. and Engeland, K. (2003). Three CCAAT-boxes and a single cell cycle genes homology region (CHR) are the major regulating sites for transcription from the human cyclin B2 promoter. *Gene* 312, 225-237.

Weinberg, D. H., Collins, K. L., Simancek, P., Russo, A., Wold, M. S., Virshup, D. M. and Kelly, T. J. (1990). Reconstitution of simian virus 40 DNA replication with purified proteins. *Proc. Natl. Acad. Sci. U. S. A* 87, 8692-8696.

Weininger, U., Haupt, C., Schweimer, K., Graubner, W., Kovermann, M., Bruser, T., Scholz, C., Schaarschmidt, P., Zoldak, G., Schmid, F. X. et al. (2009). NMR solution structure of SlyD from Escherichia coli: spatial separation of prolyl isomerase and chaperone function. *J. Mol. Biol.* 387, 295-305.

Weininger, U., Jakob, R. P., Kovermann, M., Balbach, J. and Schmid, F. X. (2010). The prolyl isomerase domain of PpiD from Escherichia coli shows a parvulin fold but is devoid of catalytic activity. *Protein Sci.* 19, 6-18.

Wells, J. and Farnham, P. J. (2002). Characterizing transcription factor binding sites using formaldehyde crosslinking and immunoprecipitation. *Methods* 26, 48-56.

Wessel, D. and Flugge, U. I. (1984). A method for the quantitative recovery of protein in dilute solution in the presence of detergents and lipids. *Anal. Biochem.* 138, 141-143.

Wheeler, D. L., Barrett, T., Benson, D. A., Bryant, S. H., Canese, K., Chetvernin, V., Church, D. M., Dicuccio, M., Edgar, R., Federhen, S. et al. (2007). Database resources of the National Center for Biotechnology Information. *Nucleic Acids Res.* 35, D5-12.

Winkler, K. E., Swenson, K. I., Kornbluth, S. and Means, A. R. (2000c). Requirement of the prolyl isomerase Pin1 for the replication checkpoint. *Science* 287, 1644-1647.

Winkler, K. E., Swenson, K. I., Kornbluth, S. and Means, A. R. (2000a). Requirement of the prolyl isomerase Pin1 for the replication checkpoint. *Science* 287, 1644-1647.

Winkler, K. E., Swenson, K. I., Kornbluth, S. and Means, A. R. (2000b). Requirement of the prolyl isomerase Pin1 for the replication checkpoint. *Science* 287, 1644-1647.

Witte, C. P., Noel, L. D., Gielbert, J., Parker, J. E. and Romeis, T. (2004). Rapid one-step protein purification from plant material using the eight-amino acid StrepII epitope. *Plant Mol. Biol.* 55, 135-147.

Wu, X., Wilcox, C. B., Devasahayam, G., Hackett, R. L., revalo-Rodriguez, M., Cardenas, M. E., Heitman, J. and Hanes, S. D. (2000). The Ess1 prolyl isomerase is linked to chromatin remodeling complexes and the general transcription machinery. *EMBO J.* 19, 3727-3738.

Wulf, G. M., Liou, Y. C., Ryo, A., Lee, S. W. and Lu, K. P. (2002). Role of Pin1 in the regulation of p53 stability and p21 transactivation, and cell cycle checkpoints in response to DNA damage. *J. Biol. Chem.* 277, 47976-47979.

Wysocka, J., Reilly, P. T. and Herr, W. (2001). Loss of HCF-1-chromatin association precedes temperature-induced growth arrest of tsBN67 cells. *Mol. Cell Biol.* 21, 3820-3829.

Xu, G. G. and Etzkorn, F. A. (2009). Pin1 as an anticancer drug target. *Drug News Perspect.* 22, 399-407.

Xu, Y. X., Hirose, Y., Zhou, X. Z., Lu, K. P. and Manley, J. L. (2003). Pin1 modulates the structure and function of human RNA polymerase II. *Genes Dev.* 17, 2765-2776.

Xu, Y. X. and Manley, J. L. (2007). Pin1 modulates RNA polymerase II activity during the transcription cycle. *Genes Dev.* 21, 2950-2962.

Yaffe, M. B., Schutkowski, M., Shen, M., Zhou, X. Z., Stukenberg, P. T., Rahfeld, J. U., Xu, J., Kuang, J., Kirschner, M. W., Fischer, G. et al. (1997). Sequence-specific and phosphorylation-dependent proline isomerization: a potential mitotic regulatory mechanism. *Science* 278, 1957-1960.

Yeh, E., Cunningham, M., Arnold, H., Chasse, D., Monteith, T., Ivaldi, G., Hahn, W. C., Stukenberg, P. T., Shenolikar, S., Uchida, T. et al. (2004). A signal-

ling pathway controlling c-Myc degradation that impacts oncogenic transformation of human cells. *Nat. Cell Biol.* 6, 308-318.

Yeh, E. S., Lew, B. O. and Means, A. R. (2006). The loss of PIN1 deregulates cyclin E and sensitizes mouse embryo fibroblasts to genomic instability. *J. Biol. Chem.* 281, 241-251.

Yeh, E. S. and Means, A. R. (2007). PIN1, the cell cycle and cancer. *Nat. Rev. Cancer* 7, 381-388.

You, H., Zheng, H., Murray, S. A., Yu, Q., Uchida, T., Fan, D. and Xiao, Z. X. (2002). IGF-1 induces Pin1 expression in promoting cell cycle S-phase entry. *J. Cell Biochem.* 84, 211-216.

Yunokuchi, I., Fan, H., Iwamoto, Y., Araki, C., Yuda, M., Umemura, H., Harada, F., Ohkuma, Y. and Hirose, Y. (2009). Prolyl isomerase Pin1 shares functional similarity with phosphorylated CTD interacting factor PCIF1 in vertebrate cells. *Genes Cells* 14, 1105-1118.

Zheng, H., You, H., Zhou, X. Z., Murray, S. A., Uchida, T., Wulf, G., Gu, L., Tang, X., Lu, K. P. and Xiao, Z. X. (2002). The prolyl isomerase Pin1 is a regulator of p53 in genotoxic response. *Nature* 419, 849-853.

Zhou, X. Z., Kops, O., Werner, A., Lu, P. J., Shen, M., Stoller, G., Kullertz, G., Stark, M., Fischer, G. and Lu, K. P. (2000). Pin1-dependent prolyl isomerization regulates dephosphorylation of Cdc25C and tau proteins. *Mol. Cell* 6, 873-883.

8. Appendix

Supplementary Table 1 List of all Par14/Par17 interactors identified by AP-MS with the exclusion of the technical contamitants and non-specifc binders as listed on Table 4.1

Protein Symbol/Name	Accession No	Scores	Peptides	MW [kDa]
ACTB cDNA FLJ52842	IPI00894365	49.6	2	39.2
ACTN4 Alpha-actinin-4	IPI00013808	31.9	1	104.8
ANXA1 Annexin A1	IPI00549413	79.3	3	22.7
ANXA2 Annexin A2	IPI00455315	114.0	4	38.6
ANXA5 Uncharacterized protein ANXA5 (Fragment)	IPI00872379	50.2	2	35.8
cDNA FLJ55692, GOT2, mitochondrial	IPI00910267	59.4	2	43.0
cDNA FLJ55705, highly similar to TARS	IPI00910719	32.9	2	70.3
cDNA FLJ59476, HARS	IPI00909075	48.9	2	35.6
CKB Creatine kinase, brain	IPI00908811	53.8	2	38.7
EEF1A2 Eukaryotic translation elongation factor 1 alpha 2	IPI00556204	73.8	2	36.9
Ezrin (EZR) 69 kDa protein	IPI00872684	388.8	14	69.3
HNRNPA2B1 34 kDa protein	IPI00916517	87.0	2	34.2
HSP90AA1 Isoform 1 of Heat shock protein HSP 90-alpha	IPI00784295	223.5	7	84.6
HSP90AB1 Heat shock protein HSP 90-beta	IPI00414676	242.5	7	83.2
HSPA4 Heat shock 70 kDa protein 4	IPI00002966	108.6	3	94.3
HSPA5 HSPA5 protein	IPI00003362	252.0	6	72.4
HSPA9 cDNA FLJ51903, highly similar to Stress-70 protein	IPI00922694	50.1	2	69.9
HSPA9 cDNA FLJ51903, mitochondrial	IPI00922694	50.1	2	69.9
LMNA Rhabdomyosarcoma antigen MU-RMS-40.12	IPI00655812	97.4	3	55.6
NCAPG2 Isoform 1 of Condensin-2 complex subunit G2	SHD00797030	31.0	2	130.9
NCL Nucleolin	IPI00444262	118.0	5	65.9
NOMO1;NOMO3 139 kDa protein	SHD00413732	44.2	2	139.3
NPFFR2 Isoform 3 of Neuropeptide FF receptor 2	SHD00221214	28.6	1	49.0
NPM1 nucleophosmin	IPI00658013	29.8	1	28.4
P4HB Protein disulfide-isomerase precursor	IPI00010796	103.3	2	57.1
PDIA3 Protein disulfide-isomerase A3 precursor	IPI00025252	201.3	7	56.7
PDIA4 Protein disulfide-isomerase A4 precursor	IPI00009904	61.0	2	72.9
Peroxiredoxin 1 PRDX1 19 kDa protein	IPI00640741	126.2	4	19.0
PPIA 13 kDa protein	IPI00925411	36.6	2	13.0
PPIB peptidylprolyl isomerase B precursor	IPI00646304	58.3	2	23.7
SFRS1 Isoform ASF-3 of Splicing factor, arginine/serine-rich 1	IPI00218592	70.8	1	22.4
SHROOM4 Isoform 2 of Protein Shroom4	IPI00845416	32.3	2	152.7
SPTAN1, Spectrin	SHD00871535	284.9	2	47.3
TLK2 Isoform 2 of Serine/threonine-protein kinase tousled-like 2	SHD00337659	21.9	1	85.4
Transketolase TKT Putative uncharacterized protein	IPI00792641	104.8	3	58.9
YWHAE 14-3-3 protein epsilon	IPI00000816	102.2	4	29.2

Supplementary Table 2 List of potential Par14/Par17 interactors that were reported to be acetylated by Choudary and co-workers. * stands for the inclusion of MPG, a DNA-repair protein that was not acetylated but its counterpart UDG (Uracil-DNA glycosylase) was reported to be acetylated in the same study

Protein Symbol	Acetylated	Reference
Protein translation		
HARS	Yes	Chouhdary et al. (2009)
TARS	Yes	Chouhdary et al. (2009)
DNA repair		
MPG	No*	
RNA processing		
HNRNPA2B1	Yes	Chouhdary et al. (2009)
SFRS1	Yes	Chouhdary et al. (2009)
Ribosome biogenesis		
NCL	Yes	Chouhdary et al. (2009)
NPM1	Yes	Chouhdary et al. (2009)
Cell adhesion & cytoskeleton		
EZR	Yes	Chouhdary et al. (2009)
LMNA	Yes	Chouhdary et al. (2009)
SPTAN1	Yes	Chouhdary et al. (2009)
EPB41	Yes	Chouhdary et al. (2009)
DMN1	Yes	Chouhdary et al. (2009)
Par14/Par17	Yes	Chouhdary et al. (2009)
Signal transduction		
YWHAE	Yes	Chouhdary et al. (2009)
Metabolism		
GOT2	Yes	Chouhdary et al. (2009)
TKT	Yes	Chouhdary et al. (2009)
Annexin		
ANXA1	Yes	Chouhdary et al. (2009)
ANXA5	Yes	Chouhdary et al. (2009)
Unclassified		
PRDX1	Yes	Chouhdary et al. (2009)

Supplementary Fig 1 Par14/Par17 mRNA displaying all the siRNA and shRNA sequences used in this study. In red are the sequences of the newly ordered siRNAs as mentioned in Section 6.

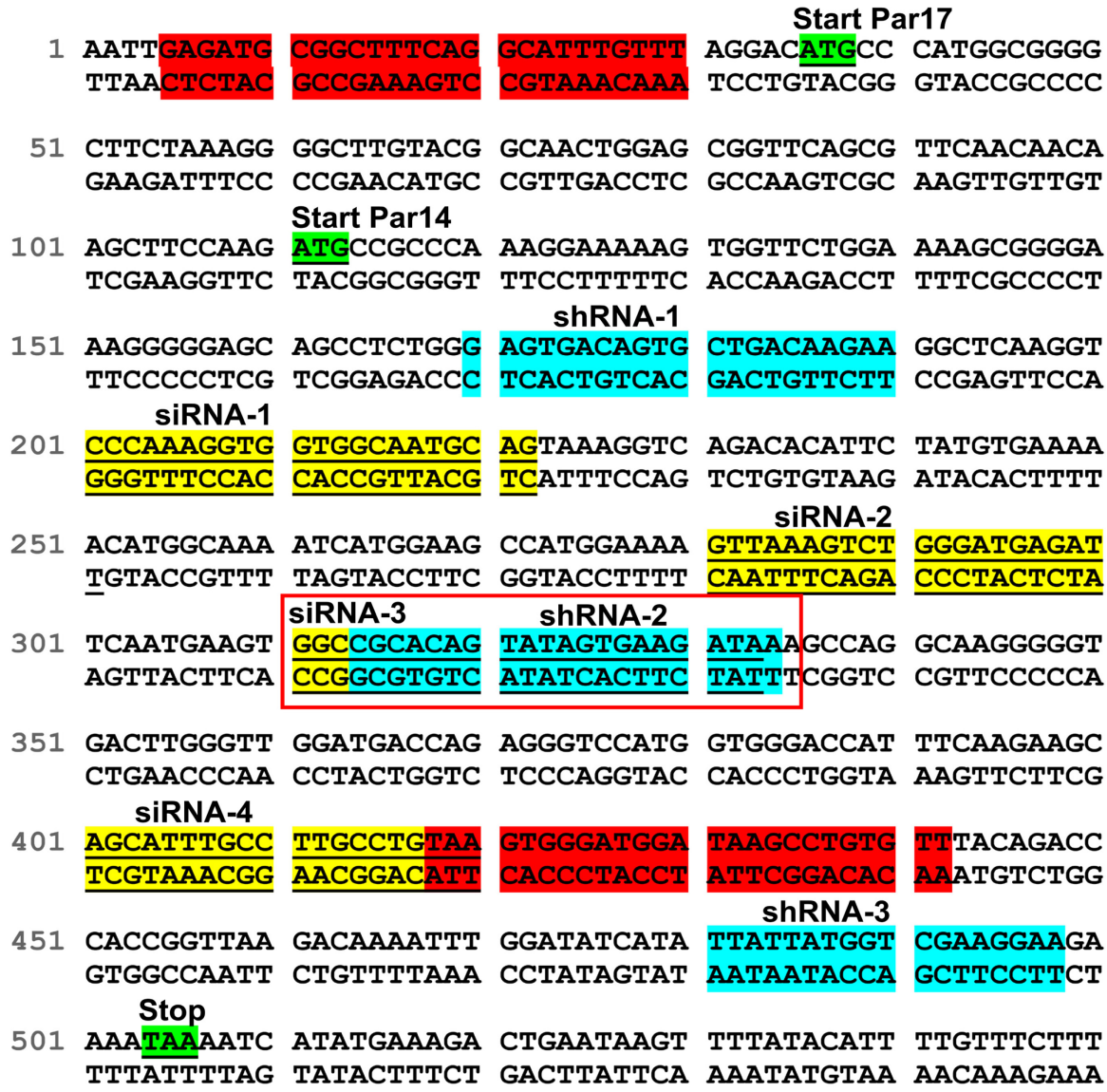

9. Acknowledgements

A sincere note of thank you goes to Prof. Dr. Peter Bayer who made it possible for me to do my thesis in the premises of the institute of Structural and Medicinal Biochemistry. I could storm his office at any given time and he always had an ear for me.

I abundantly thank my scientific supervisor and mentor Dr Jonathan Mueller for his time and patience. Dear Jonathan, our working together was a very interesting one. I'd like to tell you that I'm happy to have profited from your diverse repertoire of expertise that is unparalleled and second to none.

I thank my mate Dr Levin Bölig (Department of Molecular Oncology, *Universitätsfrauenklinik* Leipzig, Germany) with whom I collaborated to produce the data of the transcription regulation experiments. The assistance of Dr Barbara Sitek (*Medizinisches Proteom-Center,* Ruhr University of Bochum, Germany) who conducted the mass spectrometry experiments is also heavily appreciated. I can't forget to say thank you to Dr Corinna Schirling (Department of Genetics, Center of Medical Biotechnology, University Duisburg-Essen, Germany) who provided the polytene chromosome squashes. Manuel Prince was very helpful in the statistical analyses of my qRT-PCR data (Department of Bioinfomatics, Center for Medical Biotechnology, University of Duisburg-Essen, Germany). Klaus Lennartz (Institute of Cell Biology, University Clinic Essen, Germany) played an invaluable role in putting me throung with the handling of the FACSCalibur flow cytometer. Tina Stratmann and Alma Rüppel were the hearts and souls of the laboratory. I am deeply indebted for their technical assistance and the time we spent together.

Dr Christian Sinnen played a crucial role in proof-reading this work. My old university mate from our days in Darmstadt, Alexander Strigun, at the moment a doctoral fellow, has been very supportive and he also helped in proof-reading this thesis. Thank you Chris! Thank you Alex! Another special person, who must be mentioned, is Anja Matena. She has been an angel and unlimited source of moral support. Our long and endless discussions are still very fresh in memory. We both stood the test of time.

I acknowledge the support that my family and particularly that of my younger sister, Lum Lilian Saningong gave to me. Thank you little sister!! You have been magnanimous.

A colossal thank you goes to some already mentioned colleagues and friends for being part of the ***Kamerun4AfrikaClub e.V.*** They have been my constituents and comrades in making education accessible to the poorest of the poor. They are: Christian Sinnen, Anja Matena, Martin Ruppert, Levin Böhlig, Katja Röser, Alma Rüppel, Alexander Strigun, Kenneth Ndango, Manuel Prince, Daniel Grum, Nikolaj Dybowski, Oliver Kuhn, Björn Thorwirth, Imad Elfaki and Stefan Franke. They agreed with me without preconditions or reservation that education is not only a right but a remedy. It is a lifeline and a path out of poverty. Your unflinching commitment towards our course touches me in a manner I can't describe. Kudos to you all pals!!

Last but not least, I want to earnestly thank the ***Elfriede und Helmut Lotz Stiftung*** for the award of a stipend enabling me to write my thesis up to the bitter end. I'm indelibly greatful. I also thank the *Deutsche Forschungsgemeintschaft* for funding this work.

10. Curriculum Vitae

Akuma Divine Saningong, MSc (TUM)

Molecular Biotechnologist

Personal Information

Date of Birth:	09.09.1978
Place of Birth:	Yaoundé – Cameroon
Nationality:	Cameroonian
Family Status:	Single

Educational Background

10/2006 – present	Doctoral Studies at the University of Duisburg-Essen, Department of Structural and Medicinal Biochemistry in the Graduate College: Transcription, Chromatin Structure and DNA Repair in Development and Differentiation **Reserach Topic**: „Functional Studies on Par14/Par17 with Emphasis on Chromatin, the Cell Cycle and Protein-Protein Interactions “ **Stipendiary of the *Deutsche Forschungsgemeinschaft (DFG)***
10/2004 – 10/2006	Graduate Studies in Molecular Biotechnology at the Technical University of Munich **Core Areas**: Protein Biochemistry, Molecular Infection Biology and Molecular Physiology Degree: Master of Science (MSc) in Molecular Biotechnology
10/2001 – 10/2004	Undergraduate Studies in Biotechnology at the University of Applied Sciences in Darmstadt **Stipendiary of the *Elfriede- und Helmut Lotz-Stiftung***
09/2000 – 08/2001	German Language Courses at the Goethe Institute in Yaoundé and at the University of Potsdam

Research Experience

02/2006 – 09/2006	Masterthesis at the *Else Kröner-Fresenius-Zentrum für Ernährungsmedizin,* Department of Nutritional Medicine, Technical University of Munich

Akuma D. Saningong Immestr. 55 D-45127 Essen
Tel. +(49)-179-6881446 E-Mail: akuma.saningong@uni-due.de

	Research Topic: Functional Characterisation of Potential Regulatory SNPs in the Proximal Promoter Region of the Human ACDC Gene Adiponectin
11/2005 – 12/2005	Research at the Nutrition and Food Research Center, Weihenstephan, Department of Physiology, Technical University of Munich **Research Topic:** Analysis of Gene Expression in Different Bovine Tissues after Treatment with the Beta-Receptor Agonist – Clenbuterol
03/2005 – 05/2005	Research Internship at the Institute for Chemistry of Bio-polymers, Technical University of Munich **Research Topic:** „Proteolyse und Massenspektrometrie als Werkzeuge für die Ermittlung der Struktur des Nogo-A Proteins“

Social Engagements and Memberships

04/2007 – present	Founder & Chairman of Kamerun4AfrikaClub e. V. (www.kamerun4afrikaclub.de)
01/2007 – present	Member of the German Society of Biochemistry and Molecular Biology (GBM) and the Federation of European Biochemical Societies (FEBS)
03/2005 – present	Public Relations Officer of **Amnesty International,** Section of the Federal Republic of Germany, Local Group in Essen

Personal Skills and Competences

Social Skills	Organising ability, capable to work in a team and alone, flexible and able to work under pressure
Computer Skills	MS-Office (Word, Excel, PowerPoint, Access), Adobe Photoshop
Language Proficiency	English: Mother Tongue; French: business fluent; German: business fluent; Spanisch: basics
Personal Interests	Sport: Jogging, Tennis and Fitness Other: Human Rights, Environment, Travelling

Akuma Divine Saningong, Essen, 26.04.2010

Akuma D. Saningong Immestr. 55 D-45127 Essen
Tel. +(49)-179-6881446 E-Mail: akuma.saningong@uni-due.de

Lebenslauf

Akuma Divine Saningong, MSc (TUM)

Molekularer Biotechnologe

Persönliche Daten

Geburtsdatum:	09.09.1978
Geburtsort:	Yaounde, Kamerun
Staatangehörigkeit:	Kamerunisch
Familienstand:	Ledig, keine Kinder

Schule und Studium

Seit 10/2006	Promotionsstudium an der Universität Duisburg-Essen, Abteilung Strukturelle und Medizinische Biochemie im Graduiertenkolleg „Transcription, Chromatin Structure and DNA Repair in Development and Differentiation“ **Forschungsthema**: „Functional Studies on Par14/Par17 with Emphasis on Chromatin, the Cell Cycle and Protein-Protein Interactions “ **Stipendiat der Deutschen Forschungsgemeinschaft (DFG)**
10/2004 – 10/2006	Studium im Master Studiengang Molekulare Biotechnologie an der TU München Schwerpunkte: Proteinbiochemie und Engineering, Molekulare Infektionsbiologie und Molekulare Physiologie Abschluss als **Master of Science** (**MSc) in molekularer Biotechnologie**
10/2001 – 10/2004	Studium der Biotechnologie an der Hochschule Darmstadt **Stipendiat der Elfriede- und Helmut Lotz-Stiftung**
09/2000 – 08/2001	Deutschkurse am Goetheinstitut in Yaounde - Kamerun und an der Universität Potsdam

Forschungserfahrung

02/2006 – 09/2006	Masterarbeit im Else Kröner-Fresenius-Zentrum für Ernährungsmedizin,

Akuma D. Saningong Immestr. 55 D-45127 Essen
Tel. +(49)-179-6881446 E-Mail: akuma.saningong@uni-due.de

	Lehrstuhl für Ernährungsmedizin der Technischen Universität München **Forschungsthema:** "Functional Characterisation of Potential Regulatory SNPs in the Proximal Promoter Region of the Human ACDC Gene Adiponectin
11/2005 – 12/2005	Forschungspraktikum im ZIEL (Zentralinstitut für Ernährung und Lebensmittelforschung); Abteilung Physiologie an der TU München **Forschungsthema:** "Analysis of Gene Expression in Different Bovine Tissues after Treatment with the Beta-Receptor Agonist – Clenbuterol".
03/2005 – 05/2005	Forschungspraktikum im Institut für Chemie der Biopolymere und Institut für Biologische Chemie an der TU München **Forschungsthema:** Proteolyse und Massenspektrometrie als Werkzeuge für die Ermittlung der Struktur des Nogo-A Proteins

Ehrenamtliches Engagement & Mitgliedschaften

04/2007 – dato	Gründer & Vorstandsvorsitzender des Kamerun4AfrikaClub e. V. (www.kamerun4afrikaclub.de)
01/2007 – dato	Mitglied der Gesellschaft für Biochemie und Molekulare Biologie (GBM) und der „Federation of European Biochemical Societies (FEBS)"
03/2005 – dato	Beauftragter für Öffentlichkeitsarbeit von **Amnesty International** Sektion Bundesrepublik Deutschland in der Ortsgruppe Essen

Weiteres

Allgemeine Fähigkeiten	Organisationstalent und Teamfähigkeit, selbständiges Arbeiten, belastbar und flexibel
EDV-Kenntnisse	MS-Office (Word, Excel, PowerPoint, Access), Adobe Photoshop
Sprachkenntnisse	Englisch: Muttersprache; Französisch: verhandlungssicher; Deutsch: verhandlungssicher; Spanisch: Grundkenntnisse
Persönliche Interessen	Sport: Joggen, Tennis und Fitness Sonstiges: Menschenrechtsarbeit, Umwelt, Reisen

Akuma Divine Saningong, Essen, 26.04.2010

Akuma D. Saningong Immestr. 55 D-45127 Essen
Tel. +(49)-179-6881446 E-Mail: akuma.saningong@uni-due.de

Publications and Conferences

Publications

- Laumen, H., **Saningong, A. D.**, Heid, I. M., Hess, J., Herder, C., Claussnitzer, M., Baumert, J., Lamina, C., Rathmann, W., Sedlmeier, E. M. et al. (2009). Functional characterization of promoter variants of the adiponectin gene complemented by epidemiological data. Diabetes 58, 984-991.
- **Saningong, A.D**, Elfaki I, Sitek B, Böhlig L, Bayer P, Müller J Functional Studies with Human Protein Isomerases of the Parvulin Type (Manuscript in Preparation)

Conferences

- Spetsai Summer School, Proteins and their Networks – from Specific to Global Analysis, Spetses, Greece, 07 – 17.09.2009
- 33rd FEBS Congress and 11th IUBMB Conference, Biochemistry of Cell Regulation, Athens, Greece, 28.06 – 03.07.2008
- Mosbach Colloquium, Epigenetics – Molecular Principles and Mechanisms, Mosbach, Germany, 27 – 29.03.2008
- Herbsttagung, Molecular Life Sciences, Hamburg, Germany, 16 –19.09.2007
- Mosbach Colloquium, Protein and Lipid Sorting in Health and Disease, Mosbach, Germany, 29 – 31.03.2007

Declaration

Erklärung:

Hiermit erkläre ich, gem. § 6 Abs. 2, Nr. 7 der Promotionsordnung der Math.-Nat. Fakultäten zur Erlangung der Dr. *rer. nat.*, dass ich das Arbeitsgebiet, dem das Thema *„Functional Studies on Par14/Par17 with Emphasis on Chromatin, the Cell Cycle, and Protein-Protein Interactions“* zuzuordnen ist, in Forschung und Lehre vertrete und den Antrag von **Akuma Divine Saningong** befürworte.

Essen, den _____ _____

Unterschrift d. wissenschaftl. Betreuers/Mitglieds der Universität Duisburg-Essen

Erklärung:

Hiermit erkläre ich, gem. § 6 Abs. 2, Nr. 6 der Promotionsordnung der Math.-Nat. Fakultäten zur Erlangung des Dr. *rer. nat.*, dass ich die vorliegende Dissertation selbständig verfasst und mich keiner anderen als der angegebenen Hilfsmittel bedient habe.

Essen, den _____ _____

Unterschrift des/r Doktoranden/in

Erklärung:

Hiermit erkläre ich, gem. § 6 Abs. 2, Nr. 8 der Promotionsordnung der Math.-Nat. Fakultäten zur Erlangung des Dr. *rer. nat.*, dass ich keine anderen Promotionen bzw. Promotionsversuche in der Vergangenheit durchgeführt habe und dass diese Arbeit von keiner anderen Fakultät abgelehnt worden ist.

Essen, den _____ _____

Unterschrift des/r Doktoranden/in